THE UNIVERSITY
of ADELAIDE

School of Mechanical Engineering

The University of Adelaide

EFFECT OF PARTICLE SIZE AND SINTERING PROCESSES ON MECHANICAL PROPERTIES OF CEMENTED CARBIDES

Md. Raihanuzzaman Rumman

PhD Thesis

May 2016

ABSTRACT

Cemented carbide has been widely used as hard materials in industrial machining as cutting tools and as moulds in metal shaping. Prior research suggests that many processing techniques have been applied to improve its manufacturing conditions, microstructural characteristics and mechanical properties, namely hardness, fracture toughness and wear resistance. Although it is considered to be one of the most stable composites in terms of industrial requirements, challenges have been faced in the areas and routes of manufacturing, and consolidation with a desired set of mechanical properties via different processing techniques.

In the field of cemented carbides, the understanding of the processes such as powder refinement and consolidation or sintering, contributing to the mechanical properties is critical. The aim of this project was to examine three different groups of powder size of Tungsten Carbide-Cobalt (WC-Co), which is the dominant compositional elements among all cemented carbides, and four consolidation techniques including plasma, microwave and conventional sintering, in order to understand the relationship between these processes and mechanical properties. This study started with analysing three different particle size for both Tungsten Carbide (WC) and Cobalt (Co), which then resulted into three different types of mixed powder samples based on their size. Once the compositions were made through either high or low energy ball milling, experiments proceeded to compaction and sintering stage. The chosen composition for the study was WC – 7.5 wt. % Co, which was kept constant, while particle size, sintering process, sintering temperature, pressure and other parameters were varied. The final and overall objective was to establish a three way relationship among particle size, processing routes and mechanical properties of WC – 7.5 wt. % Co.

It was found that Pulse Plasma Sintering (PPS) method is the most successful in achieving excellent physical and mechanical properties including density (fully dense), hardness (2000 HV) and fracture toughness (15.3 MPa√m), and displays significantly improved microstructural behaviour in cemented carbides sintered at lower than conventional temperature, ensuring time and energy efficiency. Spark Plasma and Microwave Sintering were found to be the most efficient and effective after PPS in terms of mechanical

properties, considering the entire particle size range and the other variable parameters.

This thesis first outlines the basic understanding of cemented carbides, their fields of application, types, and processes that are involved during their manufacture. It then presents an overview article which is a chapter as well that presents an understanding of what has been done specifically in the areas of processing techniques, through powder refinement and consolidation highlighting the areas where challenges are faced. The mechanical properties along with certain microstructural aspects like grain growth and phases are also elaborated as part of this paper. The second paper discusses the processing of particles before sintering processes are applied and how a homogeneous and optimized mixture can be achieved. Four more chapters come from four papers that are either published or under review focusing on the different consolidation processes and their effects on mechanical properties and microstructural behaviour of WC- 7.5 wt. % Co. The thesis finally brings together a conclusion from all the separate segments of the project, highlighting the key findings and comparisons and provides information on future work.

Future work will involve further investigation on sintering mechanisms and to resolve one of the most critical question, whether the presence of plasma can be confirmed during the use of some of the modern sintering methods.

I certify that this work contains no material which has been accepted for the award of any other degree or diploma in my name, in any university or other tertiary institution and, to the best of my knowledge and belief, contains no material previously published or written by another person, except where due reference has been made in the text. In addition, I certify that no part of this work will, in the future, be used in a submission in my name, for any other degree or diploma in any university or other tertiary institution without the prior approval of the University of Adelaide and where applicable, any partner institution responsible for the joint-award of this degree.

I give consent to this copy of my thesis when deposited in the University Library, being made available for loan and photocopying, subject to the provisions of the Copyright Act 1968.

The author acknowledges that copyright of published works contained within this thesis resides with the copyright holder(s) of those works.

I also give permission for the digital version of my thesis to be made available on the web, via the University's digital research repository, the Library Search and also through web search engines, unless permission has been granted by the University to restrict access for a period of time.

Md Raihanuzzaman Rumman, 11th May 2016

Prima facie, I am thankful to God for bestowing upon me the patience, will and wellbeing necessary to complete this work.

I would like to express my gratitude to my principal supervisor Reza Ghomashchi; you have been a tremendous mentor for me. It was an honor having an opportunity to work with you, which needless to say allowed me to grow as a research scientist over these past few years. Your advice on different aspects of research as well as on my career have been priceless. I would also like to thank my co supervisor Zonghan Xie for his invaluable assistance and guidance throughout the entire duration of the project. Your feedback and suggestions on my work have been incredibly helpful.

I am immensely grateful to my collaborators, Professors Marcin Rosinski (Warsaw University, & GeniCore, Poland), Soon Jik Hong (Kongju National University, South Korea) and Lee Chang Chuan (University Malaysia Perlis, Malaysia) for their generous help in granting us access to the experimental units required for several parts of the study. I would also like to mention Ken Neubauer and the entire team of Adelaide Microscopy for their continuous support towards the microstructural study of this work. Also, special thanks to Dr Erwin Gamboa and Dr John Codrington for their continuous support with inductions on materials processing.

Mom, your words of inspiration and prayers resonated greatly with me recounting all the curiosities you entertained as I learned to categorize the world around me in a way I would like to believe, conscientious. You were, are, and always will be priceless.

[1] **Raihanuzzaman RM**, Xie Z, Hong SJ, Ghomashchi R. Powder Refinement, Consolidation and Mechanical Properties of Cemented Carbides—An Overview. Powder Technology. 2014;261:1-13.

[2] **Raihanuzzaman RM**, Jeong TS, Ghomashchi R, Xie Z, Hong S-J. Characterization of Short-Duration High-Energy Ball Milled WC–Co Powders and Subsequent Consolidations. Journal of Alloys and Compounds. 2014;615:S564-S8.

[3] **Raihanuzzaman RM**, Han S-T, Ghomashchi R, Kim H-S, Hong S-J. Conventional Sintering of WC with Nano-sized Co Binder: Characterization and Mechanical Behavior. International Journal of Refractory Metals and Hard Materials. 2015.

[4] **Raihanuzzaman RM**, Xie Z, Hong S-J, Ghomashchi R. Effect of Spark Plasma Sintering Pressure on Mechanical Properties of WC–7.5 wt% Nano Co. Materials & Design. 2015;68:221-7.

[5] **Raihanuzzaman RM**, Lee Chang Chuan, Zonghan Xie, Reza Ghomashchi Mechanical Properties and Microstructural Behaviour of Microwave Sintered WC – Co (Under Review).

[6] **Raihanuzzaman RM**, Marcin Rosinski, Zonghan Xie, Reza Ghomashchi Mechanical Properties and Microstructural Behaviour of Pulse Plasma Sintered WC – Co (Under Review).

[1] **Raihanuzzaman RM**, Chuan LC, Xie Z, Ghomashchi R. Microwave Sintering and Its Application on Cemented Carbides. World Academy of Science, Engineering and Technology, International Journal of Chemical, Molecular, Nuclear, Materials and Metallurgical Engineering. 2015;9:930-3.

[2] Song J-W, **Raihanuzzaman RM**, Lee I, Hong S-J, Myung Koo J. Refinement Behavior of Scrap Silicon by Mechanical Milling. Current Nanoscience. 2014;10:441-4.

[3] **Raihanuzzaman RM**, Park H, Ghomashchi R, Kwon T, Son H-T, Hong S. Effect Of Ti Powder Addition On The Fabrication Of TiO_2 Nanopowders. Archives of Metallurgy and Materials. 2015;60:1473-7.

[4] Song J-W, **Raihanuzzaman RM**, Hong S-J. Consolidation of WC–Co Alloys by Magnetic Pulsed Compaction and Evaluation of their Mechanical Properties. Powder Technology. 2013;235:723-7.

[5] Song J-W, **Raihanuzzaman RM**, Hong S-J. Mechanical Properties of WC-Co Alloys with Various Mixing and Milling Conditions using High Energy Ball Miller. Current Nanoscience. 2014;10:62-5.

Paper 1 (Published)

Cemented carbides, owing to their excellent mechanical properties, have been of immense interest in the field of hard materials for the past few decades. Although a number of processing techniques have been developed to obtain nanostructured cemented carbide powders with grain size of less than 100 nm, they are expensive, as such, the challenge remains for producing nano-sized powders economically. The lack of understanding and control of grain growth and its effect on deformation and fracture of the resulting carbide materials is another area that requires proper attention. In addition, the effect of binder materials and their content on the mechanical properties of cemented carbides is not clearly understood yet. This review aims to address some of the key issues and challenges faced in the research and development of cemented carbides, especially on powder refinement and consolidation, and their effect on mechanical properties.

Paper 2 (Published)

The aim of this study was to observe the effect of short-duration, high-energy ball milling on the mechanical properties of sintered WC–Co. Mixed powders of WC–7.5 wt. % nano Co were ball milled at three different time using WC vial and balls, while other parameters were kept constant. The powders were then consolidated using spark plasma sintering. Density and hardness of the sintered samples were measured as a function of milling time, used to mix the powders prior to consolidation. It was found that both density and hardness increased with milling time, with hardness reaching a maximum of 14.95 GPa for the sample milled for 10 min. Microstructures of the sintered samples suggested a slight decline in grain size and increase in Co distribution with increasing milling time. It was also evident that milling of WC–Co powders resulted in the sintered samples having overall irregular shaped grains.

Paper 3 (Published)

In this study, WC particles of 1–3 μm were blended with two different sizes of Co particles and sintered conventionally at two different temperatures. Compaction of initial powders was carried out using a relatively new dynamic compaction method called Magnetic Pulsed compaction (MPC). The maximum Vickers hardness for the samples found was around 1353 HV (13.27 GPa), while the maximum fracture toughness was observed at 4.6 MPa · m$^{1/2}$. The marked changes in density, hardness, fracture toughness and crack behaviour observed in the samples indicate strong correlations among particle size, sintering process and mechanical properties of cemented carbides. In addition, the nature of crack initiation and propagation, which is indicative of the trend in fracture toughness of materials, was observed and analysed.

Paper 4 (Published)

In this study, Spark Plasma Sintering (SPS), a relatively fast consolidation method assisted with simultaneous application of heat and pressure, was used to produce bulk carbides from mixed WC–7.5 wt. % Nano Co powders. Different pressures ranging from 30 to 80 MPa were applied during sintering to explore its effect on the mechanical properties of resulting carbides. The maximum hardness was found for the samples pressed at 80 MPa, which is ~1925 HV (18.88 GPa), higher than that of the commercially available cemented carbide tools. The marked changes in porosity, hardness, and crack propagation observed in the samples show that the sintering pressure have considerable impact on the mechanical properties of cemented carbides. In particular, the nature of crack initiation and propagation, which is indicative of the fracture toughness of materials, was studied and clarified.

Paper 5 (Under Review)

Tungsten or in general cemented carbides have been of great interest within industrially manufacturable hard materials for their excellent mechanical properties, especially in the last few decades, with a number of new and revamped processing techniques emerging in order to develop high performance carbide tools. Microwave sintering or heating is known for its application on a range of materials, which includes ceramics as well. Although it has

been widely used, its effect however on grain growth of materials still requires clear understanding. Furthermore, the effect of sintering temperature and initial particle size and how they influence microwave behaviour for such range of materials is another area that requires clear understanding. This article focuses on microwave sintering being used on cemented carbides using a range of final sintering temperatures and initial particle sizes, which sheds light on the entire process and its effectiveness on ceramic processing. The microstructural features associated to the sintering process have also been focused as part of the study, addressing some of the key issues and challenges faced in the research.

Paper 6 (Under Review)

Tungsten carbides-based inserts have been considered as one of the dominant hard materials in the cutting industry, receiving great interest for their excellent combination of mechanical properties. Pulse plasma sintering (PPS) process has been applied to a series of WC-Co samples with varying sintering temperature, initial particle size and sintering pressure in order to study the mechanical and microstructural behaviour. The quality of the products as well as the mechanical properties and microstructural features this process yields are commendable and worth looking into. A high hardness of more than 2000 HV has been achieved while a maximum fracture by toughness of 15 MPa. $m^{1/2}$ was found in samples that were sintered at 1100 ºC and 100 MPa. Microstructural features like grain growth and other properties are discussed with respect to the varying parameters. While grain size shows an incremental pattern with increasing temperature, it was still possible to limit them to a great extent ensuring high mechanical properties. The effect of sintering pressure in the range of 60-100 MPa, while keeping sintering temperature constant was found to be almost negligible.

Cemented carbides are a group of composites which are essentially aggregates of particles of refractory carbides and a metallic binder like Co or Ni, forming a body through compaction and/or sintering displaying a unique combination of properties, namely high hardness, fracture toughness and wear resistance. The most well-known cemented carbides are WC-Co composites. From a technical and commercial point of view, these carbides are one of the oldest and most successful powder metallurgy (P/M) products. They are a typical example of the benefits of manufacturing composite materials from disparate phases.

The overall advances made on sintered carbides are mainly due to three important events that occurred chronologically [1].

a) The discovery of multi-carbides in 1930's with inclusions of commercial grain growth inhibitors like TiC, TaC, NbC, Mo_2C and so on.

b) The introduction of the indexable insert tips in metal cutting and mining industry after Second World War.

c) The emergence of coated tools in late 1960's in sintered carbides technology.

1.1. Processing of Cemented Carbides: Powder Metallurgy

Powder metallurgy has been considered as the most successful and dominant route for the production of cemented carbides irrespective of their composition or area of application. As stated previously, WC-Co is the most popular compound within the class of hard materials, although it can vary in terms of composition and presence of other commercial grain growth inhibitors used in most conventional processes. A number of stages can be involved for the manufacture of these carbides depending on what process is being used to consolidate the materials. Some of the important stages in powder metallurgy include, but not limited to:

1.1.1   Powder Refinement and Mixing

1.1.2   Compaction

1.1.3   Sintering

1.1.1. Powder Refinement and Mixing

Powder synthesis often requires an additional step or refinement that ensures that average particle size and shape are in sync with the requirement of the product that needs to be fabricated. A conventional ball mill is generally employed for mixing purposes. Straightforward mixing is found to be fully effective after only a few hours of ball milling [2, 3]. In fact, manufacturers tend to prefer extended ball milling for several days or even more, as they require the grinding action to take place properly, so the carbide powder becomes finer, influencing final sintering by reducing porosity content [4-7]. The exact mechanism of milling was once an interesting research topic, but mixing preferences have now been industrially standardized and do not cause manufacturing difficulties in the later stages. Nevertheless, investigations have indicated that continued milling reduces the particle size within the aggregates when equilibrium is reached where further combination is balanced by aggregation [2]. Powder refinement and mixing can also be carried out together although it may be advised against considering the fact that there is presence of metallic binder as part of the composition, which is essentially a softer material as opposed to the carbide compounds used. This mixing primarily, with or without refinement, depends on the types of particles involved in the composition and the requirement of the product. Once a composition is prepared through refinement and mixing, the mixed particles are ready to be processed for compaction and sintering, which are two of the most critical steps in the manufacturing chain.

1.1.2. Compaction

Compaction (or compression, briquetting, pressing, consolidation) is the procedure where purposely designed dies are used and pressure is applied on powders to consolidate into desired shaped parts. Conventional compaction is carried out at room temperature as a stand-alone process involving pressing at high pressure. The purpose of this process primarily is to consolidate these loose particles into a shape, often referred to as green sample or green body that can later be used for heating. This stage often increases the

contact areas between particles, imparting the required strength to a compact, disintegrating the agglomerates of particles and sometimes even the particles themselves, and goes through several stages of deformation, rearrangement and fragmentation [8]. Fig. 1 illustrates schematic diagrams showing particle deformation, rearrangement and fragmentation in some parts of the powder during compaction stage.
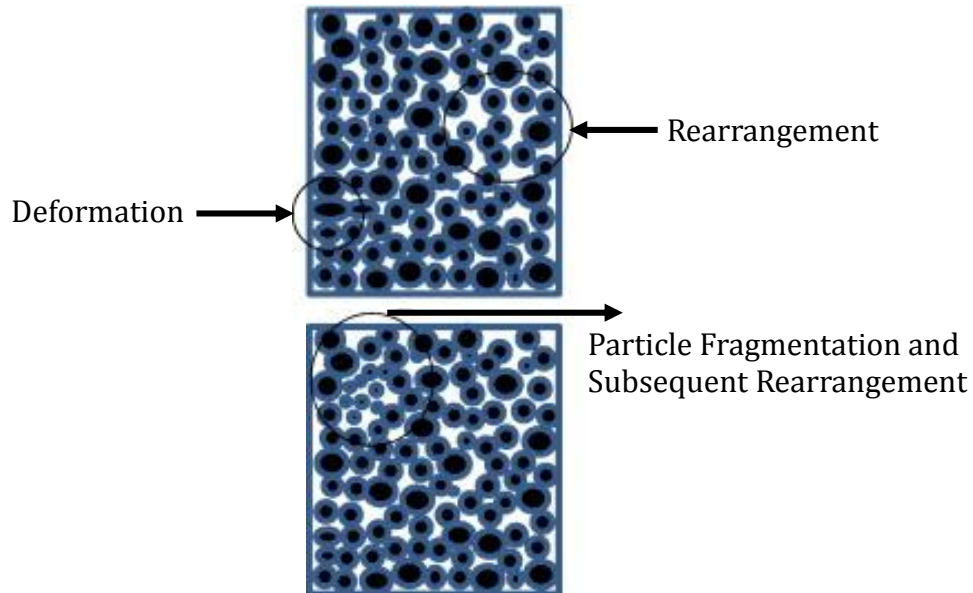

Fig.1: Schematic illustrations of particle deformation, rearrangement and fragmentation in some parts of the powder during compaction [8]

Conventional uniaxial compaction is the dominant mode of powder compaction, although other forms of dynamic compactions have been of great interest in recent times [9-15]. As a result of uniaxial compaction, pressure gradients evolve along the height of the powder bed and can be expressed as [16]:

$$P_x = pe^{(-4uzx/D)} \tag{1}$$

Where P is punch pressure, P_x is the pressure undergone by powders at any position x below the punch, u is the die wall friction coefficient, z is the radial to axial stress ratio, and D is the compact diameter. All parameters here are quite important in the sense that they all contribute to the compaction results. It is often seen that in order to avoid pressure gradient, the final thickness of compacted samples are kept within specific ranges, which

also ensures a homogeneous mechanical behaviour throughout the compacted sample. The applied pressure, as well as the pressure experienced by the particles and die walls also need to be observed and used carefully, especially when dealing with hard materials that are not prone to rapid deformation without substantial amount of softer binder presence. The diameter of the sample, thickness of the die wall and their ratio also factor in, in deciding the pressure threshold for specific compaction arrangements.

During compaction, it is important to make sure that consolidation is even in all directions of the samples. For WC particles, a homogeneous sedimentation in solid or liquid binder, either during compaction or sintering, leads to ensuring enhanced density of WC-Co samples. The way compaction works on hard and brittle particles has been a topic of discussion in a few studies [17-19]. Initially when the process starts, mixed powder with a certain distribution of particle size and shape along with its pore distribution is inserted into a die. In most cases, frictional force is observed among particles, and between particles and the inner wall of the die. In order to reduce the frictional resistance between particles and wall, a high temperature resistant boron nitride or similar spray is often used. Even after that, it may be seen that the exact applied pressure is not translated within the particles due to the difference in nature of frictional forces. Hence it is possible that a pressure gradient is present along the length of the consolidated green sample. During the compaction stage, most particles go through two different phases that can also be observed simultaneously; rearrangement and deformation. While some particles may experience only deformation, others may go through both deformation and rearrangement, either sequentially or simultaneously, depending on the shape and orientation of the particle with respect to the adjacent particles. Irrespective of the nature of particles or amount of pressure applied, it is safe to assume that rearrangement is a dominant mechanism within the compaction stage. Having said that, there is a level of unpredictability in determining what mechanism a particle may go through, and more importantly, when. This effect may cause a difference in density in compacted or even sintered samples. The presence of a liquid phase may eliminate the defects within a sample to an extent, or even generate some pores when infiltrates through the bulk due to capillary effect and therefore can't be considered as a completely effective method in case of pressure less sintering.

There have been a number of compaction techniques employed to perfect the production of green samples [8, 9, 20], although they mostly vary in terms of pressing time and number

of pressing steps involved during the process. It can sometimes involve the particles to go through a preheating stage for ensuring better alignment, but is not enough for them to change their characteristics [21]. Once the powders are compacted into green samples, they are ready to go through the sintering stage.

1.1.3. Sintering

Sintering is a major stage in the manufacture of sintered carbides. This stage usually consists of two overlapping steps, pre-sintering (includes delubrication around 300-400 ℃) and final sintering. The main purpose of pre-sintering is to burn out the lubricant added to the powders prior to further heating (also termed de-waxing), although slight sintering or densification, usually in solid state can be observed, where WC-Co green compacts are subject to a temperature up to 700-750 ℃ [9]. Green density [21], composition [22], particle size and distribution [23, 24], atmosphere [25], sintering temperature [26, 27], pressure [20], time and heating rate [28] are known to heavily influence the state of sintering. The final temperature during sintering is quite influential as it suggests what condition, liquid or solid, the constituent materials will be in and for how long.

If the final sintering temperature is around the melting point of binder metal, a liquid phase is expected to form, which is known as liquid phase sintering (LPS). Much attention has been concentrated on exploring the mechanisms of LPS as it promotes the idea of faster sintering rate [29]. A wetting liquid here exhibits adequate capillary force so that external forces are not required to attain full density. The liquid also reduces the inter-particular friction and dissolves sharp particle edges, thereby aiding rearrangement of the solid particles. Furthermore, the liquid phase provides for faster atomic diffusion [22, 30-32]. A common problem of LPS is shape distortion, which occurs when too much liquid is formed during sintering [33]. It is however possible to achieve liquid phase sintering even at a temperature lower than the melting point of the binder, provided a reasonably high pressure during sintering is applied [34, 35]. This may be possible due to the quick particle heating as opposed to conventional conduction method, which allows for faster diffusion in the process. In contrast, sintering may be carried out where particles are still at solid state, and hasn't formed a liquid phase. If sintering occurs at a temperature where presence of a liquid phase can't be confirmed, it is known as solid phase sintering.

Several types of sintering processes have been involved in the processing of industrially graded cemented carbides, including but not limited to:

1.1.3.1 Conventional Sintering [27, 34, 36, 37]

1.1.3.2 Microwave Sintering [38-40]

1.1.3.3 Spark Plasma Sintering (SPS) [20, 36, 41-52]

1.1.3.4 Pulse Plasma Sintering (PPS) [35, 53-58]

In case of conventional and microwave sintering, pressure is not used as part of the sintering process, and requires the powders to be pre-compacted into green shapes prior to heating. In contrast, processes like SPS and PPS use both temperature and pressure as part of the sintering step, eliminating the necessity of a separate compaction process for mixing of powders. All four types of sintering techniques mentioned above are part of this work, and have been employed on cemented carbides in order to observe their effects on mechanical properties and microstructural behaviour. Chapter five focuses on conventional sintering, while chapter six explains how spark plasma sintering process along with the use of pressure influence mechanical behaviour of carbides. Chapter seven and eight aim to cover the remaining two techniques, microwave and pulse plasma sintering while keeping most of the processing conditions constant, which would enable us to make a four way comparison between all the processes in terms of the mechanical properties tested, and the microstructural features analysed.

1.1.3.1. Conventional Sintering Mechanism

In conventional sintering, the mechanisms that are thought to be responsible for ensuring bonding are quite varied, and often complicated to comprehend. Diffusion is however considered as the main reason behind materials bonding. It suggests that some of the hard WC dissolves into the binder phase which is Co in this study, a rather softer counterpart. This dissolution is achieved through migration and re-precipitation on the surface [59], resulting in the final product, which is a three dimensional WC grain structure where Co acts as a binder matrix. A number of studies [60, 61] have looked into the sintering mechanism of WC-Co considering both fine and coarse grained materials. Although it is perceived that the basic mechanism is roughly the same irrespective of the particle size, smaller mean grain size was observed for test samples that started with finer particles,

resulting in displaying better mechanical properties and microstructural features. It was concluded that fine grained materials are capable of being sintered at relatively lower temperature as opposed to coarse grained materials. In addition to diffusion, other features like plastic deformation or flow, grain growth, recrystallization, liquid or vapour phase material transport can also be considered as potential sintering mechanisms depending on the manufacturing process and the nature of the material. Irrespective of the presence of diffusion, particle bonding during sintering can define the effectiveness of the process that is being considered. Fig. 2 shows two different types of bonding mechanism. It shows that diffusion bonding reduces inter particle space resulting in shrinkage in an attempt to join particles, while material transport fills the inter particle space to achieve bonding.
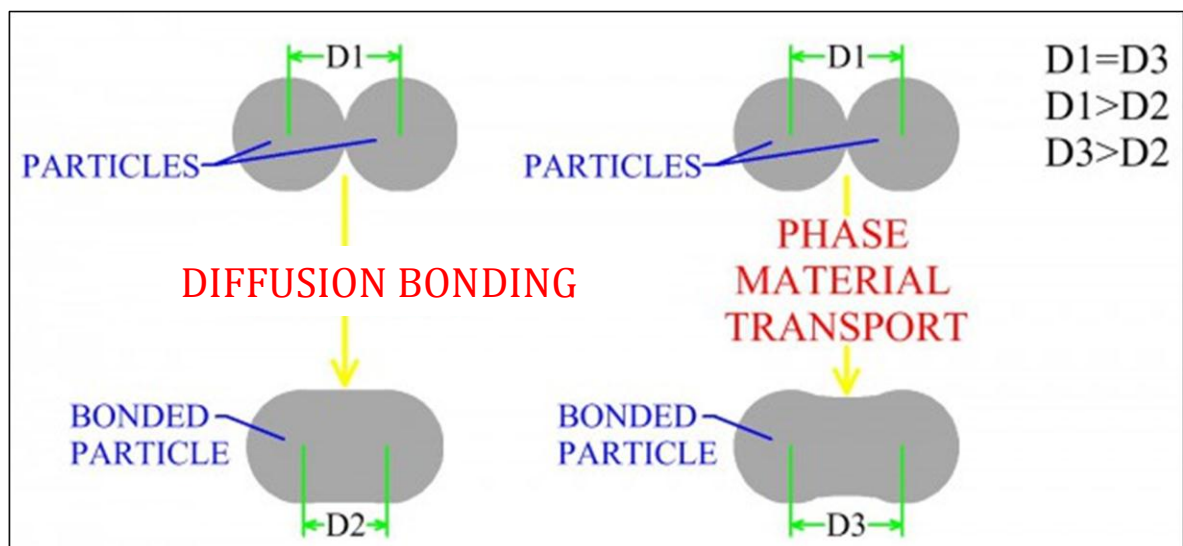

Fig. 2: Bonding mechanisms in sintering [62]

The heating process during conventional sintering occurs as a result of surface heating, which is generated from the heat source which is the heating element, and thermally conducts through the oven and holding chamber, propagating from the outside of the sample to the inside. This process of heating is quite time consuming as it has to ensure that the entire heat energy necessary for sintering of the sample goes through the surface [63]. WC [110 W/(m·K)] and Co [100 W/(m·K)] both are known to be thermally conductive, and to an almost equal degree, which ensures that both particles are contributing towards the conduction of heat during sintering.

A number of studies have tried to explain the sintering mechanism in four distinguishable stages, which were later confirmed by [64]. The stages are briefly mentioned below:

Stage 1: Dispersion of Co within WC grains, which is considered as one of the first indicators of sintering, and can be achieved at temperatures as low as 700 °C, and could go up to more than 1000 °C. This is where particle size plays as a differentiator, since fine grained materials (<0.2 μm) are capable of reaching this state faster (~1100 °C) than coarse grained (>3 μm) materials (~1275 °C)

Stage 2: Coating of Co around WC particles while simultaneously being agglomerates into the matrix. Even for this stage, fine grained WC are thought to perform faster than coarse grained materials.

Stage 3: Formation of an agglomerate network, which can be achieved via coalescence or as a result of Oswald Ripening. During this process, the pores present as part of the microstructure are eliminated by capillary forces provided there is presence of a liquid phase, eventually forcing WC particles towards vertical sedimentation.

Stage 4: WC grain growth through Tungsten and Carbon dissolved into binder, which is Co.

Fig. 3 shows the production process of a conventional sintering facility starting from powder mixing to finish product stage.
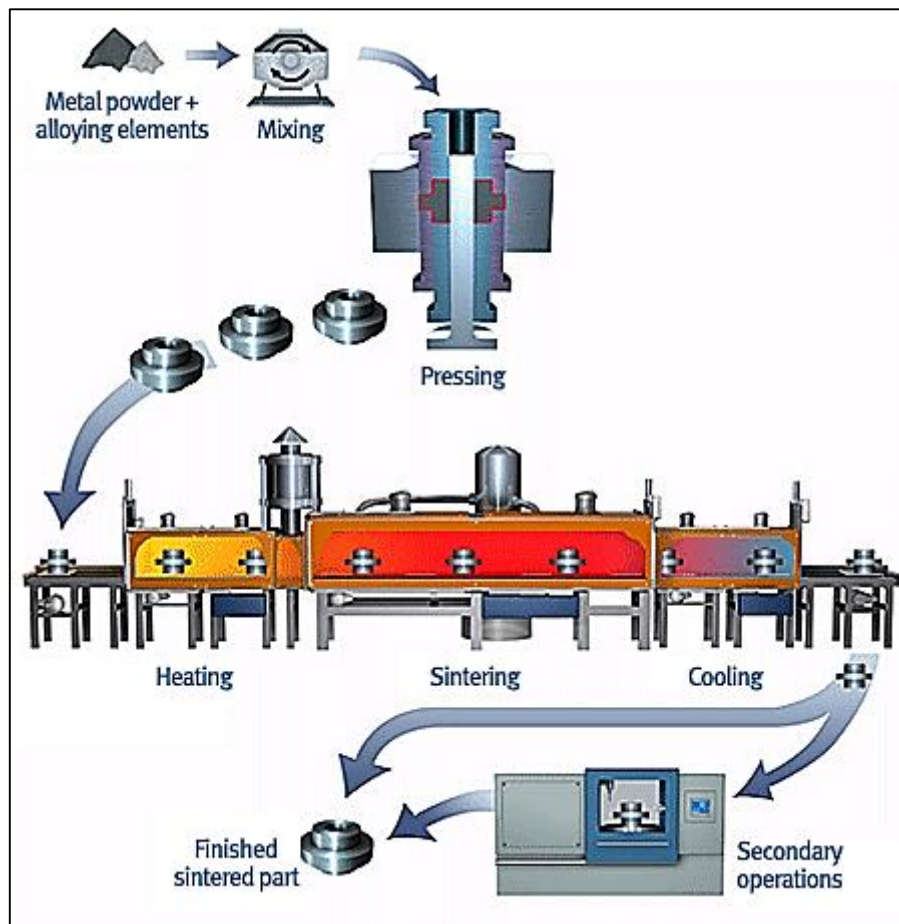
Fig. 3: Production process of a conventional sintering facility [65].

1.1.3.2. Microwave Sintering Mechanism

Microwave sintering is one of the relatively modern sintering techniques that has gained popularity since early 90s. The process itself as well as the mechanism are significantly different from the principles of conventional sintering which is why it has been of great interest [34, 66] in the past few decades.

Unlike the heating source in conventional sintering, and much like the one in a typical microwave oven, the heat source in this form of sintering are the oscillations (Fig. 2) of the free electrons usually generated at a high frequency microwave (~2.45 GHz) into the binder material (Co), the free carbon, and ions in WC [63, 67, 68].
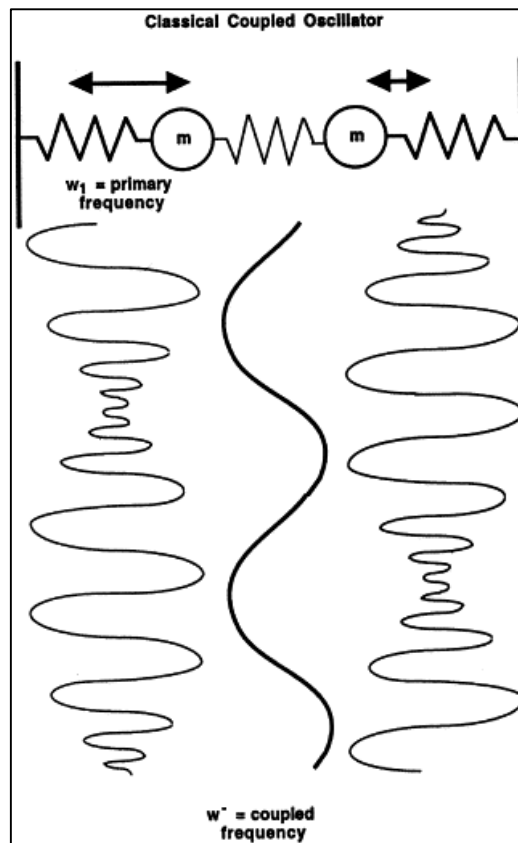
Fig. 4: Schematic diagram of a coupled oscillator of a microwave sintering unit [69]

It needs to be mentioned here that microwaves have the capacity to penetrate dielectric materials but tend to reflect back when a metal particle goes into micrometre range [70]. This reflection also occurs when the particles have a smooth surface, like Co within WC-Co. However, since WC particles are quite brittle in nature and comes with irregular shaped and more importantly sharp corners causing sparks, added to the fact that there may be smaller Co particles present, WC and Co are both thought as contributors towards microwave heating. As a result, the entire volume of the sample can be heated instantly attributing to the interaction of microwave energy with both particles, and throughout the entire length of the sample. This is a major differentiating factor when it comes to the heating time between microwave and conventional sintering. Since this process of microwave heating is quite rapid for WC-Co samples, it doesn't frequently cause thermal gradient along the length of the sample, eliminating the need to heat the samples for several hours [71]. Fig. 5 shows a schematic diagram of a microwave sintering assembly.
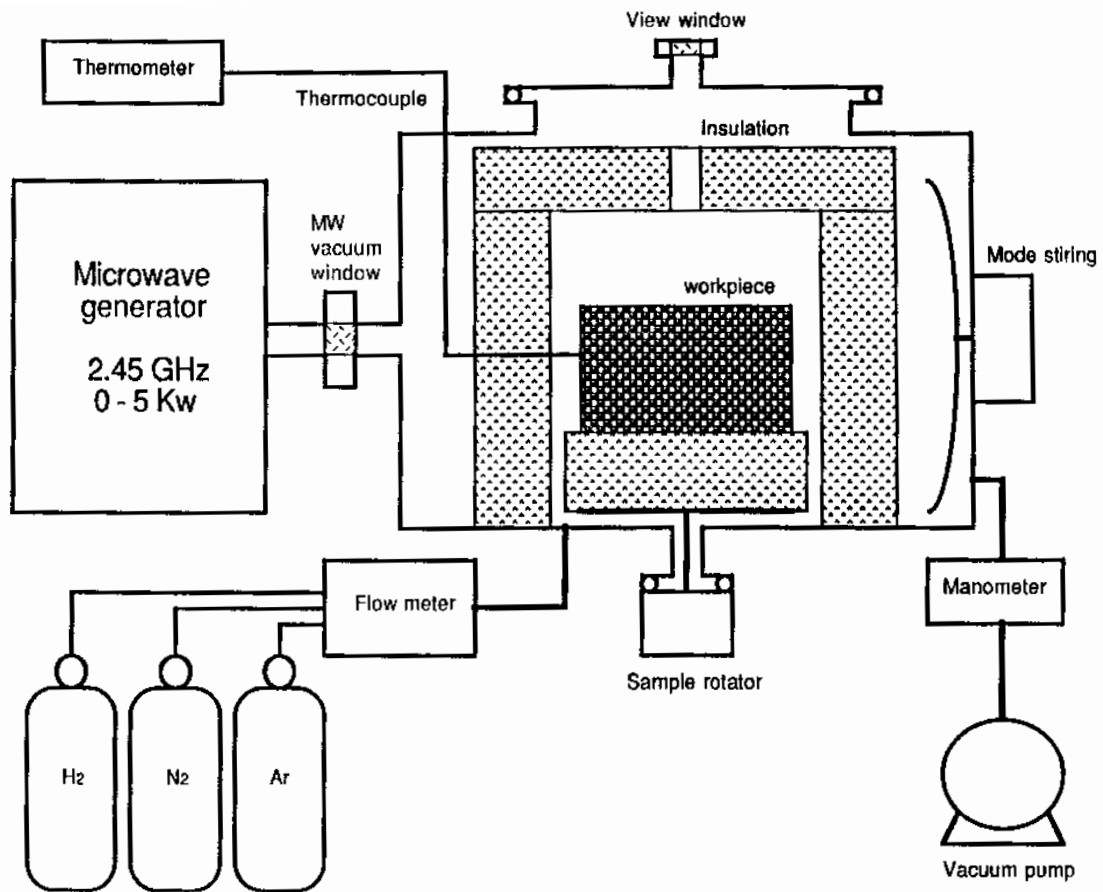
Fig. 5: Schematic diagram of a microwave sintering assembly [72]

1.1.3.3. Spark Plasma Sintering (SPS) Mechanism

The exact mechanism of spark plasma sintering is a topic of debate. The reason why it is a critical question is because of the fact that it is a process that is capable of sintering materials significantly faster than what is expected off a conventional approach. The complexity in understanding the spark plasma mechanism attributes to a combination of electrical, mechanical and thermal factors that are involved during the process [73]. It is thought that the electric pulses, with or without varying frequency and time intervals, are generated and delivered to the electrodes, leading towards the particles irrespective of their positions, instantaneously. As a result, the microscopic electric discharges (Fig. 6) that are present within the gaps of particles and within an electric field tend to generate plasma which escalates sintering [74, 75].
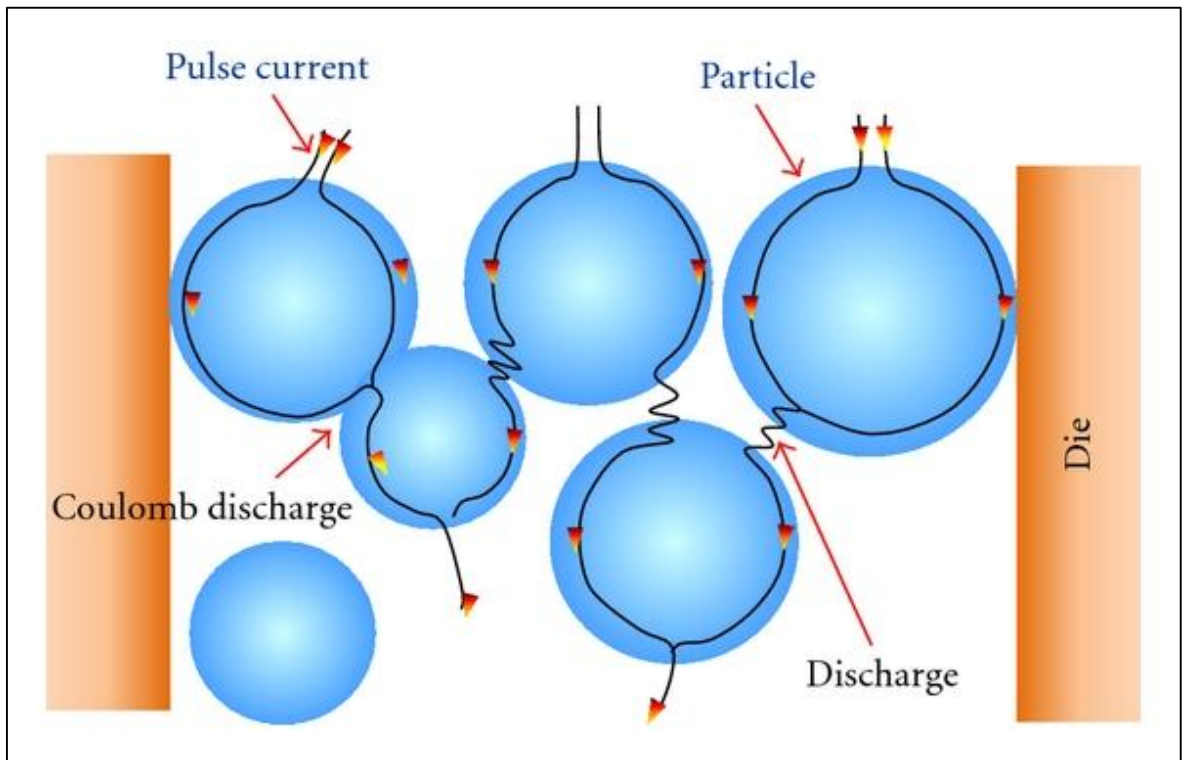
Fig. 6: DC pulse current flow through particles [76]

This generated discharge is thought of as a major contributor towards elimination of most adsorptive gases, impurities and oxide thin films within and around the surface of the particles [77-79], which then effectively leads to enhancing thermal diffusion [80-83]. Joule heating also contributes in densifying particles during the process [84, 85]. All of these combined act as a fast and significantly improved way to enhance diffusion and restrict grain growth, which is otherwise limited in other conventional processes to a certain extent [86-88]. Fig. 7 shows a schematic diagram of the energy dispersion process on a microscopic scale, along with mechanism of partial localised heating.

Fig. 7: Energy dispersion in microscopic scale [89]

1.1.3.4. Pulse Plasma Sintering (PPS) Mechanism:

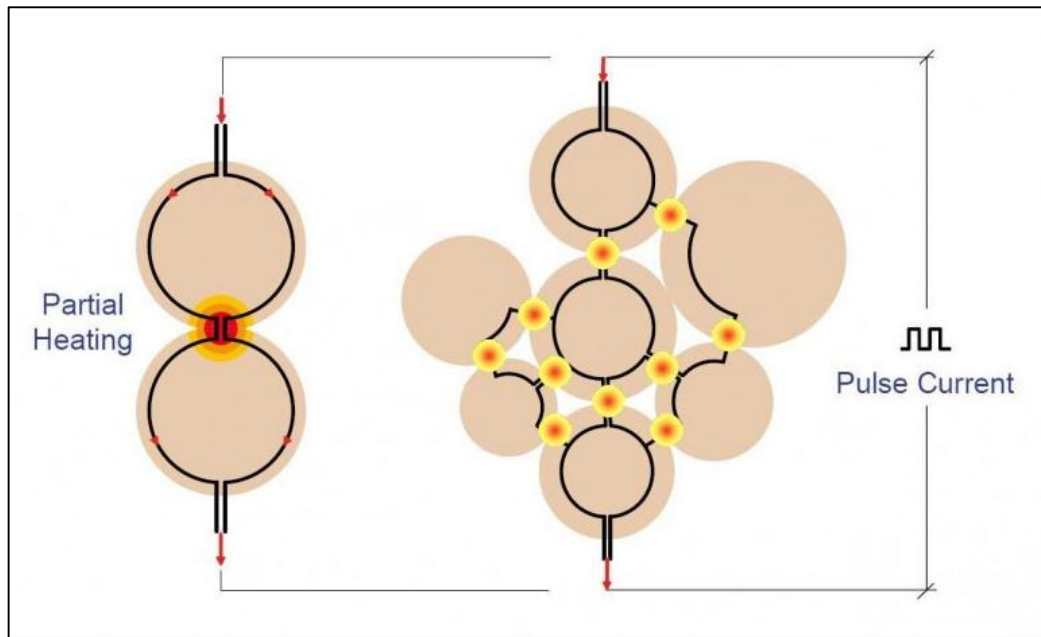The pulse plasma sintering process is unique in terms of efficiency of the heating process involved. In this process the reaction is initiated by periodically generated high current electric pulses that are charged at a maximum of 6kV by the energy source, which is a battery of capacitors. During this process energy is released on to the powder particles for repeated duration of a fraction of a second (frequency 1-20Hz), while they are already under a constant set pressure. This process of heating by very narrow high-current pulses with duration in the order of hundreds of microsecond, along with the applied pressure on the powders help the particles reach the ignition temperature faster in comparison with conventional heating processes. From a physical point of view, compressed particles are heated by Joule heating at contact points with the help of repeated spark discharges occurring between particles and within pores helping faster diffusion [56], along with building momentum of atoms due to the plasma ion-atoms interaction that are active during the sintering process. Fig. 8 shows a schematic diagram of a pulse plasma sintering unit, while Fig. 9 shows the behavior of pulse current and voltage waveforms during a capacitor discharge [54]
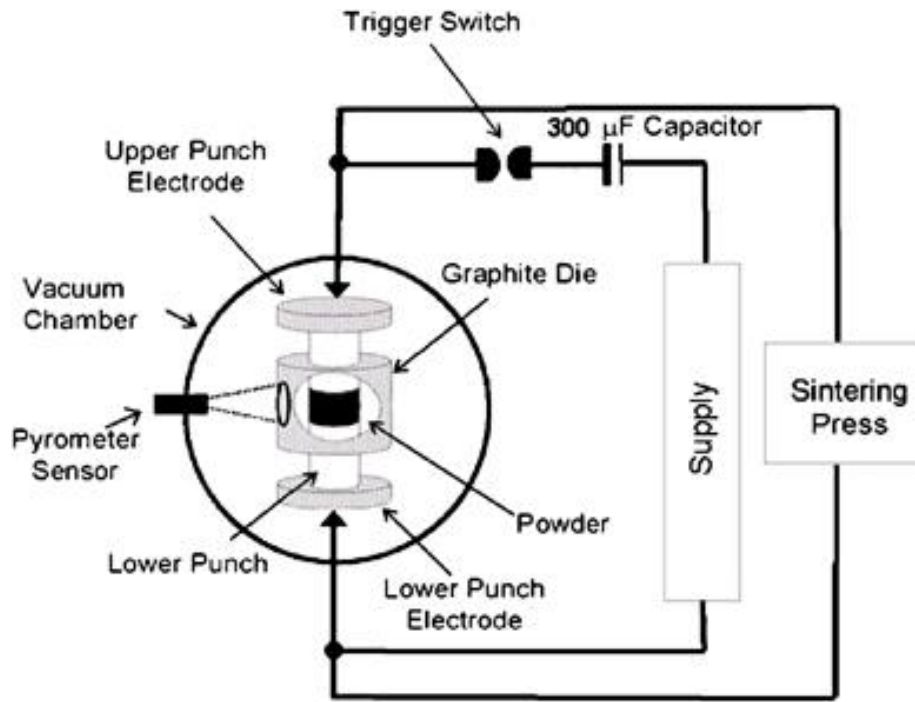
Fig. 8: Schematic diagram of a pulse plasma sintering (PPS) unit [54]
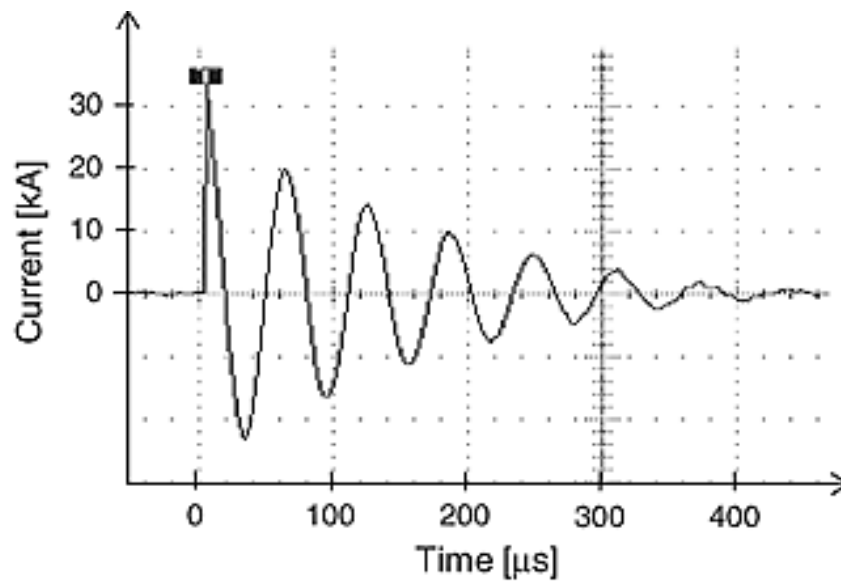

Fig. 9: Behavior of pulse current and voltage waveforms during a capacitor discharge [54]

1.2. Applications of Cemented Carbides

The applications of sintered carbides are in a sense a mirror to show the features of this group of composites [90-92]. Their utilisation covers almost every industry. These applications may be classified into the following five basic categories.

1.2.1. Metal Cutting

Metal cutting tools should be able to withstand high temperatures, severe thermal shocks, fatigue, abrasion, attrition, and adhesive wear, because of the contact between work piece and tool materials during chip removal [93]. Contact stress may reach up to several hundred MPa where temperature can go above 1000°C [94]. Sintered carbides usually have a high modulus of elasticity and exhibit little ability to undergo plastic deformation. Therefore these carbide tips have been widely used as indexable inserts. The majority of carbides consumed in industry are for metal cutting applications. A total of 90-95% of the cutting tool market is covered by steels and sintered carbides, and almost 95% of the available sintered carbides are WC based [95]. Generally, the hardest grades of sintered carbides are selected for light continuous finishing cuts, while the tougher grades are used for roughing and heavy cuts or for intermittent cutting involving vibrational or impact forces [94, 96, 97]

1.2.2. Metal Forming

Both hot and cold metal forming operations are carried out using sintered carbides tools and dies. Cold drawing of rods, wires, and tubes employs sintered carbides dies and mandrels, while in the cold rolling of strips and foils with good surface finish, carbide rolls are advantageous [98, 99]. Hot working tools, including extrusion dies and drop-stamping dies, have been made of sintered carbides, although they suffer from lack of toughness and thermal shock resistance in comparison with nickel-base high-temperature alloys which are dominant materials in this field [100].

1.2.3. Earth Drilling

In mining industry, carbide tools are widely used for picks, rotary drills, percussion drills,

and other tools subjected to severe wear by the minerals involved. It is estimated that almost 90% of all pneumatic drilling of hard rocks is done with carbide insert tips [101]. Carbides insert tips are almost mandatory for drilling rocks harder than limestone, and their use has all but made the conventional hard faced steel teeth obsolete, both on the basis of performance and economics [94]

1.2.4. Wear Protection

Owing to their resistance to abrasive wear, sintered carbides are also effective in applications where abrasive wear is of prime concern. Typical examples using sintered carbides [59, 102, 103] for wear protection include nozzles and valves in plastic processing, guides and cones for wire drawing, brick mold liners, facing for hammers in hammer mills, jaw crushers, ball milling linings, sand blast nozzles and wear pads in machining.

1.2.5. High-Rigidity Structural Components

The high modulus of sintered carbides, which is significantly higher than steel, enables them to be used in applications where high rigidity [104, 105] is of prime importance, like industrial drilling.

1.3. Summary

The objective of this study is to observe the effect of sintering processes and initial particle size on mechanical properties and microstructural characteristics of WC-Co. The thesis is divided into 8 chapters. Chapter one briefly introduces the type of cemented carbides that are being considered in this work and highlights the area of applications for cemented carbides from a broader perspective and focuses on the background of the work and explaining the powder metallurgy (PM) route often chosen for the manufacture of cemented carbides. It also elaborates on several sintering techniques that are essentially a part of the PM process and used in this study. Chapter two includes a published review article discussing powder refinement and consolidation techniques of WC-Co with special focus on progressive research that has been of interest in this area in the past few decades. Chapter three includes another published article that highlights the effect of powder

refinement on mechanical properties of cemented carbides. The intention is to determine the ideal initial processing conditions that would eventually lead to demonstrating better mechanical properties and microstructural characteristics. Chapter four includes a published paper where conventional sintering route has been approached on WC-Co samples, a method that is industrially preferred and has been used for more than a century. Chapter five adds a paper where Spark Plasma Sintering, a modern sintering process has been applied on WC-Co particles in order to observe the differences and effectiveness of the process in terms of industrially recognised properties. Chapter six and seven include two papers that are under review, focusing on Microwave and Pulse Plasma Sintering and how they influence the mechanical and microstructural behaviour of cemented carbides. Finally chapter eight concludes this thesis by summarising the entire work with the help of a comparison between all sintering processes and parameters that were considered influential to these series of cemented carbides. It also provides some insights for further research on cemented carbides.

1.4. References

[1] Upadhyaya GS. Materials science of cemented carbides—an overview. Materials & Design. 2001;22:483-9.

[2] Fang ZZ, Wang X, Ryu T, Hwang KS, Sohn H. Synthesis, sintering, and mechanical properties of nanocrystalline cemented tungsten carbide–a review. International Journal of Refractory Metals and Hard Materials. 2009;27:288-99.

[3] Raihanuzzaman RM, Xie Z, Hong SJ, Ghomashchi R. Powder refinement, consolidation and mechanical properties of cemented carbides—An overview. Powder Technology. 2014;261:1-13.

[4] Fecht H, Hellstern E, Fu Z, Johnson W. Nanocrystalline metals prepared by high-energy ball milling. Metallurgical and Materials Transactions A. 1990;21:2333-7.

[5] Liu S, Huang Z-L, Liu G, Yang G-B. Preparing nano-crystalline rare earth doped WC/Co powder by high energy ball milling. International Journal of Refractory Metals and Hard Materials. 2006;24:461-4.

[6] Song J-W, Hong S-J. Mechanical Properties of WC-Co Alloys with Various Mixing and Milling Conditions using High Energy Ball Miller. Current Nanoscience. 2014;10:62-5.

[7] Zhang F, Wang C, Zhu M. Nanostructured WC/Co composite powder prepared by high energy ball milling. Scripta materialia. 2003;49:1123-8.

[8] Aryanpour G, Farzaneh M. Application of a piston equation to describe die compaction of powders. Powder Technology. 2015;277:120-5.

[9] Hong S-J, Rumman MR, Rhee CK. Effect of Magnetic Pulsed Compaction (MPC) on Sintering Behavior of Materials. In: Lakshmanan DA, editor. Sintering of Ceramics - New Emerging Techniques. Croatia: InTech Publication; 2012. p. 159-76.

[10] Kim JH, Md Raihanuzzaman R, Rhee CK, Lee JG, Lee MK, Hong S-J. Fabrication and Densification Behavior Analysis of Metalizing Targets Using ZrO2 Nanopowders by Magnetic Pulsed Compaction. Materials Transactions-JIM. 2011;52:1156.

[11] Lee JG, Lee M, Hong S, Lee H, Pyun S, Rhee C. Consolidation of mixed diamond and cobalt granule powders by magnetic pulsed compaction. Materials Letters. 2010;64:35-7.

[12] Lee JG, Lim C, Kim H, Hong S, Kim M, Kang B, et al. Highly dense steel components prepared by magnetic pulsed compaction of iron-based powders. Powder Technology. 2012;228:254–7.

[13] Park H-Y, Kilicaslan MF, Hong S-J. Effect of multiple pressures by Magnetic Pulsed Compaction (MPC) on the density of gas-atomized Al-20Si powder. Powder Technology. 2012;224:360-4.

[14] Raihanuzzaman RM, Kim JH, Lee JK, Yoon JS, Son H-T, Hong S-J. Wear Behavior of Al-Fe-Cr-Ti Alloys fabricated by Magnetic Pulsed Compaction. Powder Technology. 2012;225:227–31.

[15] Raihanuzzaman RM, Song J-W, Hong S-J. Evaluation of Mechanical Properties and Processing Conditions of WC-Co alloys Fabricated by Magnetic Pulsed Compaction. Journal of alloys and Compounds. 2011.

[16] German RM. Powder metallurgy science: Metal Powder Industries Federation, Princeton, N. J. 08540,; 1984.

[17] Chandler H, Sands C, Song J, Withers P, McDonald S. A plasticity model for powder compaction processes incorporating particle deformation and rearrangement. International Journal of Solids and Structures. 2008;45:2056-76.

[18] Martin C, Bouvard D, Shima S. Study of particle rearrangement during powder compaction by the discrete element method. Journal of the Mechanics and Physics of Solids. 2003;51:667-93.

[19] Lamy P, Brunet L, Thomas G. Modeling the porosity evolution of a powder under uniaxial compression. Propellants, Explosives, Pyrotechnics. 2005;30:397-403.

[20] Rumman MR, Xie Z, Hong S-J, Ghomashchi R. Effect of spark plasma sintering pressure on mechanical properties of WC–7.5 wt% Nano Co. Materials & Design. 2015;68:221-7.

[21] Song J-W, Raihanuzzaman RM, Hong S-J. Consolidation of WC–Co alloys by magnetic pulsed compaction and evaluation of their mechanical properties. Powder Technology. 2013;235:723-7.

[22] Raihanuzzaman RM, Song J-W, Hong S-J. Evaluation of mechanical properties and processing conditions of WCCo alloys fabricated by magnetic pulsed compaction. Journal of alloys and Compounds. 2012;536:S211-S5.

[23] Zhao S, Song X, Wei C, Zhang L, Liu X, Zhang J. Effects of WC particle size on densification and properties of spark plasma sintered WC–Co cermet. International Journal of Refractory Metals and Hard Materials. 2009;27:1014-8.

[24] Gurland J. A study of the effect of carbon content on the structure and properties of sintered WC-Co alloys. Transactions AIME. 1954;200:285-90.

[25] Simchi A, Pohl H. Effects of laser sintering processing parameters on the microstructure and densification of iron powder. Materials Science and Engineering: A. 2003;359:119-28.

[26] Morton C, Wills D, Stjernberg K. The temperature ranges for maximum effectiveness of grain growth inhibitors in WC–Co alloys. International Journal of Refractory Metals and Hard Materials. 2005;23:287-93.

[27] Raihanuzzaman RM, Han S-T, Ghomashchi R, Kim H-S, Hong S-J. Conventional sintering of WC with nano-sized Co binder: Characterization and mechanical behavior. International Journal of Refractory Metals and Hard Materials. 2015.

[28] Stanciu L, Kodash V, Groza J. Effects of heating rate on densification and grain growth during field-assisted sintering of α-Al2O3 and MoSi2 powders. Metallurgical and Materials Transactions A. 2001;32:2633-8.

[29] Tandon R, Johnson J. Liquid-phase sintering. ASM Handbook. 1998;7:565-73.

[30] Schreiner M, Schmitt T, Lassner E, Lux B. On the Origins of Discontinuous Grain Growth During Liquid Phase Sintering of WC--Co Cemented Carbides. Powder Metall Int. 1984;16:180-3.

[31] Eso O, Fang ZZ, Griffo A. Kinetics of cobalt gradient formation during the liquid phase sintering of functionally graded WC–Co. International Journal of Refractory Metals and Hard Materials. 2007;25:286-92.

[32] Kim S, Han S-H, Park J-K, Kim H-E. Variation of WC grain shape with carbon content in the WC–Co alloys during liquid-phase sintering. Scripta materialia. 2003;48:635-9.

[33] Campbell LG, German RM. Gravitational Effects on Microstructures in Liquid-Phase Sintering. Advances in powder metallurgy and particulate materials. 2007;2:8.

[34] Breval E, Cheng J, Agrawal D, Gigl P, Dennis M, Roy R, et al. Comparison between microwave and conventional sintering of WC/Co composites. Materials Science and Engineering: A. 2005;391:285-95.

[35] Michalski A, Rosinski M. Pulse Plasma Sintering and Applications. Advances in Sintering Science and Technology: Ceramic Transactions. 2010;87:219.

[36] Demirskyi D, Borodianska H, Agrawal D, Ragulya A, Sakka Y, Vasylkiv O. Peculiarities of the neck growth process during initial stage of spark-plasma, microwave and conventional sintering of WC spheres. Journal of Alloys and Compounds. 2012;523:1-10.

[37] Oghbaei M, Mirzaee O. Microwave versus conventional sintering: A review of fundamentals, advantages and applications. Journal of Alloys and Compounds. 2010;494:175-89.

[38] Agrawal D. Microwave sintering, brazing and melting of metallic materials. Sohn International Symposium; Advanced Processing of Metals and Materials Volume 4: New, Improved and Existing Technologies: Non-Ferrous Materials Extraction and Processing2006. p. 183-92.

[39] Katz JD. Microwave sintering of ceramics. Annual Review of Materials Science. 1992;22:153-70.

[40] Raihanuzzaman RM, Chuan LC, Xie Z, Ghomashchi R. Microwave Sintering and Its Application on Cemented Carbides.

[41] Cha SI, Hong SH, Kim BK. Spark plasma sintering behavior of nanocrystalline WC–10Co cemented carbide powders. Materials Science and Engineering: A. 2003;351:31-8.

[42] Hungría T, Galy J, Castro A. Spark Plasma Sintering as a Useful Technique to the Nanostructuration of Piezo-Ferroelectric Materials. Advanced Engineering Materials. 2009;11:615-31.

[43] Jia C-C, Tang H, Mei X-Z, Yin F-Z, Qu X-H. Spark plasma sintering on nanometer scale WC–Co powder. Materials Letters. 2005;59:2566-9.

[44] LIU X-q, LIN T, GUO Z-m, CUI F-e, Luo J. Consolidation of ultrafine binderless cemented carbide by spark plasma sintering. Journal of Iron and Steel Research, International. 2007;14:82-4.

[45] Maizza G, Grasso S, Sakka Y, Noda T, Ohashi O. Relation between microstructure, properties and spark plasma sintering (SPS) parameters of pure ultrafine WC powder. Science and Technology of Advanced Materials. 2007;8:644-54.

[46] Sivaprahasam D, Chandrasekar S, Sundaresan R. Microstructure and mechanical properties of nanocrystalline WC–12Co consolidated by spark plasma sintering. International Journal of Refractory Metals and Hard Materials. 2007;25:144-52.

[47] Sun L, Jia C, Cao R, Lin C. Effects of Cr 3 C 2 additions on the densification, grain growth and properties of ultrafine WC–11Co composites by spark plasma sintering. International Journal of Refractory Metals and Hard Materials. 2008;26:357-61.

[48] SUN L, JIA C-c, LIN C-g, CAO R-j. VC addition prepared ultrafine WC-11Co composites by spark plasma sintering. Journal of Iron and Steel Research, International. 2007;14:85-9.

[49] Wang X, Xie Y, Guo H, Van der Biest O, Vleugels J. Sintering of WC-Co powder with nanocrystalline WC by spark plasma sintering. Rare Metals. 2006;25:246-52.

[50] Yaman B, Mandal H. Spark plasma sintering of Co–WC cubic boron nitride composites. Materials Letters. 2009;63:1041-3.

[51] Yingfang X, Xingqing W, Lidong C, Xiaodong L, Hailiang G. Preparation of superfine-cemented carbide by spark plasma sintering. Journal of Wuhan University of Technology--Materials Science Edition. 2006;21:42-5.

[52] Zhao H, Zhu L, Huang Q. Nanocrystalline WC-10% Co-0.8% VC cemented carbides prepared by spark plasma sintering. Rare Met Mat Eng. 2005;34:82-5.

[53] Ciupiński Ł, Siemiaszko D, Rosiński M, Michalski A, Kurzydłowski KJ. Heat sink materials processing by pulse plasma sintering. Advanced Materials Research: Trans Tech Publ; 2009. p. 120-4.

[54] Michalski A, Rosiński M. Sintering diamond/cemented carbides by the pulse plasma sintering method. Journal of the American Ceramic Society. 2008;91:3560-5.

[55] Michalski A, Rosiński M, Siemiaszko D, Jaroszewicz J, Kurzydłowski KJ. Pulse plasma sintering of nano-crystalline Cu powder. Solid State Phenomena: Trans Tech Publ; 2006. p. 239-44.

[56] Rosinski M, Fortuna E, Michalski A, Pakiela Z, Kurzydlowski K. W/Cu composites produced by pulse plasma sintering technique (PPS). Fusion Engineering and Design. 2007;82:2621-6.

[57] Rosinski M, Michalski A. WCCo/cBN composites produced by pulse plasma sintering method. Journal of Materials Science. 2012;47:7064-71.

[58] Rosinski MS, Fortuna E. W/Cu composites produced by low temperature Pulse Plasma Sintering (PPS).

[59] Schwarzkopf P, Kieffer R. Cemented carbides: Macmillan; 1960.

[60] Da Silva A, Schubert W, Lux B. The role of the binder phase in the WC-Co sintering. Materials Research. 2001;4:59-62.

[61] Cha SI, Hong SH, Ha GH, Kim BK. Microstructure and mechanical properties of nanocrystalline WC-10Co cemented carbides. Scripta materialia. 2001;44:1535-40.

[62] Pressing and Sintering, http://thelibraryofmanufacturing.com/pressing_sintering.html).

[63] Meredith RJ. Engineers' handbook of industrial microwave heating: Iet; 1998.

[64] Gillia O, Bouvard D. Phenomenological analysis of densification kinetics during sintering: application to WC–Co mixture. Materials Science and Engineering: A. 2000;279:185-91.

[65] Sintered Soft Magnetic Products, http://www.gkn.com/sintermetals/capabilities/soft-magnetic-pm/process/Pages/Sintered-Soft-Magnetic-products.aspx).

[66] Cheng J, Agrawal D, Komarneni S, Mathis M, Roy R. Microwave processing of WC-Co composites and ferroic titanates. Material Research Innovations. 1997;1:44-52.

[67] Calinescu J, Martin D. Microwaves involvement in materials synthesis and processing. Symposium Avantajele strategice ale tehnologiei informationale si transferui de tehnologie in economia romaneasca, Chiminform Data SA Bucuresti2000. p. 17.

[68] Meredith B, Milner D. Densification Mechanisms in the Tungsten Carbide—Cobalt System. Powder Metallurgy. 1976;19:38-45.

[69] Clark DE, Folz DC, West JK. Processing materials with microwave energy. Materials Science and Engineering: A. 2000;287:153-8.

[70] Agrawal DK. Microwave processing of ceramics. Current Opinion in Solid State and Materials Science. 1998;3:480-5.

[71] Cheng J, Roy R, Agrawal D. Radically different effects on materials by separated microwave electric and magnetic fields. Material Research Innovations. 2002;5:170-7.

[72] Agrawal D, Cheng J, Lackner A, Fersti W. Microwave sintering of commercial WC/Co based hard metal tools. European Conference on Advances in Hard Materials Production as held at the EURO PM 99 Conference1999. p. 175-82.

[73] Chaim R. Densification mechanisms in spark plasma sintering of nanocrystalline ceramics. Materials Science and Engineering: A. 2007;443:25-32.

[74] Perera D, Tokita M, Moricca S. Comparative study of fabrication of Si 3 N 4/SiC composites by spark plasma sintering and hot isostatic pressing. Journal of the European Ceramic Society. 1998;18:401-4.

[75] Song S-X, Wang Z, Shi G-P. Heating mechanism of spark plasma sintering. Ceramics International. 2013;39:1393-6.

[76]Spark Plasma Sintering of Metal Matrix Composite, http://www.hindawi.com/journals/jnm/2012/983470/fig3/.

[77] Orru R, Licheri R, Locci AM, Cincotti A, Cao G. Consolidation/synthesis of materials by electric current activated/assisted sintering. Materials Science and Engineering: R: Reports. 2009;63:127-287.

[78] Nowak S, Perrière L, Dembinski L, Tusseau-Nenez S, Champion Y. Approach of the spark plasma sintering mechanism in Zr 57 Cu 20 Al 10 Ni 8 Ti 5 metallic glass. Journal of Alloys and Compounds. 2011;509:1011-9.

[79] Tang Y, Xue J-X, Zhang G-J, Wang X-G, Xu C-M. Microstructural differences and formation mechanisms of spark plasma sintered ceramics with or without boron nitride wrapping. Scripta Materialia. 2014;75:98-101.

[80] Kasperski A, Weibel A, Estournes C, Laurent C, Peigney A. Preparation-microstructure-property relationships in double-walled carbon nanotubes/alumina composites. Carbon. 2013;53:62-72.

[81] Dutel G-D, Langlois P, Tingaud D, Dirras G. Room-temperature deformation micro-mechanisms of polycrystalline nickel processed by spark plasma sintering. Materials Characterization. 2013;79:76-83.

[82] Li X, Yan M, Imai H, Kondoh K, Schaffer G, Qian M. The critical role of heating rate in enabling the removal of surface oxide films during spark plasma sintering of Al-based bulk metallic glass powder. Journal of Non-Crystalline Solids. 2013;375:95-8.

[83] Zhang Z-H, Liu Z-F, Lu J-F, Shen X-B, Wang F-C, Wang Y-D. The sintering mechanism in spark plasma sintering–proof of the occurrence of spark discharge. Scripta Materialia. 2014;81:56-9.

[84] Zhang F, Mihoc C, Ahmed F, Lathe C, Burkel E. Thermal stability of carbon nanotubes, fullerene and graphite under spark plasma sintering. Chemical physics letters. 2011;510:109-14.

[85] Jabbar H, Monchoux J-P, Thomas M, Couret A. Microstructures and deformation mechanisms of a G4 TiAl alloy produced by spark plasma sintering. Acta Materialia. 2011;59:7574-85.

[86] Hungría T, Amorín H, Algueró M, Castro A. Nanostructured ceramics of BiScO 3–PbTiO 3 with tailored grain size by spark plasma sintering. Scripta Materialia. 2011;64:97-100.

[87] Olevsky E, Bogachev I, Maximenko A. Spark-plasma sintering efficiency control by inter-particle contact area growth: a viewpoint. Scripta Materialia. 2013;69:112-6.

[88] Li X, Jiang D, Zhang J, Lin Q, Chen Z, Huang Z. Densification behavior and related phenomena of spark plasma sintered boron carbide. Ceramics international. 2014;40:4359-66.

[89]Spark Plasma Sintering Technology, http://www.fct-systeme.de/en/content/Spark Plasma Sinter Technologie/~nm.19~nc.40/SPS Technology.html#x).

[90] Exner H. Physical and chemical nature of cemented carbides. International Materials Reviews. 1979;24:149-73.

[91] Gurland J. New scientific approaches to development of tool materials. International Materials Reviews. 1988;33:151-66.

[92] Roebuck B, Almond E. Deformation and fracture processes and the physical metallurgy of WC–Co hardmetals. International Materials Reviews. 1988;33:90-112.

[93] Jack D. Ceramic cutting tool materials. Materials & Design. 1986;7:267-73.

[94] Fischer UK, Hartzell ET, Akerman JG. Cemented carbide body used preferably for rock drilling and mineral cutting. Google Patents; 1988.

[95] Yao Z, Stiglich JJ, Sudarshan T. Nano-grained tungsten carbide-cobalt (WC/Co). Mater Modif. 1999:1-27.

[96] Lundell L-G. Drill bit with cemented carbide inserts. Google Patents; 1990.

[97] Stiffler SP. Cemented carbide tip. Google Patents; 1992.

[98] Forming rolls. Google Patents; 1971.

[99] Dearnaley G, Hartley NE. Metal-forming dies. Google Patents; 1978.

[100] Oblak J, Paulonis D, Duvall D. Coherency strengthening in Ni base alloys hardened by DO22 γ' precipitates. Metallurgical Transactions. 1974;5:143-53.

[101] Kumar A, Pelty LP. High-strength tungsten carbide material for use in earth-boring bits. Google Patents; 1994.

[102] Fischer U, Waldenstrom M, Hartzell T. Cemented carbide body with increased wear resistance. Google Patents; 1999.

[103] Beste U, Jacobson S. A new view of the deterioration and wear of WC/Co cemented carbide rock drill buttons. Wear. 2008;264:1129-41.

[104] Hara A, Yazu S. Tungsten carbide, hot pressing. Google Patents; 1980.

[105] Hosoi R. Drill having cutting edges with the greatest curvature at the central portion thereof. Google Patents; 1980.

Powder Refinement, Consolidation and Mechanical Properties of Cemented Carbides — An Overview

Rumman Md Raihanuzzaman[a], Zonghan Xie[a], Soon Jik Hong[b], Reza Ghomashchi[a*]

[a]School of Mechanical Engineering, The University of Adelaide,
South Australia 5005, Australia
[b]Division of Advanced Materials Science, Kongju National University,
331-717, South Korea

Statement of Authorship

Title of Paper	Powder Refinement, Consolidation and Mechanical Properties of Cemented Carbides — An Overview
Publication Status	☑ Published ☐ Accepted for Publication ☐ Submitted for Publication ☐ Unpublished and Unsubmitted work written in manuscript style
Publication Details	Raihanuzzaman RM, Xie Z, Hong SJ, Ghomashchi R. Powder Refinement, Consolidation and Mechanical Properties of Cemented Carbides—An Overview. Powder Technology. 2014;261:1-13.

Principal Author

Name of Principal Author (Candidate)	Md Raihanuzzaman Rumman		
Contribution to the Paper	I was responsible for the literature review required for this work, and conducting the preliminary tests to support the processes described in the paper. I performed all the tests, wrote the first draft of the manuscript and incorporated and addressed all comments and suggestions by other authors in subsequent revisions of the manuscript. Interpretation of data was primarily my responsibility.		
Overall percentage (%)	90%		
Certification:	This paper reports on original research I conducted during the period of my Higher Degree by Research candidature and is not subject to any obligations or contractual agreements with a third party that would constrain its inclusion in this thesis. I am the primary author of this paper.		
Signature		Date	22/12/15

Co-Author Contributions

By signing the Statement of Authorship, each author certifies that:
i.   the candidate's stated contribution to the publication is accurate (as detailed above);
ii. permission is granted for the candidate in include the publication in the thesis; and
iii. the sum of all co-author contributions is equal to 100% less the candidate's stated contribution.

Name of Co-Author	Reza Ghomashchi		
Contribution to the Paper	I was principal supervisor for the work, contributed to addressing the outline and refining the manuscript.		
Signature		Date	23/12/2015

Name of Co-Author	Zonghan Xie		
Contribution to the Paper	I jointly supervised this work, and contributed to refining the manuscript.		
Signature		Date	15/01/2016

Name of Co-Author	Soon Jik Hong		
Contribution to the Paper	I jointly contributed to refining the manuscript.		
Signature		Date	10/02/2016

Review

Powder refinement, consolidation and mechanical properties of cemented carbides — An overview

Rumman Md Raihanuzzaman [a], Zonghan Xie [a], Soon Jik Hong [b], Reza Ghomashchi [a,*]

[a] School of Mechanical Engineering, University of Adelaide, South Australia 5005, Australia
[b] Division of Advanced Materials Science, Kongju National University, 331-717, South Korea

ARTICLE INFO

ABSTRACT

Cemented carbides, owing to their excellent mechanical properties, have been of immense interest in the field of hard materials for the past few decades. Although a number of processing techniques have been developed to obtain nanostructured cemented carbide powders with grain size of less than 100 nm, they are expensive, as such, the challenge remains for producing nano-sized powders economically. The lack of understanding and control of grain growth and its effect on deformation and fracture of the resulting carbide materials is another area that requires proper attention. In addition, the effect of binder materials and their content on the mechanical properties of cemented carbides is not clearly understood yet. This review aims to address some of the key issues and challenges faced in the research and development of cemented carbides, especially on powder refinement and consolidation, and their effect on mechanical properties.

© 2014 Elsevier B.V. All rights reserved.

Contents

1. Introduction

The first synthesis of cemented tungsten carbides, also known as cemented carbides, dates back to a century ago [1]. They have been the subject of intensive research and industrial applications for the past few decades, especially for metal cutting, forming and earth drilling industries [2–6]. Cemented carbides have very high melting temperatures; consequently, it is quite impractical to fabricate carbide parts by casting route. Historically, powder metallurgy (P/M) was used to manufacture this class of materials, and so far has been the predominant processing technique. The properties of cemented carbides prepared by this technique are quite high and unparalleled, as compared to those fabricated by other methods [7–9].

It is worth noting that most studies on cemented carbides used coarse (3.5–5 μm) to ultrafine powders (0.2–0.5 μm) [9]. Recent developments in the field of nanostructured materials [10] suggest that the formation of nanocrystalline grain structure has the potential to significantly improve the mechanical properties of cemented carbides. However, the mechanisms that govern the deformation of nanocrystalline carbides have not been well explored and understood yet. On the other hand, the possibilities of improving the properties of tungsten carbide based materials through nanostructural engineering have triggered considerable interest in manufacturing fine, nanoscale powders. Processes used to synthesize nanosized tungsten carbide powders include, but not limited to, ball milling, spray conversion and chemical vapor phase reaction [11–13]. In addition, various consolidation methods have been utilized and modified in an attempt to control grain growth during sintering stage and to produce bulk nanocrystalline materials [14,15], which is an active research area considered to be critical in the studies of cemented carbides. To optimize mechanical,

---

* Corresponding author. Tel.: +61 8 8313 3360.
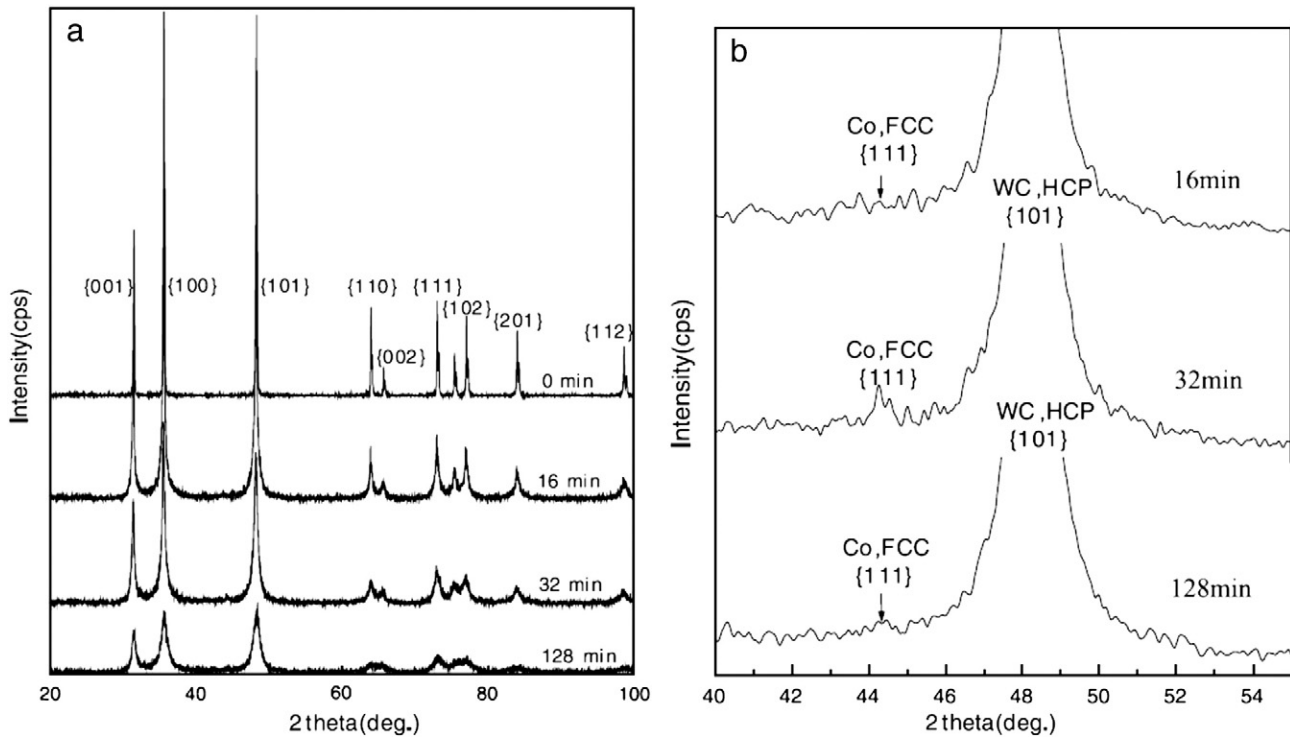E-mail address: reza.ghomashchi@adelaide.edu.au (R. Ghomashchi).

Fig. 1. X-ray diffraction patterns of WC–10Co–0.8VC–0.2Cr$_3$C$_2$ powders after milling for different times: (a) full spectrum; (b) partial enlarged spectrum [20].

physical and chemical properties, focus has been placed on selecting appropriate binder materials, ranging from soft and ductile metals to their alloys [16]. While many studies indicate high hardness can result from powder refinement and/or grain growth control [17,18], the literature is still insufficient in clarifying whether or not nanosized particles have any effect on the fracture toughness of the materials.

This paper presents an overview of recent developments of nanostructured cemented carbides, with a focus on some non-conventional processing approaches having the potential to be commercialized. To do so, first, we will look into various methods used for powder refinement and synthesis to establish general requirements for such process. Second, techniques used for consolidation of cemented carbides will be discussed, in which some of the promising methods will be highlighted. Finally, the overview will take a close look at the microstructure and mechanical properties of cemented carbides and some key challenges.

2. Powder refinement and synthesis

Fine grain size has proven to be quite effective in improving the mechanical properties of cemented carbides. This is one of the main reasons why numerous studies in the past two decades have focused on synthesis of nanocrystalline powders, involving various processing methods. Here it is important to emphasize that particle size and grain size are quite different in nature, although they can be correlated depending on the process parameters employed during the consolidation stage. Before consolidation of powders, be it at room or elevated temperature, we are necessarily focusing on particle size of powders. These particles may consist of one single grain or multiple grains, which can only be differentiated through further microstructural analysis. By powder refinement, it is referred to the process or mechanism by which particle size is reduced, through breaking of either particles or
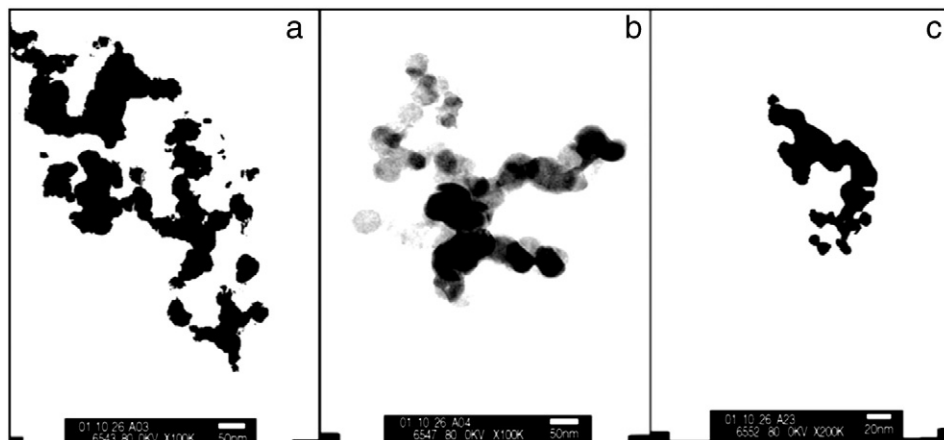

Fig. 2. TEM images of nanocrystalline WC–Co powder mixture milled for (a) 16 min, (b) 32 min and (c) 128 min [20].
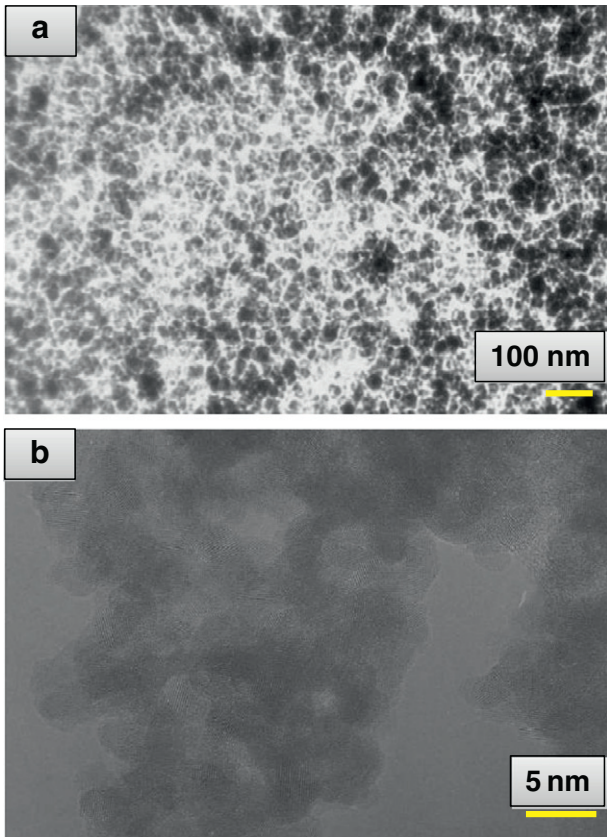
Fig. 3. (a) Low magnification bright field image (BFI) for mechanically solid-state reacted WC powders after ball milling of 256 ks (nearly 71 h), and (b) high resolution TEM image of WC powders after 436 ks (nearly 121 h) of milling [23].

grains. When grain size is considered, it usually refers to the grains that are formed after consolidation and sintering of the powder particles, i.e. within the microstructural context. In this review, there are mentions of grains in sintered WC–Co samples fabricated by a consolidation process carried out at high temperature and pressure, allowing the initial particles to change in shape and size and transform into single and/or multiple grains. In usual cases, fine grained samples resulting from the prevention of grain growth to a certain extent in response to consolidation allows them to display improved mechanical properties. But since particles in their nano forms have excellent properties, nanorefinement has been a topic of interest in most materials, including cemented carbides. In addition, it is useful to mention that the methods employed for measurement of particle size and grain size are totally different. The most widely used technique for powder sizing is laser diffraction

based particle size analysis which relies on a basic principle that particles passing through a laser beam will scatter light at an angle that is directly related to their size. The more traditional method is of course the screening technique using a range of sieves. The grain size however is measured completely differently.

Grain size measurement is quite critical in understanding the microstructure and having an idea about some mechanical properties, like hardness and toughness. Although a number of approaches [61] have been used to measure grain size, there are basically three methods as specified in ASTM E112-13 standard;

1. Comparing the grain structure to a series of graded images,
2. Planimetric method which involves an actual count of the number of grains within a known area,
3. Intercept method which involves an actual count of the number of grains intercepted by a superimposed test line on the microstructure or the number of grain boundary intersections with a test line, per unit length of test line.

Mechanical alloying [19] is considered to be the predominant means for synthesis of nano-sized powders. A few of these studies that focused on producing nanosized WC powders through various processing routes are discussed below:

To prepare fine powders for making nanocrystalline WC–10Co composite, Sun et al. [20] employed a unique high energy ball milling process that involved four different rotational speeds for nearly half an hour, producing 25 nm particle sized WC–Co composite powders from an initial 300 nm WC–Co particle size. The milling was carried out using WC–Co vial and balls under argon atmosphere, with presence of a small percentage of VC and Cr_3C_2, which are known to be grain growth inhibitors for cemented carbides. Figs. 1 and 2 show the X-ray diffraction (XRD) traces and transmission electron microscopy (TEM) images of WC–Co particles with respect to milling time. Although the XRD traces indicate peak broadening and a decrease in intensity that represents powder refinement, it was difficult to properly identify VC, Cr_3C_2 and even Co phase due to the small fractions of these phases. The TEM analysis indicates that the particle shape is predominantly spherical, while the size is quite non-uniform.

In another study, Xueming et al. [21] took a different approach, starting with elemental W, C and Co powders (WC–6Co), which were mixed and then milled for nearly 100 h in a stainless steel vial, with a ball (WC) to powder weight ratio of 30:1. A complete transformation to nano size tungsten carbide occurred, with diffusion of Co along the grain boundaries of WC. This study suggested that nano sized WC–Co can be successfully prepared using mechanical alloying. The understanding of phase transformation during mechanical alloying states a possible involvement of an interdiffusion mechanism, as in the solid state reaction of multilayered films [22]. In cemented carbides, it was suggested that carbon powders are preferentially broken soon after milling starts due to their ease of pulverization, which eventually get positioned between ductile tungsten particles. Continued milling in its
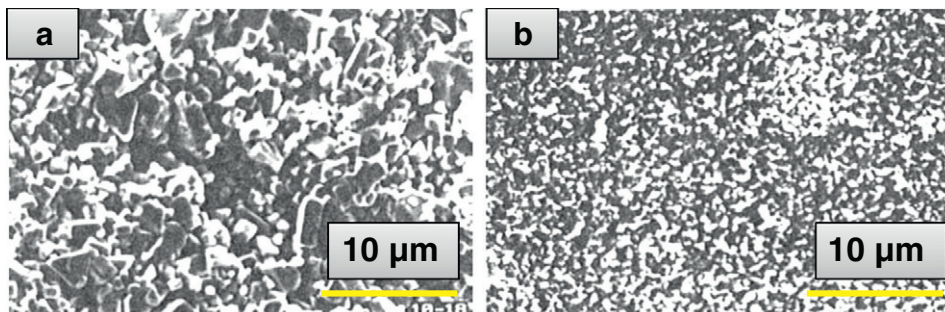

Fig. 4. SEM micrograph of the alloys (a) WC–Co; (b) WC–Co-rare earth [24].
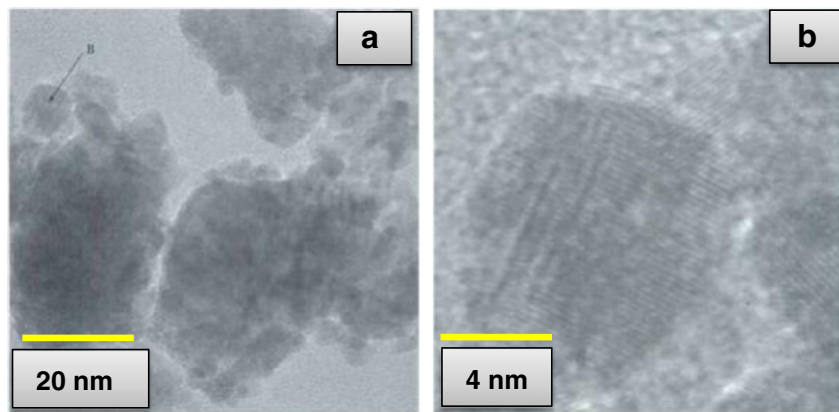
Fig. 5. (a) HR-TEM image of WC powder after 24 h of dual drive planetary milling. (b) Magnified image of region B [11].

second step would refine tungsten crystallites and at the same time produce a more homogeneous distribution of C. The study identified the formation of tungsten carbide involving two stages:

 i) Nucleation occurring at the nanometer sized interface between W/C,
ii) Growth of the nuclei.

It was tried to establish that the heat of formation of WC, provided by mechanical alloying, has helped the reaction to occur, while the defects and interfaces induced by mechanical attrition would lead the reaction process towards the completion of the transformation to WC.

Although the experiment succeeded in producing nano-grained WC of nearly 11 nm, it struggled to initiate solid WC from elemental C and W in the first 20 h. The study suggests that it takes about 100 h for a complete transformation under such milling conditions, although it was still difficult to confirm the presence of Co phase in the microstructure.

In a similar study, with elemental W and C and without grain growth inhibitors, El-Eskandarany et al. [23] used high energy ball milling with a different ball-to-powder weight ratio of 10:1 for a total of 120 h, managing to produce 70–90 nm grain size particles by the end of 71 h, and 5–7 nm by the end of 120 h, which is slightly higher than the study by Xueming et al. [21]. The XRD analysis that was done as part of the study suggested that after 256 ks (nearly 71 h) of milling, all Bragg reflections representing pure elemental W and C disappeared, revealing the completion of solid state reaction and the formation of one single phase of HCP-WC. Even with further milling, no changes in the WC phase were identified. Fig. 3 shows low magnification bright field image and high resolution TEM image of milled WC powders.

A relatively recent work by Liu et al. [24] presented the idea of milling rare earth doped WC–Co powders. Interestingly, it was found that the grain size of these rare earth doped (Y_2O_3–La_2O_3–CeO_2) cemented carbides become two times smaller upon high energy ball milling between 25 and 45 h, as opposed to milling without the inclusion of rare earth oxides. The study has successfully obtained less than 10 nm grain sized WC–Co-rare earth composite powders in 45 h of milling, from an initial average grain size of nearly 1.8 μm (Fig. 4). However, the function of these rare earth oxides with respect to the usual grain growth inhibitors (VC, Cr_3C_2, etc.) for cemented carbides, in terms of mechanical properties, is yet to be fully explored.

But in terms of time consumption during milling, most of these results were outperformed when Butler et al. [11] used a new high energy dual-drive planetary mill (HE-DPM) for producing nanosized WC–Co powders, with significantly improved efficiency. Nanosized (10–20 nm) WC and WC–Co powders were produced from initial 0.8 μm powders in approximately 10 h milling time, as seen in Fig. 5. The combined revolution and rotation of the mill canister in this design has created an acceleration field that is nearly 60 times higher than the force of gravity. As a result, the increased acceleration allowed the small

grinding medium (two different sizes) used in the study to generate higher kinetic energy as opposed to conventional planetary milling, and has been successful in increasing the frequency of effective collision between particles and grinding bodies, resulting in higher attrition and abrasion, or impact, leading to faster particle size reduction.

The work of Butler goes quite well with one of our continued works (Fig. 6) that employed high energy ball milling to mix and refine WC–7.5 wt.%Co and WC–12 wt.%Co, respectively. However in both studies, it was suggested that the presence of Co is rather difficult to identify in the milled powder but could be observed in sintered samples, which will be further elaborated in the sintering section of this article. But it is safe to state that it may conform to the principles of Sun et al.'s work [20] as explained earlier.

Although these milling techniques are essentially the most predominant ones for obtaining nano-sized powders, they are not generally energy, time and cost efficient [25–31], therefore, search continued towards optimization of these processes or new methods in this field.

In an attempt to overcome these issues, Mccandlish et al. [12] invented a process called spray conversion, capable of manufacturing ultrafine nanocomposites, based on a series of work from 1939 to 1990 [32–43]. The process started with preparing a mixing solution, followed by the formation of a chemically homogeneous precursor (a chemical/product/material/solution that is transformed into another compound, through a chemical reaction, and therefore precedes that compound in the synthetic pathway) powder through spray drying, and finally the precursor to nanometric particle conversion, which is a thermochemical process. One important feature of the process is the successful production of homogeneous spherical particles of mixed WC–Co. While the process is capable of producing nanoparticles from a wide range (Table 1) of single and multiphase systems, one of the first involvements of this process was on WC–Co composite powders. Unlike conventional processes, here, the constituent metallic elements are premixed at a molecular level, allowing a greater control over chemical and microstructural uniformity. The entire process can be explained by the following simplified stages:

 i) Preparation of a starting solution
ii) Precipitation and spray drying of precursor powder from the initial solution (e.g.: W and Co)
iii) Reduction (reaction) of precursor powder with the help of a reducing gas followed by carburization in controlled carbon–oxygen environment, resulting in biphasic particles of nanosize WC–Co.

Following the same suggested pathway, Cha et al. [47,48] successfully produced 100 nm grain sized WC–10Co composite powders, which later were found to be within 300–700 nm range after sintering, with inclusion of several grain growth inhibitors (Fig. 7).
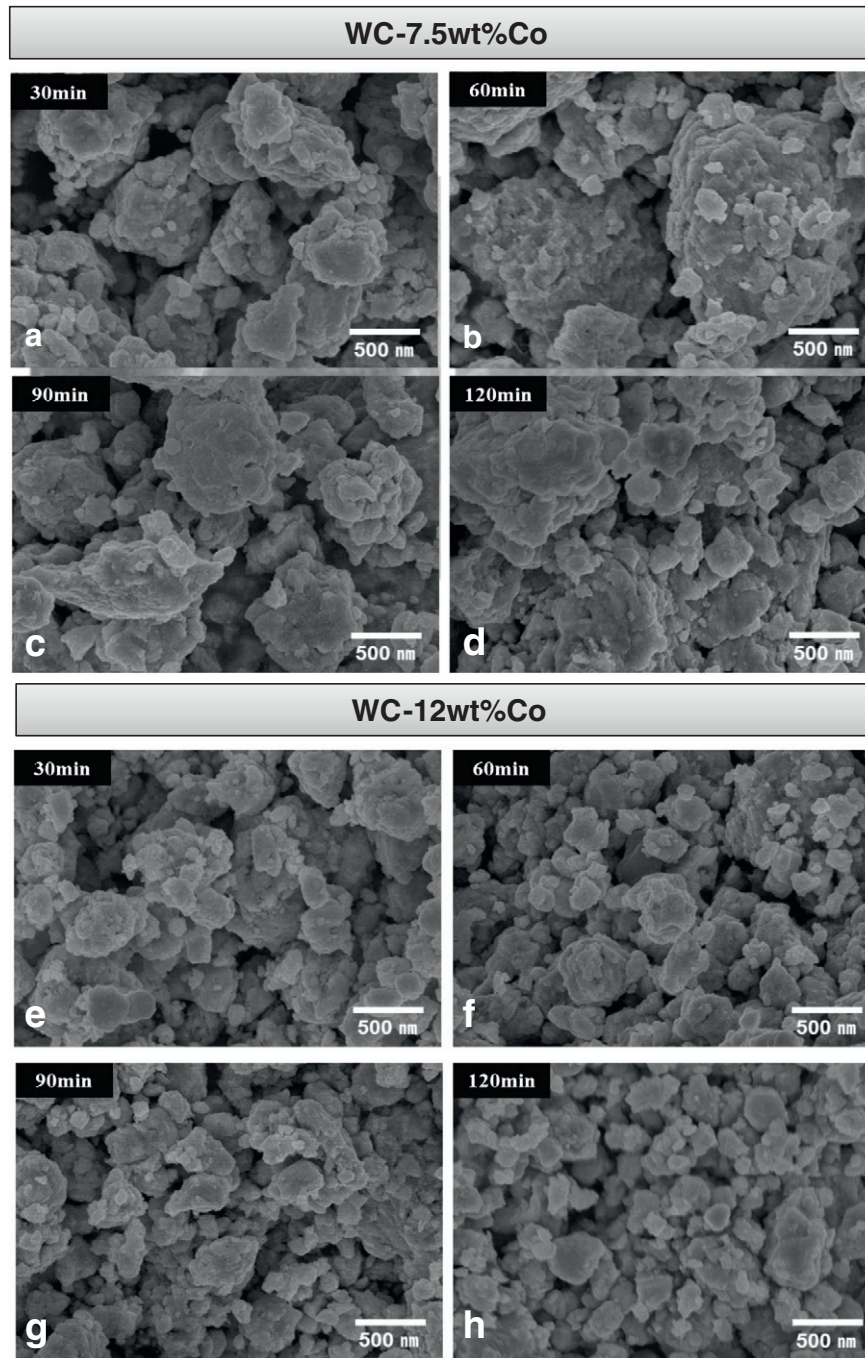
WC-7.5wt%Co

WC-12wt%Co

Fig. 6. SEM images of high energy ball milled WC–7.5 wt.%Co and WC–12 wt.%Co particles, milled for (a, e) 30 min (b, f) 60 min (c, g) 90 min (d, h) 120 min, at a rotational speed of 1100 rpm using stainless steel vial and ball, with a ball to powder ratio of 1:20.

In addition, it was one of the few studies [21,23] that tried to relate nanorefinement with mechanical properties, namely fracture toughness, and suggested that nanocrystalline WC–Co illustrated low fracture toughness as opposed to conventional WC–Co. Contrary to the popular belief that the fracture toughness would increase with increasing Co mean free path [49,51], this study suggested that there might be more factors affecting the toughening mechanism. In addition to the acknowledgment of ductile phase reinforcement theory [76] and Co ligament theory [50], the study added, that with decreasing HCP/FCC ratio of Co binder phase by HCP → FCC phase transformation during liquid phase sintering, fracture toughness would decrease. This ratio was thought to be dependent on the C content within the binder phase. Now, in

nanocrystalline WC–Co, the C content within the Co phase was found to be lower than that of conventional sample, resulting in the material illustrating low HCP/FCC value (<0.2) [47].

However, hardness of the sintered samples with 300 nm of grain size showed significantly higher values as opposed to medium coarse grained (4 μm) samples [47], which may have followed the Hall–Petch relationship. Although it is more applicable to pure metals and alloys and has less significance for composites, it has been argued for both cases. Now depending on the nature of the phases and how diffusion occurs within the microstructure, it may be possible to apply this relationship on WC–Co composites as well. The possibility of having a relationship between fracture toughness or hardness with respect to

Table 1
List of hard metal composites for which spray conversion process can be applied [7,44–47].

Examples of cemented carbides			
WC based		**WC-free**	
Years	Cemented carbides	Years	Cemented carbides
1922–25	WC–Co	1929–31	TiC + MoC + Ni, Cr, Mo
1927	Graphite free WC + Co	1930–31	TaC + Ni, Co
1928–29	WC + Stellite binders	1931	TiC + Cr, Mo, W, Ni, Co
1931	WC + TiC + Co WC + TaC(VC, NbC) + Co	1931	TiC + TaC + Co
1932	WC + TiC + (TaNb)C + Co	1938	TiC + VC + Ni, Fe
1938	WC + Cr$_3$C$_2$ + Co	1944	TiC, NbC + Ni, Co
1951	WC + Ni	1948–50	TiC(Mo$_2$C, TaC) + Ni, Co, Cr
1956	WC + TiC + Ta(Nb)C + Cr$_3$C$_2$ + Co	1949	TiC + VC + NbC + Mo$_2$C + Ni
1959	WC + TiC + HfC + Co	1952–81	TiC + heat treatable binder
1965	HIP	1965–70	TiC + Mo$_2$C + Ni, Mo
1966	Submicron WC–Co	1968–70	TiMoC+Ni,Mo,Cr
1968–69	WC + TiC + (TaNb)C + HfC + Co	1990–2005	WC–(5–15)% Co
1969–80	Coated carbides		

processing techniques and grain size will be further elaborated in the mechanical property section of this paper. It is worth mentioning though that processing techniques also have strong influence on grain size in cemented carbides [14,15].

Kim et al. [52] also used the spray conversion process where 50 nm grain size WC–Co was produced using a 3 step thermochemical process. In contrast with the other works that had employed the same method, this study has tried to identify an optimized processing condition in relation with both hardness and transverse rupture strength, which is also an indication of the fracture toughness of the material.

In addition to the powder production methods mentioned above, a number of studies have used vapor phase reactions [13,53–59] or plasma processing techniques [60] as their preferred way of manufacturing nanosized WC powders, with possible inclusions of several hydrocarbons as carburizing agent.

The work by Medeiros et al. [13] is one such study that employed a gas–solid reaction between ammonium paratungstate (APT) or tungsten blue oxide (TBO) and a mixture of hydrogen (H$_2$) and methane (Ch$_4$) at a relatively short time of 2 h as opposed to hundreds of milling hours, and has successfully produced WC powders (<1 μm) without much change in size and shape of the particles from initial APT/TBO particles. Due to high reactivity of APT and greater contacts between the reactants, it was possible to complete the process within such short duration. It was mentioned in the study that the decomposition and reduction steps have contributed to the high reactivity of APT and TBO particles. The reduction step was considered crucial in controlling

the nature of the particles (size and shape) produced using this process, as a change in atmosphere from dry to wet can significantly affect the final particle size and shape.

3. Consolidation of powders: compaction and sintering

Consolidation is essentially the most important step towards production of cemented carbides, be it in the form of compaction and/or sintering, and affects directly the mechanical properties of the final product. Cemented carbides, both nanostructured and conventional, have been consolidated using a variety of compaction and sintering processes either simultaneously or separate, including, but not limited to,

a) Sintering

   i) Hot isostatic pressing (HIP) [62]
   ii) Ultrahigh pressure rapid hot sintering [63]
   iii) Spark plasma sintering [64–67]
   iv) Pulse plasma sintering [14]
   v) Vacuum sintering [29,68]
   vi) Microwave sintering [69,70]
   vii) High frequency induction heated sintering [71–73]

b) Compaction

   i) Magnetic pulse compaction [29,30,74,75]
   ii) Rapid omni compaction [76]
   iii) Equal channel angular pressing [77]
   iv) Conventional uniaxial pressing (single or double action)
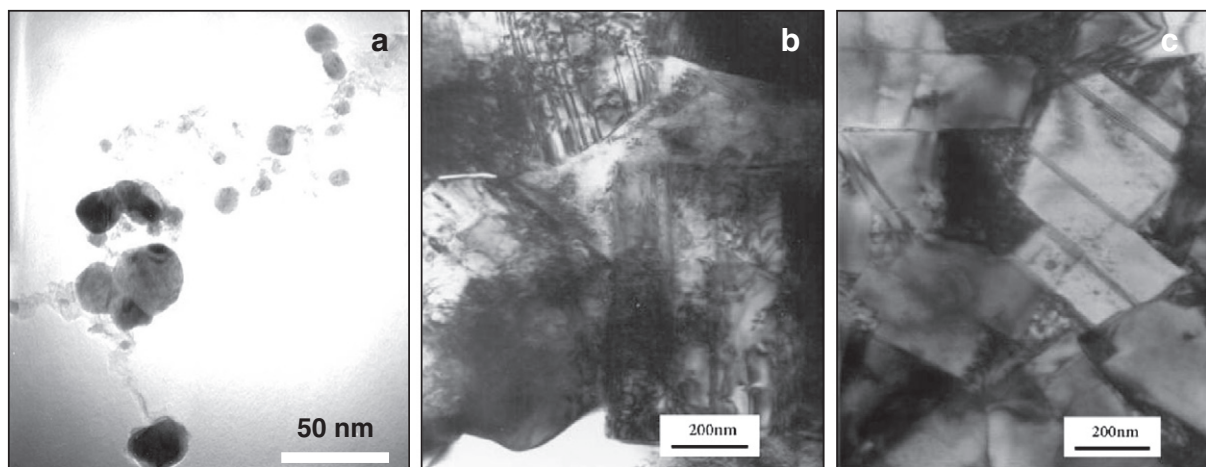

Fig. 7. (a) TEM images of WC–10Co–0.7TaC/VC powders fabricated by spray conversion process (before sintering). The darker phase represents WC phase with average diameter of 100 nm and the brighter phase represents Co phase. TEM micrographs of cemented carbides sintered at 1375 °C for 1 h under vacuum for (b) conventional WC–10Co, and (c) nanocrystalline WC–10Co–0.7TaC/VC [47].
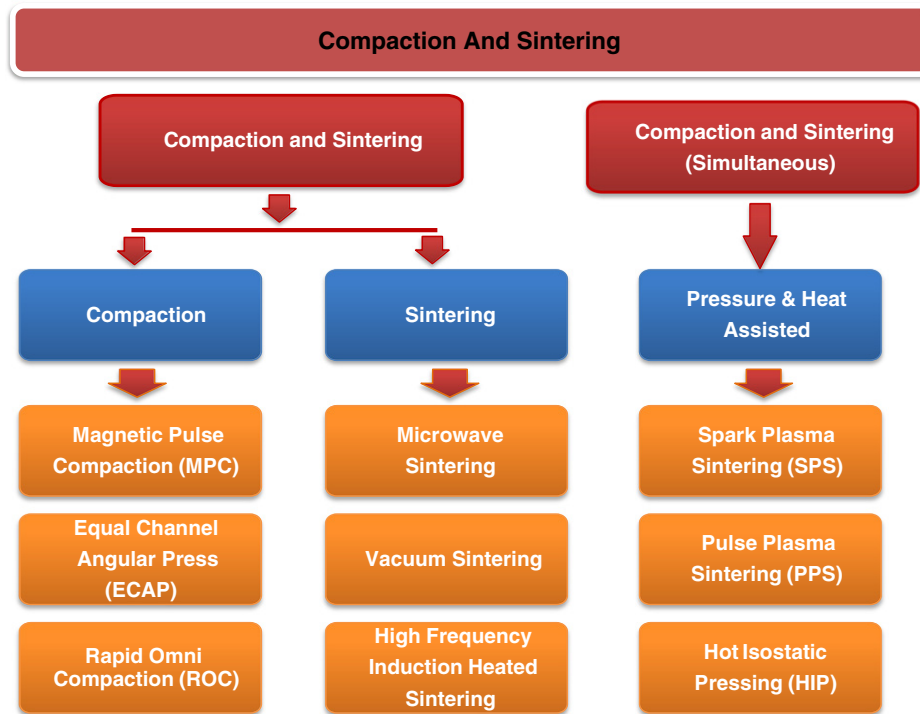
Fig. 8. Various compaction and sintering processes. Note: For HIP, SPS and PPS, it is possible, although not practiced, to compact and sinter the powders separately.

While sintering is primarily employed for joining particles together with the aid of thermal energy, compaction involves joining of particles by mechanical means which has the potential to be improved by incorporation of thermal energy as a result of sintering. Fig. 8 shows how these processes can be classified in terms of the timing of compaction and sintering. In terms of pressing direction, most of the compaction and sintering can be classified into single or double action processes. While most of these compaction methods are well-known, and are compatible to a wide range of materials and composites, rapid omni compaction and magnetic pulse compaction (MPC) are especially suitable for chemically incompatible non wetting ceramic–metal systems [78].

Some recent studies [29,30,74,75], including our previous works (see Figs. 9 and 10), have used magnetic pulse compaction (MPC), where a wide variety of powders were compacted into either nearly dense (ceramics) or high initial (green) density (cemented carbide) disk shaped samples at room temperature. While using MPC, it was possible to apply a high pressure (up to 5 GPa) to powders within a short duration of time (~500 μs). This ultra high pressure in 500 μs is capable of inducing a better powder rearrangement, resulting in an improved green density [79]. The process starts with identifying the discharge voltage which translates to the pressure that will be applied to the powders kept in the die, eventually contributing to the relative density and compressive strength of compacts. Since the capacitance is fixed in this setup, the increase of discharge voltage enhances the discharge energy, which improves the combination strength of particles. So, the relative density and compressive strength of compacts increase owing to the intensified kinetic energy acting on the powder body. Further details of the working principle can be obtained from [80], and is outside the scope of this article.

Equal channel angular pressing (ECAP) is another compaction technique that has been gaining interest in recent times, in which particles experience severe plastic deformation, and has proven to be effective for grain size control [77,81]. During this process, powder particles are pressed using a die where two channels of exactly equal cross-section intersect at a certain angle that defines the arc of curvature at the outer edge of the intersection. Studies [77,81] have shown that it is

quite practical to use this process several times on the same sample in order to obtain a high total strain, as the cross sectional area of the single passage die remains the same.

Most of the above-mentioned methods involve changes in the structure and properties of the powders, through increase in contact areas between particles, imparting the required strength to a compact, disintegrating the agglomerates of particles and sometimes even the particle themselves [82]. Among the compaction techniques named above, conventional uniaxial compaction is the predominant mode for powder consolidation, where pressure is an important parameter to get stable green samples.

A few works from the literature that have tried to employ sintering processes with or without the involvement of prior compaction, in the studies of cemented carbides are mentioned below.

In an attempt to differentiate the characteristics between conventional sintering involving a liquid phase, and microwave sintering, Breval et al. [70] used both sintering methods on several compositions of WC–Co. The heating profiles of both methods are compiled in Table 2. The study concludes that microwave sintering plays a crucial role in limiting grain growth of WC, as opposed to conventional sintering, and ensured greater uniformity of Co or other binder phases in the matrix. Between microwave and conventionally sintered samples, the difference in WC grain size was quite large, which eventually resulted in a better and finer distribution of cobalt in the microwave-sintered sample. Unlike the conventional process, according to the principles, the major source of the heating in the microwave oven is oscillations of the free electrons at high frequency microwave in cobalt and in free carbon, and of ions in WC [83]. It is worth noting that the contribution of heat from oscillations of magnetic domains in Co is very small because of its small hysteresis [84].

Although this work [70] did not focus on nanostructured materials, the fact that microwave sintering is capable of inhibiting grain growth due to a less extended period of a liquid phase, without any inclusion of commercial inhibitors, opens new avenues for WC nano composites.

Spark plasma sintering (SPS), which is a pressure assisted high temperature compaction, has attracted great interest in recent years, especially for hard to consolidate materials. In addition, the idea of being
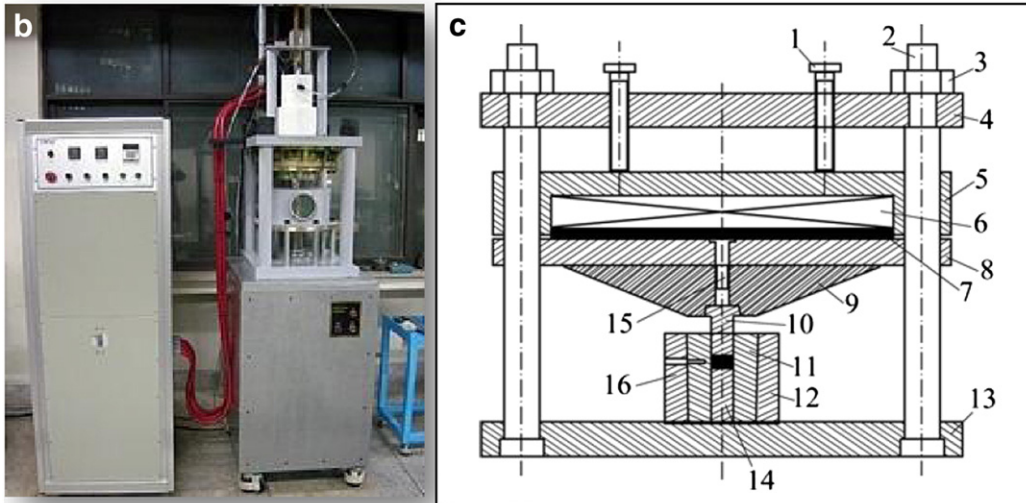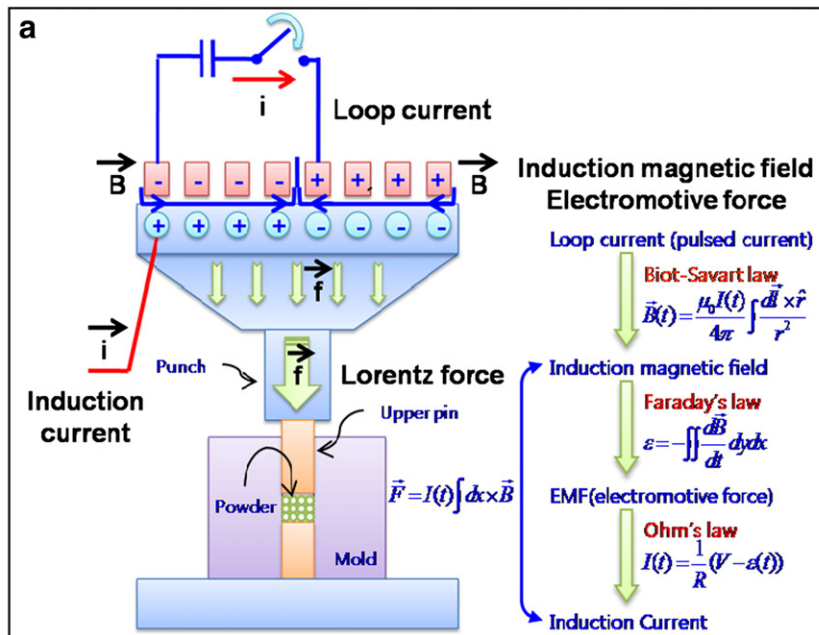
Fig. 9. (a) Working principle of magnetic pulse compaction (MPC), (b) image of the MPC unit, (c) schematic diagram of magnetic pulse forming setup [80]: 1—screw; 2—guide pillar; 3—nut; 4—upper template; 5—coil sleeve; 6—coil; 7—driver; 8—backing plate; 9—amplifier; 10—punch; 11—cavity die; 12—die sleeve; 13—lower template; 14—pad; 15—screw; and 16—heating sleeve.

able to use single or multiple pressure while heating at a gradually increasing temperature suggested the possibility of controlling nanograin growth in cemented carbides, although not much has been accomplished to capitalize the idea. Jia et al. [15] used SPS for consolidation of nano WC–11Co with varying temperature from 900 to 1100 °C and compared that with the grain growth behavior of regular (about 600 nm) WC–11Co powder (Fig. 11). They have concluded that grain growth was enhanced for regular samples, where nano WC–Co showed less grain growth for the same sintering temperature and pressure. The study however did not comment on how the sintered samples would behave in the presence of commercial grain growth inhibitors (TaC, VC etc.).

In addition to the dominant effects of pressure, SPS as opposed to conventional sintering incorporates the phenomena, where both the die and the powder are heated by the Joule effect of the dc current the process uses. Although the process is capable to reaching highly elevated temperature of nearly 2000 °C or even more with a remarkably high heating rate, the role of dc current on the mechanism of sintering is yet to be fully understood [85].

Although there have been applications of advanced sintering processes like spark plasma sintering, pulse plasma sintering and so on, controlling grain growth still remains a critical challenge. To overcome this issue, studies have primarily focused on varying compaction and sintering parameters without compromising the desired mechanical properties, which is discussed in our next section.

4. Mechanical properties: hardness and fracture toughness

Previous investigations [86–89] on mechanical properties of sintered carbides have covered almost every aspect while the current overview will focus on mainly hardness, and toughness of WC-based cemented carbides.

Hardness, a parameter indicating the resistance to change in shape of a material, is a paramount variable describing mechanical properties. Generally, hardness increases with an increasing volume fraction of the hard phase particles, but also with decreasing grain size and increasing contiguity [91]. Fig. 12 exhibits hardness and compression strength of
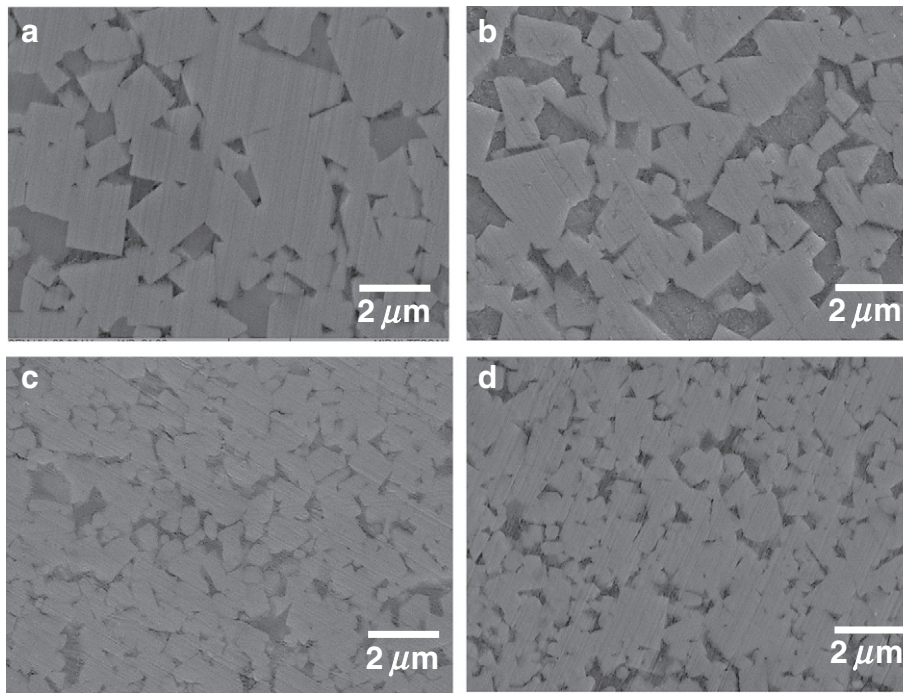
Fig. 10. Field emission scanning electron microscopy (SE) showing changes in microstructure of MPC + sintered samples (a) WC–7.5 wt.%Co at 1 GPa, (b) WC–7.5 wt.%Co at 3 GPa, (c) WC–12 wt.%Co at 1 GPa and (d) WC–12 wt.%Co at 3 GPa [29].

WC–Co hard metals as a function of composition and WC grain size. Now it is well established that for cemented carbides, hardness is inversely proportional to both WC and Co grain sizes. Studies that focused on conventional cemented carbides suggest an improbability of having high hardness and toughness for a particular grain size of WC–Co. Now on the other hand, nanostructured materials (WC–Co), that are proven to be hard in nature, yet brittle, have been reported to suggest a different possible mechanism when it comes to establishing a relationship between grain size and fracture toughness. The hypothesis [92,93] says that due to a large volume fraction of grain boundaries in nanostructured materials, it is possible to impede propagations of cracks, which essentially translates into high fracture toughness and high hardness values at the same time.

The Vickers indentation test also helps in evaluating the fracture toughness of the material. Using the following equation [94], it is possible to calculate the fracture toughness (K_{1c}):

$$K_{1c} = 0.016 \, (E/H)^{1/2} \left(P/c^{3/2} \right) \qquad (1)$$

where E is Young's modulus, P is the indentation load, c is half of the average indentation crack length usually forms during hardness testing (Fig. 13), and H is the hardness of the material.

A compilation of mechanical properties in nanostructured WC–Co materials by Fang et al. [95] is presented in Table 3. It shows that these properties are somewhat controlled by grain size and fabrication processes applied.

Table 2
Comparison of heating and cooling steps in conventional and microwave sintering [95].

Stages	Microwave sintering (min)	Conventional sintering
Heating cycle, 850–1250 °C	10–30	150 min
Soaking time at peak temperature	10	1 h
Cooling cycle 1250–850 °C	30	5–10 h
Estimated duration of Co in liquid state	15	4 h

Out of all these studies, probably the most successful one is the work by Michalski A. and Siemiaszko D. [14], where pulse plasma sintering (PPS) method was used on commercially available WC–12Co with an initial grain size of 40–80 nm. The final grain size in the sintered samples were about 50 nm at 1100 °C, which later increased up to 110 nm at a sintering temperature of 1200 °C, with displayed hardness of nearly 2250 HV (22.07 GPa) and fracture toughness of 15.3 MPa/m$^{1/2}$, which is significantly higher than what could be retrieved from other studies mentioned in literature.

Fracture toughness has become one of the most critical subjects of study for cemented carbides due to the ambiguity in understanding what primarily influences this material property. In addition, since this is fundamentally related to other mechanical properties of materials like hardness and wear, it is all the more crucial to focus on how fracture toughness varies, and why. The work of Kenny [96] and Yen [97] were two of the most important studies of fracture toughness of cemented carbides, which practically defined the understanding of the features of fracture toughness, and have been followed over the decades. Although these were successful studies, they were limited in a sense that they could not be applied to all cemented carbides, when it comes to predicting fracture toughness and other mechanical properties. The values reported by Kenny [96] were only in the range of 5.6 to 8.8 MPa/m$^{1/2}$ with the idea of toughness increasing with increasing cobalt content and grain size, while Yen's [97] work focused on two different specimen types combined with two pre-crack initiation techniques. To further extend the practical understanding of this topic, Ingelstrom and Nordberg [98] conducted a series of experiments with twelve experimental grades of tungsten carbide–cobalt composites, six different cobalt contents, three different grain sizes and two different pre-crack types, in an attempt to comment on the generalized fracture toughness behavior in cemented carbides. The pre-crack types used were:

i) A continuous series of indentation across a specimen surface with least possible spacing in between pre-cracks with a depth of 0.2–0.5 mm [96].

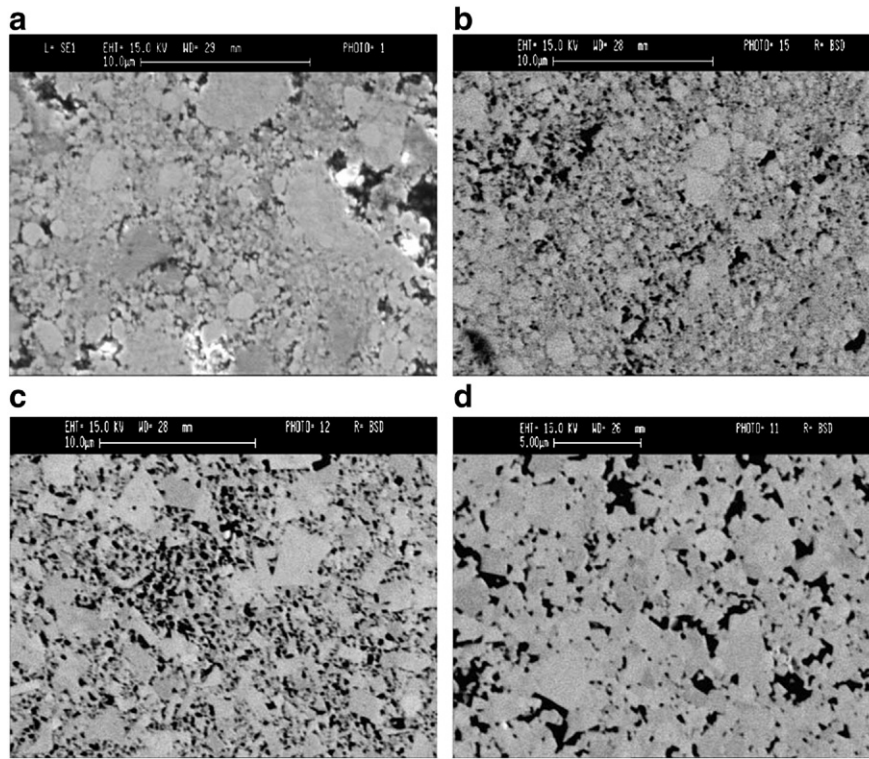ii) Single indentation with a semi-elliptical pre-crack impression; a method being used till date.

Fig. 11. SEM photographs of WC–11Co cemented carbides sintered from nanometer scale and conventional powders by SPS under pressure of 25 MPa. The photographs of WC–11Co cemented carbides sintered at 900 °C, 1000 °C and 1100 °C respectively. (a) Nanometer scale powder (900 °C); (b) nanometer scale powder (1000 °C); (c) nanometer scale powder (1100 °C); and (d) common powder (1100 °C) [15].

A compilation of several test results that were conducted on the compositions of cemented carbides is presented in Table 4.

The study by Ingelstrom and Nordberg [98] commented on the fracture toughness behavior and confirmed that fracture toughness decreases almost linearly with hardness, and increases with increasing grain size for cemented carbide compositions ranging from 6 wt.%Co to 25 wt.%Co. While this has been the basis of understanding fracture toughness and how it behaves in cemented carbides for several decades, several recent studies [14,64–67] have suggested otherwise. It has been mentioned that processes like spark plasma sintering and pulse plasma

sintering with controlled sintering parameters have been fairly successful in demonstrating high hardness and fracture toughness [14,15,99], even with low initial and final grain size and growth (refer to Table 3), in addition to their success in limiting grain growth during sintering. This inconsistency between grain size and growth control and fracture toughness mechanisms is the subject of a detailed study in our laboratories [Adelaide Materials Research Group, 2013] [100] to provide better understanding of fracture toughness and other mechanical properties of cemented carbides against particle size and processing routes with fixed or variable binders.
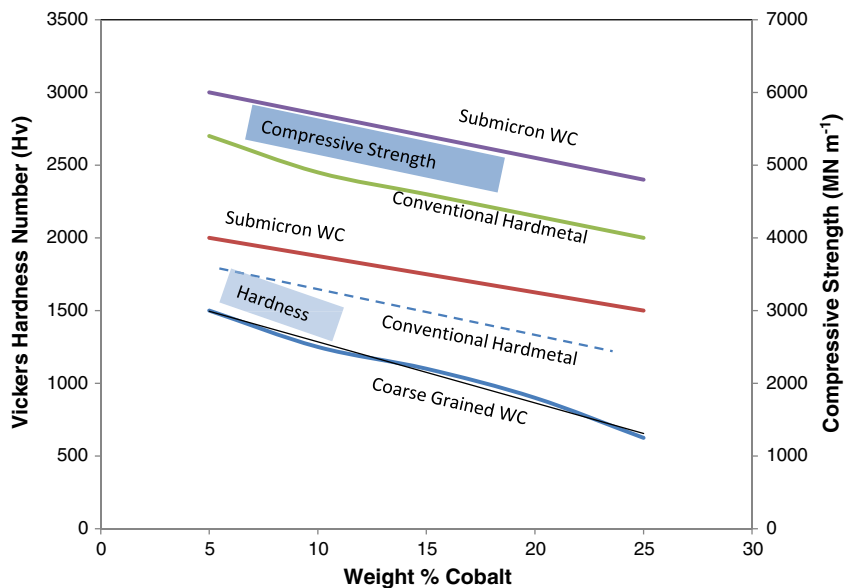

Fig. 12. Hardness and compressive strength of WC–Co hard metals as a function of composition and WC grain size [90].
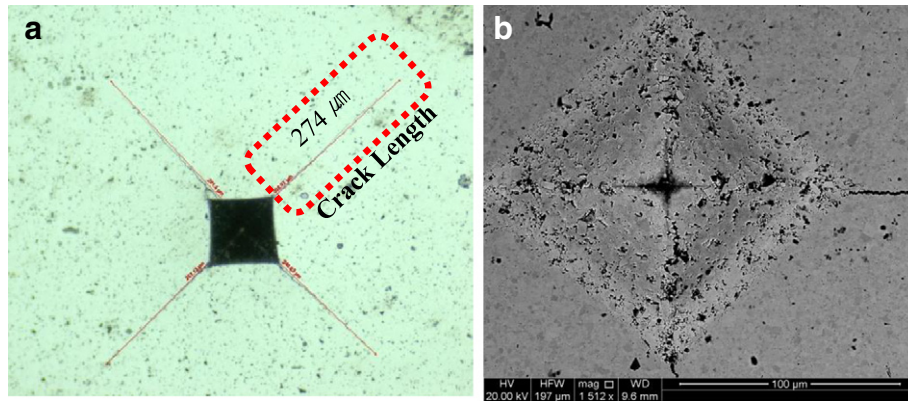
Fig. 13. (a) Optical Micrograph showing nature of indentation along with cracks generating from the edges (b) magnified SEM image. Both images are of spark plasma sintered WC–7.5 wt.% nano Co, compacted at 60 MPa.

Table 3
Hardness and fracture toughness of sintered WC–Co using nanosized powders as reported in literature [95].

Consolidation process	Sintered grain size (nm)	Hardness[a] (HV/GPa)	Fracture toughness (MPa mm1/2)
PPS	50	2250/22.07	15.3
Hot pressing	95	1100[b]/10.79[b]	14
UPRC	~97	1845/18.09	10.2[c]
SPS	<100	1887/18.51	11.5
ROC	150	1936/18.99	9.8
Hot pressing	169	2084/20.44	8.8
SPS	170	1726/16.93	9.5
HIP	~200	1910/18.73	–
SPS	200	2030/19.91	–
SPS	230	2030/19.91	13.5
SPS	280	1569/15.39	9.3
HFIHS	323	1886/18.5	13.5
SPS	~350	1800/17.65	12
HIP	~400	1740/17.06	–
SPS	470	1570/15.4	11.42
Hot pressing	780	1575/15.45	–
SPS	780	1725/16.92	–
SPS	800	1450/14.22	10.9

[a] For convenience of comparison, the original hardness values (units in GPa) from papers were converted to Vickers hardness (HV) values.

[b] Addition of ductile Co improves its toughness so that the latter is monotonically increased with increasing volume fraction of metallic Co. Contrary to this, the hardness is significantly decreased with increasing the ductile phase to reach a value of 11 GPa (14 wt.%Co).

[c] This value was measured by standard short-rod method based on ASTM-B771, which may not always be comparable with the other method (Palmquist) used in the study but is mentioned to give a rough idea since grain size and other parameters are also part of the comparison within the table.

5. Conclusions

In the studies of cemented carbides, namely WC–Co, which started nearly over a century ago, the idea of using nanocrystalline powders instead of regular ones is relatively new, being practiced only in the past two decades. This suggested theory has triggered numerous successful studies in fabricating true nanograined WC–Co powders (<100 nm) with desired properties and microstructural features. To take it to the next level, researchers have even challenged the natural phenomenon of grain growth during consolidation of these nano particles, at high temperatures, and have employed several treatments, starting from using grain growth inhibitors to using a wide range of compaction and sintering techniques. The target was simple; inhibiting grain growth in the final consolidated samples without compromising mechanical properties like hardness, wear resistance and fracture toughness. While some studies have succeeded in presenting reasonable

Table 4
Compilation of properties and fracture toughness of cemented carbide alloys [98].

Composition	Grain type	Density (g/cm³)	Mean grain size (μm)	Hardness (HV)	Fracture toughness (MN/m^{3/2})
WC–6 wt.%Co	Fine	14.85	1.0	1700	10.0
WC–6 wt.%Co	Medium	14.92	1.5	1530	12.4
WC–8 wt.%Co	Fine	14.69	1.3	1550	12.3
WC–8 wt.%Co	Coarse	14.72	3.2	1250	18.2
WC–11 wt.%Co	Medium	14.44	1.9	1210	17.5
WC–11 wt.%Co	Coarse	14.39	3.3	1140	17.4
WC–15 wt.%Co	Medium	14.01	1.9	1130	17.6
WC–15 wt.%Co	Coarse	13.97	3.3	1050	18.5
WC–20 wt.%Co	Medium	13.36	1.8	1000	20.3
WC–25 wt.%Co	Medium	13.00	3.0	800	20.3

outcomes, industrial involvement and practice of the same methods are yet to be seen. But even with all these advancements, achieving a truly nano grained consolidated product with highly improved mechanical properties and with well explained i) grain growth control mechanism, ii) grain boundary nature, iii) WC and Co bonding, iv) grain boundary orientation, and v) binder contribution, is still considered to be one of the biggest areas where focus needs to be drawn. It is equally critical and challenging based on the understanding of the studies in the field of cemented carbides/hard metals to clarify the relationship between particle or grain size and mechanical properties.

References

[1] V.K. Sarin, Cemented carbide cutting tools, Adv. Powder Technol. (1981) 253–288.
[2] J. Larsen-Basse, Effect of composition, microstructure and service conditions on the wear of cemented carbides, J. Met. 35 (1983) 35–42.
[3] H.-O. Andren, Microstructure development during sintering and heat-treatment of cemented carbides and cermets, Mater. Chem. Phys. 67 (2001) 209–213.
[4] S. Imasato, K. Tokumoto, T. Kitada, S. Sakaguchi, Properties of ultra-fine grain binderless cemented carbide 'RCCFN', Int. J. Refract. Met. Hard Mater. 13 (1995) 305–312.
[5] P.K. Mirchandani, R.E. Thomas, M. Cippel, "Multiple grade cemented carbide articles and a method of making the same," ed: Google Patents, 1996.
[6] G. Upadhyaya, Materials science of cemented carbides—an overview, Mater. Des. 22 (2001) 483–489.
[7] K. Brooks, World Directory and Handbook of Hardmetals, Engineering Digest, New York, 1979.
[8] N. Romanova, N. Kuzmina, Sintered Metal Carbides, Mir Publishers, Moscow, 1972.
[9] J.S. Hirschhorn, K.H. Roll, Advanced Experimental Techniques in Powder Metallurgy, vol. 5, Plenum Press, 1970.
[10] Y. Gao, X. Song, X. Liu, C. Wei, H. Wang, J. Fu, On the formation of WC_{1-x} in nanocrystalline cemented carbides, Scr. Mater. 68 (2) (2013) 108–110.
[11] B.G. Butler, L. Jun, Z.Z. Fang, R.K. Rajamani, Production of nanometric tungsten carbide powders by planetary milling, J. Powder Metall. 43 (2007) 35–43.
[12] L.E. McCandlish, B.H. Kear, S.J. Bhatia, "Spray conversion process for the production of nanophase composite powders," ed: Google Patents, 1994.
[13] F. Medeiros, S. De Oliveira, C. De Souza, A. Da Silva, U. Gomes, J. De Souza, Synthesis of tungsten carbide through gas–solid reaction at low temperatures, Mater. Sci. Eng. A 315 (2001) 58–62.
[14] A. Michalski, D. Siemiaszko, Nanocrystalline cemented carbides sintered by the pulse plasma method, Int. J. Refract. Met. Hard Mater. 25 (2007) 153–158.
[15] C.-C. Jia, H. Tang, X.-Z. Mei, F.-Z. Yin, X.-H. Qu, Spark plasma sintering on nanometer scale WC–Co powder, Mater. Lett. 59 (2005) 2566–2569.
[16] L. Zhang, M.-w. Xie, X. Cheng, Q. Nan, Z. Wang, Y.-p. Feng, Micro characteristics of binder phases in WC–Co cemented carbides with Cr–V and Cr–V–RE additives, Int. J. Refract. Met. Hard Mater. 36 (2013) 211–219.
[17] K. Jia, T. Fischer, Abrasion resistance of nanostructured and conventional cemented carbides, Wear 200 (1996) 206–214.
[18] K. Jia, T. Fischer, B. Gallois, Microstructure, hardness and toughness of nanostructured and conventional WC–Co composites, Nanostruct. Mater. 10 (1998) 875–891.
[19] J.S. Benjamin, Dispersion strengthened superalloys by mechanical alloying, Metall. Mater. Trans. B 1 (1970) 2943–2951.
[20] J. Sun, F. Zhang, J. Shen, Characterizations of ball-milled nanocrystalline WC–Co composite powders and subsequently rapid hot pressing sintered cermets, Mater. Lett. 57 (2003) 3140–3148.
[21] M. Xueming, Z. Ling, J. Gang, D. Yuanda, Preparation and structure of bulk nanostructured WC–Co alloy by high energy ball-milling, J. Mater. Sci. Lett. 16 (1997) 968–970.
[22] F. Petzoldt, B. Scholz, H.-D. Kunze, Study of the mechanism of amorphization by mechanical alloying, Mater. Lett. 5 (1987) 280–284.
[23] M.S. El-Eskandarany, A.A. Mahday, H. Ahmed, A. Amer, Synthesis and characterizations of ball-milled nanocrystalline WC and nanocomposite WC–Co powders and subsequent consolidations, J. Alloys Compd. 312 (2001) 315–325.
[24] S. Liu, Z.-L. Huang, G. Liu, G.-B. Yang, Preparing nano-crystalline rare earth doped WC/Co powder by high energy ball milling, Int. J. Refract. Met. Hard Mater. 24 (2006) 461–464.
[25] R. Uribe, C. Baudin, L. Mazerolles, D. Michel, Sub-micron sized Al2TiO5 powders prepared by high-energy ball milling, J. Mater. Sci. 36 (2001) 5105–5113.
[26] F. Zhang, C. Wang, M. Zhu, Nanostructured WC/Co composite powder prepared by high energy ball milling, Scr. Mater. 49 (2003) 1123–1128.
[27] H. Fecht, Synthesis and properties of nanocrystalline metals and alloys prepared by mechanical attrition, Nanostruct. Mater. 1 (1992) 125–130.
[28] H. Fecht, E. Hellstern, Z. Fu, W. Johnson, Nanocrystalline metals prepared by high-energy ball milling, Metall. Mater. Trans. A 21 (1990) 2333–2337.
[29] R.M. Raihanuzzaman, J.-W. Song, S.-J. Hong, Evaluation of mechanical properties and processing conditions of WCCo alloys fabricated by magnetic pulsed compaction, J. Alloys Compd. 536 (2012) S211–S215.
[30] J.H. Kim, R. Md Raihanuzzaman, C.K. Rhee, J.G. Lee, M.K. Lee, S.-J. Hong, Fabrication and densification behavior analysis of metalizing targets using ZrO_2 nanopowders by magnetic pulsed compaction, Mater. Trans. JIM 52 (2011) 1156.
[31] R. Porat, S. Berger, A. Rosen, Sintering behavior and mechanical properties of nanocrystalline WC/Co, Mater. Sci. Forum, 1996, pp. 629–648.
[32] M.E. Shaffer, E.R. Kimmel, "Method for preparation of WC–NI grade powder," ed: Google Patents, 1991.
[33] H.-E. Schutz, B. Szesny, B.E. Krismer, "Agglomerated metal composite powders," ed: Google Patents, 1990.
[34] R.S. Polizzotti, L.E. McCandlish, "Multiphase composite particle," ed: Google Patents, 1989.
[35] E.R. Kimmel, M.E. Shaffer, T.R. Pinkowski, G.L. Harris, "Method of producing monotungsten carbide powder," ed: Google Patents, 1987.
[36] R.C. Lueth, "Method for carbon control of carbide preforms," ed: Google Patents, 1986.
[37] J.J. Oakes, W. Scheithauer Jr, "Intimate mixtures of refractory metal carbides and a binder metal," ed: Google Patents, 1982.
[38] F.P. Gortsema, "Process for the preparation of fine grain metal carbide powders," ed: Google Patents, 1976.
[39] F.C. Holtz, "Cobalt–tungsten carbide alloy and process," ed: Google Patents, 1970.
[40] J.F. Hardy, "Process and composition for the production of cemented metal carbides," ed: Google Patents, 1970.
[41] W.L. Robb, "Process for producing carbides," ed: Google Patents, 1963.
[42] J. Komp, "Method of making hard metal alloys," ed: Google Patents, 1939.
[43] M. Oswald, "Method of manufacturing hard," ed: Google Patents, 1939.
[44] R. Kieffer, F. Benesovsky, "Hartmetalle," 1965, 541 P, Springer-verlag, Molkerbastei 5, a-1010 Wien, Germany, 1966.
[45] R. Kieffer, P. Ettmayer, Recent advances in the knowledge and applications of transition metal nitrides, High Temp. High Pressure 6 (1974) 253–260.
[46] H. Exner, Analysis of grain-and-particle-size distributions in metallic materials, Int. Mater. Rev. 17 (1972) 25–42.
[47] S.I. Cha, S.H. Hong, G.H. Ha, B.K. Kim, Mechanical properties of WC–10Co cemented carbides sintered from nanocrystalline spray conversion processed powders, Int. J. Refract. Met. Hard Mater. 19 (2001) 397–403.
[48] S.I. Cha, S.H. Hong, G.H. Ha, B.K. Kim, Microstructure and mechanical properties of nanocrystalline WC–10Co cemented carbides, Scr. Mater. 44 (2001) 1535–1540.
[49] M. Kotoul, On the shielding effect of a multiligament zone of a crack in WC–Co, Acta Mater. 45 (1997) 3363–3376.
[50] K. Ravichandran, Fracture toughness of two phase WC–Co cermets, Acta Metall. Mater. 42 (1994) 143–150.
[51] L.S. Sigl, H. Fischmeister, On the fracture toughness of cemented carbides, Acta Metall. 36 (1988) 887–897.
[52] B. Kim, G. Ha, D. Lee, Sintering and microstructure of nanophase WC/Co hardmetals, J. Mater. Process. Technol. 63 (1997) 317–321.
[53] J. Kim, B. Kim, Synthesis of nanosized tungsten carbide powder by the chemical vapor condensation process, Scr. Mater. 50 (2004) 969–972.
[54] G. Leclercq, M. Kamal, J. Giraudon, P. Devassine, L. Feigenbaum, L. Leclercq, A. Frennet, J. Bastin, A. Löfberg, S. Decker, Study of the preparation of bulk powder tungsten carbides by temperature programmed reaction with $CH_4 + H_2$ mixtures, J. Catal. 158 (1996) 142–169.
[55] J. Hojo, T. Oku, A. Kato, Tungsten carbide powders produced by the vapor phase reaction of the $WC_{16}–CH_4–H_2$ system, J. Less-Common Met. 59 (1978) 85–95.
[56] M. Fitzsimmons, V.K. Sarin, Comparison of $WC_{16}–CH_4–H_2$ and $WF_6–CH_4–H_2$ systems for growth of WC coatings, Surf. Coat. Technol. 76 (1995) 250–255.
[57] L. Gao, B. Kear, Low temperature carburization of high surface area tungsten powders, Nanostruct. Mater. 5 (1995) 555–569.
[58] X. Tang, R. Haubner, B. Lux, B. Kieffer, Preparation of ultrafine CVD WC powders deposited from WC_{16} gas mixtures, J. Phys. IV 5 (1995) 5.
[59] C.-W. Won, B.-S. Chun, H. Sohn, Preparation of ultrafine tungsten carbide powder by CVD method from $WC_{16}–C_2H_2–H_2$ mixtures, J. Mater. Res. 8 (1993) 2702–2708.
[60] Y. Moriyoshi, M. Futaki, S. Komatsu, T. Ishigaki, The preparation and characterization of ultrafine tungsten powder, J. Mater. Sci. Lett. 16 (1997) 347–349.
[61] G.F. Vander Voort, Grain size measurement, Adv. Powder. Metall. Part. Mater. (1984) 85–181.
[62] I. Azcona, A. Ordonez, J. Sanchez, F. Castro, Hot isostatic pressing of ultrafine tungsten carbide-cobalt hardmetals, J. Mater. Sci. 37 (2002) 4189–4195.
[63] X. Wang, Z. Fang, H. Sohn, Nanocrystalline cemented tungsten carbide sintered by an ultra-high-pressure rapid hot consolidation process, Adv. Powder. Metall. Part. Mater. 2 (2007) 8.
[64] D. Sivaprahasam, S. Chandrasekar, R. Sundaresan, Microstructure and mechanical properties of nanocrystalline WC–12Co consolidated by spark plasma sintering, Int. J. Refract. Met. Hard Mater. 25 (2007) 144–152.
[65] H. Zhao, L. Zhu, Q. Huang, Nanocrystalline WC–10% Co–0.8% VC cemented carbides prepared by spark plasma sintering, Rare Met. Mater. Eng. 34 (2005) 82–85.
[66] X. Yingfang, W. Xingqing, C. Lidong, L. Xiaodong, G. Hailiang, Preparation of superfine-cemented carbide by spark plasma sintering, J. Wuhan Univ. Technol., Mater. Sci. Ed. 21 (2006) 42–45.
[67] G. Maizza, S. Grasso, Y. Sakka, T. Noda, O. Ohashi, Relation between microstructure, properties and spark plasma sintering (SPS) parameters of pure ultrafine WC powder, Sci. Technol. Adv. Mater. 8 (2007) 644–654.
[68] D. Carroll, Sintering and microstructural development in WC/Co-based alloys made with superfine WC powder, Int. J. Refract. Met. Hard Mater. 17 (1999) 123–132.
[69] D. Agrawal, J. Cheng, P. Seegopaul, L. Gao, Grain growth control in microwave sintering of ultrafine WC–Co composite powder compacts, Powder Metall. 43 (2000) 15–16.
[70] E. Breval, J. Cheng, D. Agrawal, P. Gigl, M. Dennis, R. Roy, A. Papworth, Comparison between microwave and conventional sintering of WC/Co composites, Mater. Sci. Eng. A 391 (2005) 285–295.

[71] H.-C. Kim, I.-J. Shon, I.-K. Jeong, I.-Y. Ko, J.-K. Yoon, J.-M. Doh, Rapid sintering of ultra fine WC and WC–Co hard materials by high-frequency induction heated sintering and their mechanical properties, Met. Mater. Int. 13 (2007) 39–45.

[72] H.-C. Kim, D.-Y. Oh, I.-J. Shon, Sintering of nanophase WC–15 vol.% Co hard metals by rapid sintering process, Int. J. Refract. Met. Hard Mater. 22 (2004) 197–203.

[73] H.C. Kim, I.K. Jeong, I.J. Shon, I.Y. Ko, J.M. Doh, Fabrication of WC–8 wt.%Co hard materials by two rapid sintering processes, Int. J. Refract. Met. Hard Mater. 25 (2007) 336–340.

[74] H.-Y. Park, M.F. Kilicaslan, S.-J. Hong, Effect of multiple pressures by magnetic pulsed compaction (MPC) on the density of gas-atomized Al–20Si powder, Powder Technol. 224 (2012) 360–364.

[75] R.M. Raihanuzzaman, J.H. Kim, J.K. Lee, J.S. Yoon, H.-T. Son, S.-J. Hong, Wear behavior of Al–Fe–Cr–Ti alloys fabricated by magnetic pulsed compaction, Powder Technol. 225 (2012) 227–231.

[76] E.M. Dubensky, R.T. Nilsson, "Dense fine grained monotungsten carbide-transition metal cemented carbide body and preparation thereof," ed: Google Patents, 1998.

[77] M. Furukawa, Y. Iwahashi, Z. Horita, M. Nemoto, T.G. Langdon, The shearing characteristics associated with equal-channel angular pressing, Mater. Sci. Eng. A 257 (1998) 328–332.

[78] A.J. Pyzik, A. Hchenik, Rapid omnidirectional compaction of ceramic–metal composites, Proceedings of the 12th Annual Conference on Composites and Advanced Ceramic Materials, Part 1 of 2: Ceramic Engineering and Science Proceedings, vol. 9, 7/8, 2008, pp. 965–974.

[79] J.G. Lee, M. Lee, S. Hong, H. Lee, S. Pyun, C. Rhee, Consolidation of mixed diamond and cobalt granule powders by magnetic pulsed compaction, Mater. Lett. 64 (2010) 35–37.

[80] M. Li, H.-P. Yu, C.-F. Li, Microstructure and mechanical properties of Ti6Al4V powder compacts prepared by magnetic pulse compaction, Trans. Nonferrous Metals Soc. China 20 (2010) 553–558.

[81] T.G. Langdon, M. Furukawa, M. Nemoto, Z. Horita, Using equal-channel angular pressing for refining grain size, JOM 52 (2000) 30–33.

[82] H. Exner, Physical and chemical nature of cemented carbides, Int. Mater. Rev. 24 (1979) 149–173.

[83] R.J. Meredith, Engineers' Handbook of Industrial Microwave Heating, vol. 25, Institution of Electrical Engineers, London, 1998.

[84] W.D. Kingery, H. Bowen, D. Uhlmann, Introduction to Ceramics, Jhon Willey & Son, New York, 1976.

[85] T. Hungría, J. Galy, A. Castro, Spark Plasma sintering as a useful technique to the nanostructuration of piezo–ferroelectric materials, Adv. Eng. Mater. 11 (2009) 615–631.

[86] T. Nishimura, O. Ishibashi, S. Imasato, Some properties of WC–Co–Ni–Cr cemented carbides, Nippon Tungsten Rev. 20 (1987) 53–60.

[87] R.A. Cutler, A.V. Virkar, The effect of binder thickness and residual stresses on the fracture toughness of cemented carbides, J. Mater. Sci. 20 (1985) 3557–3573.

[88] R. Viswanadham, P. Lindquist, J. Peck, Preparation and properties of WC–(Ni, Al) cemented carbides, Sci. Hard Mater. (1981) 873–889.

[89] Z. Yin, X. Yang, B. Sun, C. Qian, T. Jin, The microstructure and properties of WC–10 (Fe, Co, Ni) cemented carbides, J. Cent.-South Inst. Min. Metall. 25 (1994) 719–722 ((China) (People's Republic of China)).

[90] P. Ettmayer, Hardmetals and cermets, Annu. Rev. Mater. Sci. 19 (1989) 145–164.

[91] H. Lee, J. Gurland, Hardness and deformation of cemented tungsten carbide, Mater. Sci. Eng. 33 (1978) 125–133.

[92] H. Gleiter, Materials with ultrafine microstructures: retrospective and perspectives, Nanostruct. Mater. 1 (1992) 1–19.

[93] R.W. Siegel, Synthesis and properties of nanophase materials, Mater. Sci. Eng. A 168 (1993) 189–197.

[94] Z.-H. Xie, M. Hoffman, Y.B. Cheng, Microstructural tailoring and characterization of a calcium α-SiAlON composition, J. Am. Ceram. Soc. 85 (2002) 812–818.

[95] Z.Z. Fang, X. Wang, T. Ryu, K.S. Hwang, H. Sohn, Synthesis, sintering, and mechanical properties of nanocrystalline cemented tungsten carbide–a review, Int. J. Refract. Met. Hard Mater. 27 (2009) 288–299.

[96] P. Kenny, Application of fracture mechanics to cemented tungsten carbides, Powder Metall. 14 (1971) 22–38.

[97] S.S. Yen, Fracture Toughness of Cemented Carbides, Lehigh University, 1971.

[98] N. Ingelstrom, H. Nordberg, The fracture toughness of cemented tungsten carbides, Eng. Fract. Mech. 6 (1974) 597–607.

[99] L. Sun, C.-C. Jia, C.-G. Lin, R.-J. Cao, VC addition prepared ultrafine WC–11Co composites by spark plasma sintering, J. Iron Steel Res. Int. 14 (2007) 85–89.

[100] R. Rumman, Effect of Particle Size and Sintering Processes on Mechanical Properties of Cemented Carbides — PhD Studies, The University of Adelaide, 2013.

Characterization of Short-Duration High-Energy Ball Milled WC–Co Powders and Subsequent Consolidations

Rumman Md Raihanuzzaman[a], Tae Sik Jeong[b], Reza Ghomashchi[a], Zonghan Xie[a], Soon-Jik Hong[b*]

[a]School of Mechanical Engineering, The University of Adelaide,
South Australia 5000, Australia
[b]Division of Advanced Materials Engineering and Institute for Rare Metals,
Kongju National University, Cheonan 330-717, South Korea

Statement of Authorship

Title of Paper	Characterization of Short-Duration High-Energy Ball Milled WC–Co Powders and Subsequent Consolidations
Publication Status	☑ Published ☐ Accepted for Publication ☐ Submitted for Publication ☐ Unpublished and Unsubmitted work written in manuscript style
Publication Details	Raihanuzzaman RM, Jeong TS, Ghomashchi R, Xie Z, Hong S-J. Characterization of Short-Duration High-Energy Ball Milled WC–Co Powders and Subsequent Consolidations. Journal of Alloys and Compounds. 2014;615:S564-S8.

Principal Author

Name of Principal Author (Candidate)	Md Raihanuzzaman Rumman		
Contribution to the Paper	I was responsible for the literature review required for this work, and designed the framework for the experimental conditions. I carried out the tests, performed the measurements and data processing, wrote the first draft of the manuscript and incorporated and addressed all comments and suggestions by other authors in subsequent revisions of the manuscript. Interpretation of data was primarily my responsibility.		
Overall percentage (%)	90%		
Certification:	This paper reports on original research I conducted during the period of my Higher Degree by Research candidature and is not subject to any obligations or contractual agreements with a third party that would constrain its inclusion in this thesis. I am the primary author of this paper.		
Signature		Date	22/12/15

Co-Author Contributions

By signing the Statement of Authorship, each author certifies that:
  i.   the candidate's stated contribution to the publication is accurate (as detailed above);
  ii.   permission is granted for the candidate in include the publication in the thesis; and
  iii. the sum of all co-author contributions is equal to 100% less the candidate's stated contribution.

Name of Co-Author	Soon Jik Hong		
Contribution to the Paper	I was supervisor of this work while it was being carried out in my lab in South Korea, and jointly contributed to refining the manuscript.		
Signature		Date	10/02/2016

Name of Co-Author	Reza Ghomashchi		
Contribution to the Paper	I was joint supervisor for the work, and contributed to refining of the manuscript.		
Signature		Date	23/12/2015

Name of Co-Author	Zonghan Xie		
Contribution to the Paper	I jointly contributed to refining of the manuscript.		
Signature		Date	15/01/2016

Name of Co-Author	Tae Sik Jeong		
Contribution to the Paper	I jointly contributed to part of the experiments.		
Signature		Date	12/02/2016

Characterization of short-duration high-energy ball milled WC–Co powders and subsequent consolidations

Rumman Md Raihanuzzaman [a], Tae Sik Jeong [b], Reza Ghomashchi [a], Zonghan Xie [a], Soon-Jik Hong [b,*]

[a] School of Mechanical Engineering, The University of Adelaide, South Australia 5000, Australia
[b] Division of Advanced Materials Engineering and Institute for Rare Metals, Kongju National University, Cheonan 330-717, South Korea

ABSTRACT

The aim of this study was to observe the effect of short-duration, high-energy ball milling on the mechanical properties of sintered WC–Co. Mixed powders of WC–7.5 wt% nano Co were ball milled at three different time using WC vial and balls, while other parameters were kept constant. The powders were then consolidated using spark plasma sintering. Density and hardness of the sintered samples were measured as a function of milling time, used to mix the powders prior to consolidation. It was found that both density and hardness increased with milling time, with hardness reaching a maximum of 14.95 GPa for the sample milled for 10 min. Microstructures of the sintered samples suggested a slight decline in grain size and increase in Co distribution with increasing milling time. It was also evident that milling of WC–Co powders resulted in the sintered samples having overall irregular shaped grains.

© 2013 Elsevier B.V. All rights reserved.

1. Introduction

Cemented carbides have been termed as one of the hardest materials, and are suitable for a number of cutting and drilling applications [1–3]. Industrial interests have grown to attain high hardness, strength, corrosion and wear resistance, and chemical and thermal stability in such carbides at elevated temperature. Among all cemented carbides, Tungsten Carbide-Cobalt (WC–Co) is the most dominant in terms of industrial applications, and displays a unique combination of mechanical properties [4].

In order to ensure desired mechanical properties in sintered WC–Co, various processing techniques and tools have been applied and modified, staring from synthesis to consolidation stage. While long duration mechanical alloying techniques have been mostly used in synthesizing hard materials, rapid MA techniques like ultrasonic field or dielectric barrier discharge plasma (DBDP) assisted ball milling [5,6] have also been successfully employed. High-energy ball milling (HEBM) is also considered quite prominent and effective in controlling initial powder size through effective refinement of both WC and Co particles [7]. The idea is to mix and refine powders to comply with the required specifications through a process that is both effective and inexpensive in nature. Such form of mechanical alloying has been widely used in mixing amorphous alloys, nitrides, nano-composites, etc. [7]. Most

reported studies that employed high energy ball milling on cemented carbides have used 10–120 h of long duration milling to either synthesize mixed WC–Co powders from elemental WC and Co, or to refine medium coarse and coarse carbides into nanocrystalline composites [8–10]. Co works as a metallic binder in the composition, has a much lower melting point than WC, and helps the hard WC grains to join upon sintering, conventionally carried out at a temperature close to the melting point of the binder. Hence, a near homogeneous mix of Co and WC prior to consolidation is highly required for ensuring good mechanical properties in the final sintered product, which is why the use of high-energy ball milling has proven to be critical. Several parameters within HEBM can affect powder morphology; namely rotational speed, milling duration, ball to powder ratio and so on [11]. Since cemented carbides are hard-to-consolidate materials, an effective change in parameters during high-energy ball milling can greatly impact the final properties of the sintered carbides. While the incorporation of conventional or nano Co as a binder increases the possibility of having reasonable fracture toughness and improved hardness, the use of HEBM introduces uneven breaking in powders, potentially leading to a change in mechanical properties upon consolidation [12,13].

The focus of the study was to observe the effect of short duration milling on the mechanical properties of sintered WC–Co, and test them against conventional non-milled, sintered sample. In addition, microstructural behavior was analyzed to understand the role of milling in ensuring a proper distribution of WC and Co before and after sintering.

---

* Corresponding author. Tel.: +82 41 521 9387; fax: +82 41 568 5776.
E-mail address: hongsj@kongju.ac.kr (S.-J. Hong).

Table 1
Specifications of WC–Co samples used in the study.

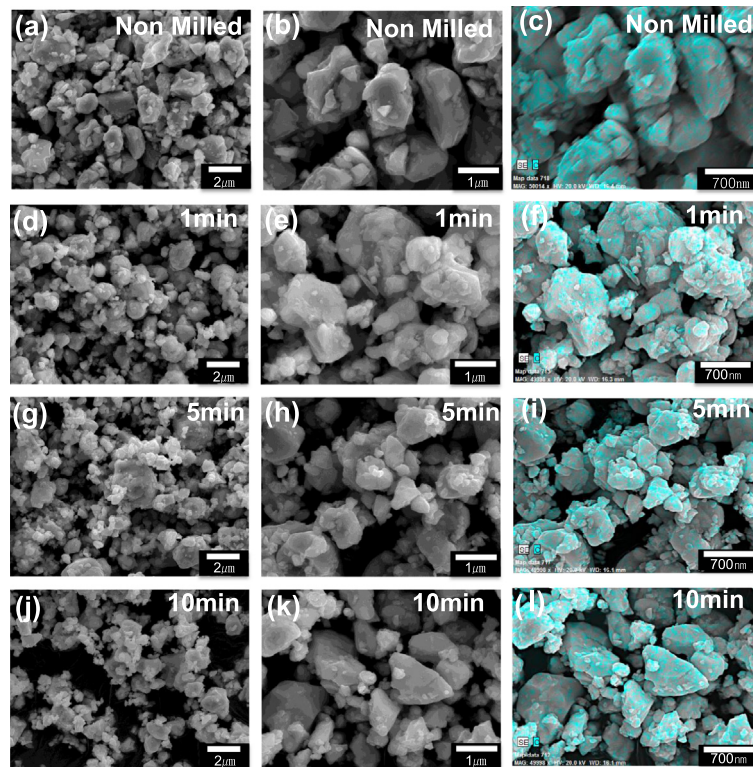| Sample	WC (wt%)	Co (wt%)	WC particle size (μm)	Co particle size (μm)	Milling time (Min)	Density (g/cm3)	Hardness (GPa)
Non milled	92.5	7.5	1–3	1–3	0	14.63	14
1 min Milled	92.5	7.5	1–3	0.3	1	15.35	14.2
5 min Milled	92.5	7.5	1–3	0.3	5	15.28	14.7
10 min Milled	92.5	7.5	1–3	0.3	10	15.5	14.95

Fig. 1. Powder morphology of (a, b) non-milled, (d, e) 1 min milled, (g, h) 5 min milled, and (j, k) 10 min milled WC–7.5 wt%Co. The non-milled powders (a–c) were commercially obtained and did not contain nano Co, whereas the milled powders (d–l) contained nano Co sized at 300 nm. Mapping of Co around WC particles are marked in cyan (c, f, i, l).

2. Experimental procedures

2.1. Powder mixing

Two types of WC–7.5 wt%Co mixed powders were used in this study. The first was commercially obtained with an average particle size of 1–3 μm, and was directly consolidated without milling. It is referred as non-milled powder in the figures. The second type of powder was of the same composition (WC–7.5 wt%Co), with the exception in Co size, which was 300 nm in average in this case. This set of WC–7.5 wt%Co was milled using a high-energy ball mill for 1 min, 5 min and 10 min, at a rotational speed of 800 rpm. For this, a WC jar and WC balls were used, without any wetting solution. The ball to powder ratio was 20:1. The jar and balls were cleaned with SiO_2 powders and ethyl alcohol solution using the high-energy ball miller, and then dried for 30 min to reduce contamination during mixing of powders.

2.2. Consolidation of powders

All four, mixed WC–7.5 wt%Co powders (commercially obtained non milled, 1 min milled, 5 min milled and 10 min milled) were consolidated using spark plasma sintering (SPS). Specifications of the samples along with their final density and hardness after consolidation are given in Table 1. At first, 2 grams of each powder mixture was poured into a graphite die, which had an inner and outer diameter of 10 mm and 40 mm, respectively. A high temperature mold release spray was applied on the die's inner wall before inserting the pins. An R-type thermocouple was

drilled into the wall of the die to read the actual temperature during sintering. The sintering temperature and pressure were set at 1350 °C and 50 MPa respectively, with a heating and cooling rate of 100 °C/min and a holding time of 10 min at sintering temperature.

2.3. Mechanical properties and microstructural analysis

After consolidation of the powders using SPS, Archimedes method was used to measure the densities of the samples. For etching of the sintered samples, Murakami reagent was used for approximately 2 min prior to using field emission scanning electron microscopy (FE-SEM). Hardness tests were carried out on polished surfaces using an Instron 2000 Vickers Hardness tester, with 30 kgf of load and 15 s of dwell time. The results are averages of 5 indentations. For both low and high magnification micrographs, TESCAN (MIRA LMH) FE-SEM was used, with secondary electron as the contrast.

3. Results and discussion

The primary understanding of how particles behave after final consolidation depends greatly on the initial information of particles. The morphologies of the mixed WC–Co powders used in this study are shown in Fig. 1. The apparent nature of the particles that can be seen from the figure is typical for WC–Co. However a

decrease in particle size with increased milling time, even if it is as low as 10 min, was observed. The non-milled powders were mostly irregular in shape although there was presence of spherical particles. With milling time, along with the decrease in size, the irregularities in shape increased, which conforms to the idea of uneven particle breaking under such high energy milling conditions. Besides, unlike most studies, the use of WC jar and balls may have caused greater and stronger inter and intra particle collision during milling. The Co mapping in the figure (c, f, i, l) also shows traces of increasing Co content around coarse WC with milling time. This enhanced distribution of a softer metallic binder around metallic carbide is critical in allowing WC particles or grains to bond during consolidation stage, at an elevated temperature. One possible explanation of the nearly homogeneous distribution within such short period of time is the contribution of the size difference between WC (1–3 μm) and Co (300 nm), which potentially can position smaller Co particles between and around larger WC particles or grains.

The XRD traces of both non-milled and milled WC–7.5 wt%Co are illustrated in Fig. 2. While Fig. 2(a) shows the XRD patterns in mixed powders before sintering, Fig. 2(b) shows the ones in sintered samples. It can be easily identified that there is a clear evidence of peak broadening in WC indicating a drop in crystalline size during milling, although it was much less than the usual decline that results only from several hours of milling [12,14]. It is worth noting that there are some fundamental differences based on experimental observations between short and long duration high-energy mall milling of cemented carbides. Unlike short duration milling, studies [9,15] that have employed long duration milling on nano or micro-crystalline WC–Co suggest that there is a usual mechanically induced, allotropic fcc-Co to hcp-Co transformation during such long milling time, which is a strong indication of the milling intensity. In addition, the presence of α-Co, which may be visible after low milling duration, completely disappears after long hours of milling, although α-Co was not seen in this study either. The sharp Bragg diffraction peaks of WC at the start of milling reconfirmed the initial coarse nature of the particles. Although it was possible to identify the presence of Co peaks in the milled powder, their intensity was very low. This is partly because of the low concentration of Co within the composition and partly due to the difference between Co and WC particle. Usual Co peaks are traced at 44, 52 and 65 theta degree angles. In the sintered samples, the reflection of the difference in milling time through peak broadening was missing, as seen in Fig. 2(b), suggesting little or no change in WC grain size in sintered carbides.

The changes in terms of cross sectional microstructure in sintered WC–7.5 wt%Co as a function of milling time is shown in Fig. 3. Fig. 3(a, d, g, j) focuses on the nature of the grains, mainly WC, while Fig. 3(b, e, h, k) primarily concentrates on the propagation of cracks, along with the presence of Co within the microstructure (inset, marked in green[1]). It can be clearly seen that the grains are mostly of WC and are quite irregular in shape. Although there has not been a huge grain growth after sintering, it was possible to see that the grain size after sintering has slightly reduced with increased milling time. The dot mapping, marked in green, also confirms that there are more Co rich zones in the 10 min milled (sintered) sample (Fig. 3(k)) than the non-milled sintered one (Fig. 3(b and e)). The apparent greater homogeneity of Co in WC helps in creating a better WC–Co grain skeleton, resulting in limiting grain growth to a reasonable extent as opposed to the less homogeneously distributed WC–Co structure [16]. In cemented carbides, metallic Co binder is known for preventing the propagation of cracks by shielding
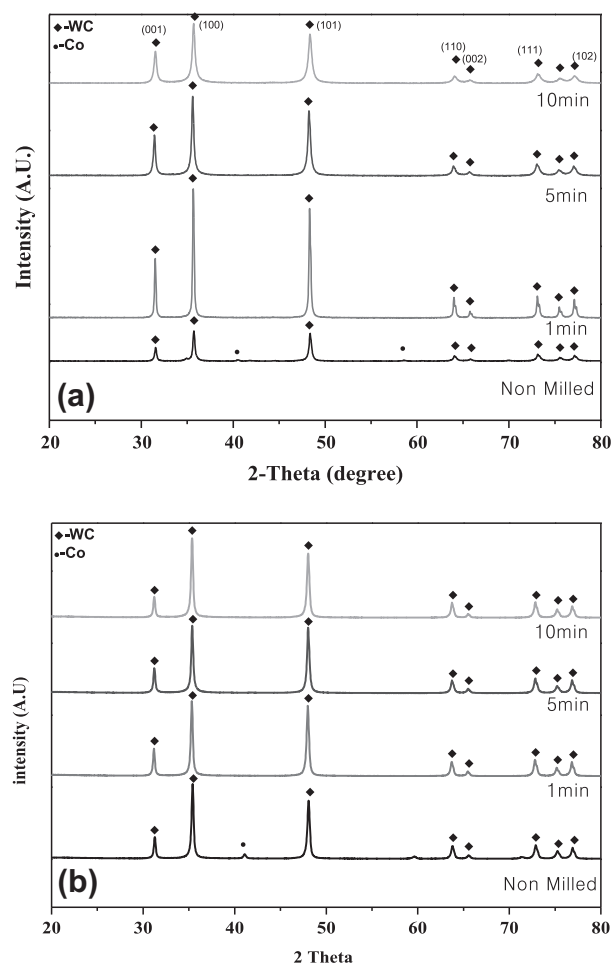

Fig. 2. XRD traces of non-milled and milled powders (a) before sintering and (b) after sintering.

a stress field around the tip of the crack. Alternatively, it can create a link or bridge between the crack ligaments after the initiation of the crack [17]. Fig. 3(c, f, i, l) shows EDS analysis of the samples, confirming the presence of all elements, although traces of Co were difficult to locate. However, the localized EDS confirmed an increase in Co content with milling time, reaching a maximum of 1.29% for the 10 min milled sintered sample, effectively contributing to the grain size, and presumably to the hardness and relative density.

The aforementioned microstructures, especially the drop in grain size with milling time, and the increased homogeneity of Co in WC matrix indicate a change in mechanical properties as well. Fig. 4 shows the relative density and hardness results with respect to milling time. Conform to expectations; both hardness and density increased with increasing milling time, reaching a maximum of 14.95 GPa and 15.5 g/cm^3, respectively. The increase in hardness is influenced by several factors: the decrease in grain size and increase in Co distribution with milling time. In addition, the sintering temperature of 1350 °C at a pressure of 50 MPa ensured liquid phase sintering of Co, migrating and re-precipitating on the surface of the original WC [18].

4. Conclusion

In this study, mixed powders of WC – 7.5 wt%Co were ball milled for 1 min, 5 min and 10 min, with subsequent consolidation using spark plasma sintering. The main conclusions are as follows:

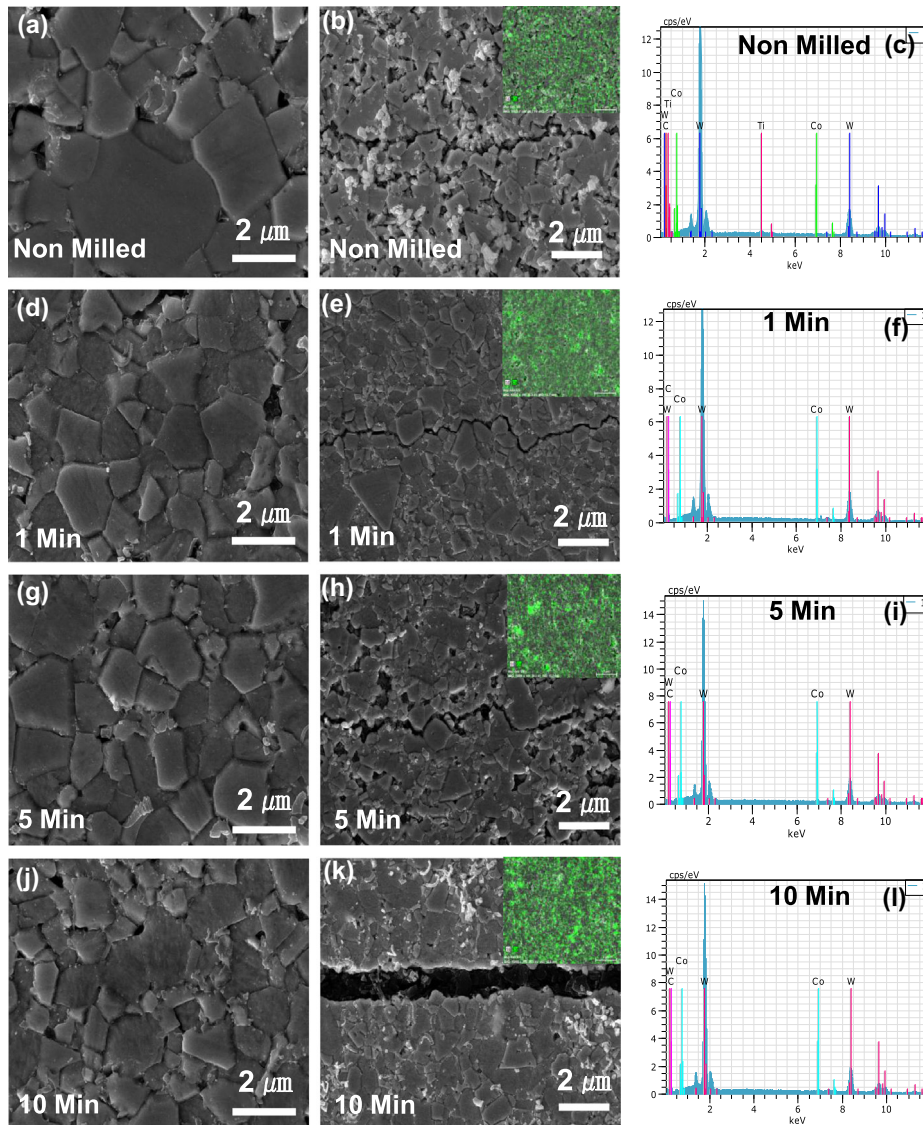[1] For interpretation of color in Fig. 3, the reader is referred to the web version of this article.

Fig. 3. Cross sectional scanning electron micrographs of (a, b) non milled, (d, e) 1 min milled, (g, h) 5 min milled and (j, k) 10 min milled sintered WC–7.5 wt%Co. The non-milled powders were commercially obtained and do not contain nano Co, whereas the milled powders contain nano Co sized at 300 nm. EDS analysis (c, f, I, l) confirms the presence of W, C and Co in all sintered samples. Insets in figures (b, e, h, k) show dot mapping of Co present in the samples.
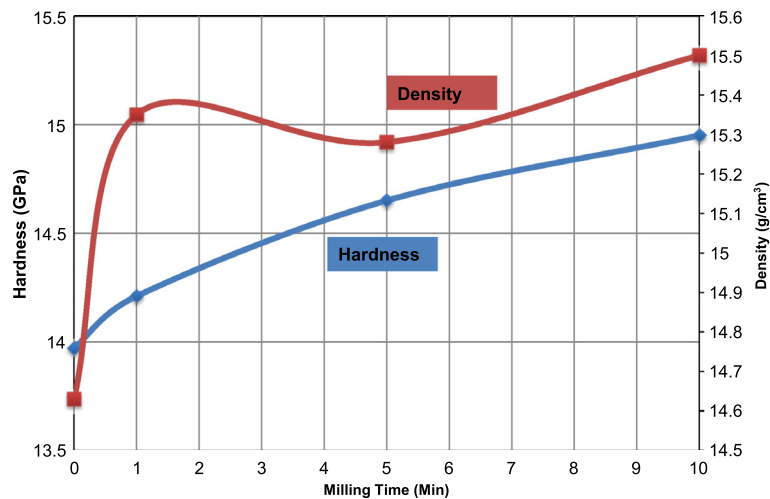

Fig. 4. Changes in hardness and relative density of WC–7.5 wt%Co samples with milling time.

(i) With an increase in milling time, finer particles of metallic Co binder got more homogeneously distributed around coarse WC.

(ii) Grain size in the sintered samples has been found to reduce with increasing milling time.

(iii) Relative density and hardness both increased due to slight drop in grain size and improved Co distribution.

(iv) Although coarse particles of WC went through uneven breaking during high-energy ball milling, the greater homogeneity of nano Co within WC matrix helped overcome the bonding adversities, and resulted in displaying reasonably high mechanical property.

Acknowledgements

References

[1] X. Wang, Y. Xie, H. Guo, O. Van der Biest, J. Vleugels, Rare Metal 25 (2006) 246–252.
[2] J. Sun, F. Zhang, J. Shen, Mater. Lett. 57 (2003) 3140–3148.
[3] V.K. Sarin, Adv. Powder Technol. (1981) 253–288.
[4] P. Ettmayer, Annu. Rev. Mater. Sci. 19 (1989) 145–164.
[5] M. Zhu, L. Dai, N. Gu, B. Cao, L. Ouyang, J. Alloys Comp. 478 (2009) 624–629.
[6] M. Zhu, X. Bao, X. Yang, N. Gu, H. Wang, M. Zeng, L. Dai, Metall. Mater. Trans. A 42 (2011) 2930–2936.
[7] M.S. El-Eskandarany, A.A. Mahday, H. Ahmed, A. Amer, J. Alloys Comp. 312 (2000) 315–325.
[8] Z.Z. Fang, X. Wang, T. Ryu, K.S. Hwang, H. Sohn, Int. J. Refract. Met. Hard Mater. 27 (2009) 288–299.
[9] M. Xueming, J. Gang, J. Alloys Comp. 245 (1996) L30–L32.
[10] S. Liu, Z-L. Huang, G. Liu, G-B. Yang, Int. J. Refract. Met. Hard Mater. 24 (2006) 461–464.
[11] M. Xueming, Z. Ling, J. Gang, D. Yuanda, J. Mater. Sci. Lett. 16 (1997) 968–970.
[12] J-W. Song, R.M. Raihanuzzaman, S-J. Hong, Powder Technol. 235 (2012) 723–727.
[13] J.H. Kim, R. Md Raihanuzzaman, C.K. Rhee, J.G. Lee, M.K. Lee, S-J. Hong, Mater. Trans. – JIM 52 (2011) 1156.
[14] B.G. Butler, Int. J. Powder Metall. 43 (2007) 35–43.
[15] F. Zhang, C. Wang, M. Zhu, Scripta Mater. 49 (2003) 1123–1128.
[16] S-J. Hong, M.R. Rumman, C.K. Rhee, Effect of magnetic pulsed compaction (mpc) on sintering behavior of materials, in: D.A. Lakshmanan (Ed.), Sintering of Ceramics – New Emerging Techniques, InTech Publication, Croatia, 2012, pp. 159–176.
[17] S.I. Cha, S.H. Hong, B.K. Kim, Mater. Sci. Eng., A 351 (2003) 31–38.
[18] K. Mohan, P. Strutt, Nanostruct. Mater. 7 (1996) 547–555.

Conventional Sintering of WC with Nano-Sized Co Binder: Characterization and Mechanical Behaviour

Rumman Md. Raihanuzzaman[a], Seung-Taek Han[b], Reza Ghomashchi[a], Hyo-Seob Kim[b], Soon-Jik Hong[b*]

[a]School of Mechanical Engineering, The University of Adelaide,
South Australia 5005, Australia
[b]Division of advanced Materials Engineering, Kongju National University,
Cheonan, Chungnam 331-717, South Korea

Statement of Authorship

Title of Paper	Conventional Sintering of WC with Nano-Sized Co Binder: Characterization and Mechanical Behaviour
Publication Status	☑ Published ☐ Accepted for Publication ☐ Submitted for Publication ☐ Unpublished and Unsubmitted work written in manuscript style
Publication Details	Raihanuzzaman RM, Han S-T, Ghomashchi R, Kim H-S, Hong S-J. Conventional Sintering of WC with Nano-sized Co Binder: Characterization and Mechanical Behaviour. International Journal of Refractory Metals and Hard Materials. 2015.

Principal Author

Name of Principal Author (Candidate)	Md Raihanuzzaman Rumman
Contribution to the Paper	I was responsible for the literature review required for this work, and designed the framework for the experimental conditions. I carried out the mechanical property and microstructural behaviour analysis, wrote the first draft of the manuscript and incorporated and addressed all comments and suggestions by other authors in subsequent revisions of the manuscript. Interpretation of data was primarily my responsibility.
Overall percentage (%)	80%
Certification:	This paper reports on original research I conducted during the period of my Higher Degree by Research candidature and is not subject to any obligations or contractual agreements with a third party that would constrain its inclusion in this thesis. I am the primary author of this paper.
Signature	Date 22/12/15

Co-Author Contributions

By signing the Statement of Authorship, each author certifies that:
  i.   the candidate's stated contribution to the publication is accurate (as detailed above);
  ii.   permission is granted for the candidate in include the publication in the thesis; and
  iii.   the sum of all co-author contributions is equal to 100% less the candidate's stated contribution.

Name of Co-Author	Soon Jik Hong
Contribution to the Paper	I was supervisor of this work while it was being carried out in my lab in South Korea in collaboration with TaeguTec Industries, and jointly contributed to refining the manuscript.
Signature	Date 10/02/2016

Name of Co-Author	Reza Ghomashchi
Contribution to the Paper	I was joint supervisor for the work, and contributed to refining the manuscript.
Signature	Date 23/12/2015

Name of Co-Author	Hyo Seob Kim
Contribution to the Paper	I jointly contributed to conducting some parts of the experiments.
Signature	Date 29/01/2016

Name of Co-Author	Seung-Taek Han
Contribution to the Paper	I jointly contributed to conducting some parts of the experiments.
Signature	Date 10/02/2016

Conventional sintering of WC with nano-sized Co binder: Characterization and mechanical behavior

Rumman Md. Raihanuzzaman [a], Seung-Taek Han [b], Reza Ghomashchi [a], Hyo-Seob Kim [b], Soon-Jik Hong [b,*]

[a] School of Mechanical Engineering, The University of Adelaide, South Australia 5005, Australia
[b] Division of advanced Materials Engineering, Kongju National University, Cheonan, Chungnam 331-717, South Korea

ARTICLE INFO

ABSTRACT

In this study, WC particles of 1–3 μm were blended with two different sizes of Co particles and sintered conventionally at two different temperatures. Compaction of initial powders was carried out using a relatively new dynamic compaction method called Magnetic Pulsed compaction (MPC). The maximum Vickers hardness for the samples found was around 1353 HV (13.27 GPa), while the maximum fracture toughness was observed at 4.6 MPa · m$^{1/2}$. The marked changes in density, hardness, fracture toughness and crack behavior observed in the samples indicate strong correlations among particle size, sintering process and mechanical properties of cemented carbides. In addition, the nature of crack initiation and propagation, which is indicative of the trend in fracture toughness of materials, was observed and analyzed.

© 2015 Elsevier Ltd. All rights reserved.

1. Introduction

Cemented carbides have been used in industrial cutting and drilling applications for over a century. Out of all carbides, Tungsten Carbide (WC), with finely distributed Cobalt (Co) or other softer materials acting as binders, have been the most successful and used constituents, as they are known to display an excellent combination of hardness and wear resistance, toughness and stiffness [1–3]. A number of early studies on such carbides have focused on issues related to finding the right composition, consolidation temperature and ways to improve mechanical properties of the final products that were expected to be commercially used [4]. In recent years, however, the focus has shifted towards the study of approaching new ways and methods of powder processing altogether in an attempt to discover convenient and effective ways to manufacture these carbides. It has ranged from introducing different types of powders to incorporating multiple stages of processing to achieve better performance [5,6].

The fabrication of these carbides is considered to be quite difficult as opposed to many other composites that are aimed towards similar applications. While some of the modern techniques use simultaneous compaction and heating as the method for carbide bits production, the conventional route still uses them as separate processes [7]. Although conventional processing takes a longer time, it is still thought of as one of the stable processing routes for the manufacture of carbide products with economic incentives. Several attempts have been made to control the grain growth of these materials during the process by either incorporating commercial grain growth inhibitors, different sizes of initial powders—from coarse to fine, (micron to nanometer range), or just by making adjustments to the timing of the processing steps involved [8,9]. Since the binder within the composition of these carbides is primarily responsible for joining the particles at elevated temperature, attention has also been given in employing ultrafine and nanograde particles as an alternative, which can potentially help study the changes in grain growth and mechanical properties of these carbides.

Over the last few years, dynamic compaction has shown promising results for a wide range of metals and composites, aimed at reducing compaction time to even fractions of a second [5,10,11]. Magnetic pulse compaction (MPC) is one of the short-duration, high-impact compaction processes that are capable of manufacturing improved cemented carbide products in green compact form [12], with reasonably high initial density. Since pressure is one of the major factors affecting the quality of the products, the study of such dynamic compaction process is all the more critical in understanding how it behaves for carbides.

In this study, two sets of WC–7.5 wt.% Co powder mixtures having different sizes of Co particles were pressed using magnetic pulse compaction, followed by conventional sintering. This study will particularly help in understanding the contribution of fine and nano/ultrafine Co towards mechanical properties and microstructural behavior of WC–Co, as well as the contribution of temperature variation during sintering.

* Corresponding author at: Division of Advanced Materials Engineering, Kongju National University, 275 Budae-dong, Cheonan, Chungnam 331–717, South Korea.
E-mail address: hongsj@kongju.ac.kr (S.-J. Hong).

2. Experimental procedure

WC particles of irregular hexagonal shape, sized at 1–3 μm, with 0.1 (wt.%) total oxygen, 0.06 (wt.%) free carbon and 6.10–6.18 (wt.%) carbon content were mixed with both 1–3 μm and 200–300 nm sized Co particles to prepare two different types of samples. The details of the samples are given in Table 1. Cobalt (Co) powders used in this study were prepared using Pulsed Wire Evaporation (PWE) equipment, and were sized at 200–300 nm and 1–3 μm range, which was controlled though changes made in input voltage. Powders were mixed using a high-energy ball mill. The process started by first placing the powders in a stainless steel container with WC inner lining and then mixing them with 10 mm diameter Ti coated stainless steel ball bearings with a ball to powder weight ratio of 5:1. The speed of rotation was set at 500 rpm and was used for 5 min to mix the powders under dry conditions. Powders were first compacted using a magnetic pulse compaction machine. Pressure was set at 1.5 GPa for all samples, while duration was observed at 0.3 s. A single action die was used for all compaction. The green compacts were then sent to TaeguTec Ltd* for conventional sintering. The samples were sintered at two different temperatures; 1400 and 1450 °C. The heating rate, cooling rate and holding time are not disclosed for this set of experiments.

The samples were sectioned after sintering, mounted and conventionally prepared (down to 1 μm diamond paste) for metallographic analysis. For etching, a batch of Murakami reagent was prepared. Density of the WC–Co samples was measured by Archimedes method, weighing them in water and air. Hardness measurements were performed on a Vickers Micro Hardness tester, with 1 kgf load. For microstructural analysis including crack length measurements, a TESCAN MIRA LMH FE-SEM was used. Since the sintered samples were quite small in size, fracture toughness values were calculated using the following equation [13]:

$$K_{1c} = 0.016\sqrt{(E \div H)}\left(P \div c^{3/2}\right) \qquad (1)$$

where E is Young's modulus [14–16], H is the hardness of the material measured using a Vickers Micro Hardness tester, P is the indentation load, and c is half of the average indentation crack length. The crack lengths are measured from the initiation points, which are along the edges of the indentation marks, till the end of the propagation.

3. Results and discussion

For hard-to-consolidate materials, it is of great importance that the composition or mixture is homogeneous in nature; which not only ensures greater chances of displaying the desired mechanical properties, but also reduces the probability of the green compacts and sintered carbides of failing through surface and/or edge cracking. Fig. 1 shows the SEM micrographs and EDS analysis of both WC–7.5 Co and WC–7.5 nano-Co. While both powders illustrate a homogeneous mixture (c and d) of WC and Co, it can also be noticed that WC–7.5 nano-Co powders are slightly more irregularly shaped than the other sample. The difference in nature in Fig. 1(b) can be attributed to the difference in size between both particles, which may have caused WC particles to collide more during the milling process, resulting them to break in

an uneven manner, slightly more than what can be seen in Fig. 1(a), where both WC and Co particles are of the same initial size. In addition, the binder content within the composition is quite low, and is only present to facilitate the bonding between particles in the presence of a liquid phase, usually observed at elevated temperatures. The size of the particles in general however does not suggest that they have gone through much agglomeration within the short duration of mechanical milling, carried out at a relatively low speed. It is also understood that most mechanical mixing processes [17,18] can potentially result in the particles being slightly unevenly shaped, except where spray conversion was used [2,19].

Fig. 2 shows the XRD patterns of both samples, sintered at two different temperatures. The WC peaks are quite prominent in all samples, which confirm the concentration. Co peaks were found to be difficult to detect due to its low concentration in the samples. It is understood that the liquid phase transformation of Co at high temperature in carbides may also be one of the reasons for displaying such low intensity. Furthermore, the presence of α-Co (fcc structured phase), which is usually visible after short duration milling [3], seemed to have disappeared after high temperature sintering. The identified peaks were detected to be of hcp structure. Traces of Co peaks are usually identified at 44 (fcc α-Co and hcp ε-Co), 52 (fcc α-Co), 65, 77 (fcc α-Co and hcp ε-Co) and 92 (fcc α-Co and hcp ε-Co) 2θ angles. In addition to the XRD traces in this study, reports, including our previous work, suggest that there is not much peak broadening observed after sintering, which is indicative of similar grain or crystalline size within the microstructure [5,20].

Fig. 3 shows the changes in density (a) and hardness (b) with respect to sintering temperature and Co particle size within the composition. It can be quite clearly interpreted that both density and hardness are illustrating incremental patterns with decreasing particle size from micron to nanolevel. However when it comes to sintering temperature, there isn't such a shift noticed for the samples. It is safe to assume that slight changes in temperature do not reflect on these properties of sintered cemented carbides. In addition, the fact that both temperatures are below the melting point of the primary binding constituent of the composition can also be related to the absence of change in density and hardness profiles. It can also be said that the change in interfacial energy between solid and liquid phase is not sufficient within this temperature range to instill a difference in wettability status between the phases. In other words, the first stage of liquid phase sintering, which is a dominant step for rearrangement of particles, has not varied enough to affect the solubility behavior of the constituents of the phases; which otherwise could contribute to a change in density, and therefore, hardness, through further microstructural evolution [4]. On the other hand, when temperature is kept constant, there seems to be an increasing pattern in both density and hardness with respect to the decrease in Co particle size. While several factors can be involved here, one possible explanation includes the idea that nanoparticles tend to impart faster diffusion between grains, promptly initiate necking behavior between constituents, as opposed to how coarse or fine grained phases would behave under such sintering conditions. It is also expected the nano-Co particles occupy WC interparticle spaces and thus increase density while this is not the case for micron size Co particles. During hardness test, indentations were generated on the surface and along the cross section of the sintered samples, which resulted in the initiation and propagation of cracks along the edges of the indentations, as shown in

Table 1
Mixing and processing conditions of WC–Co powders.

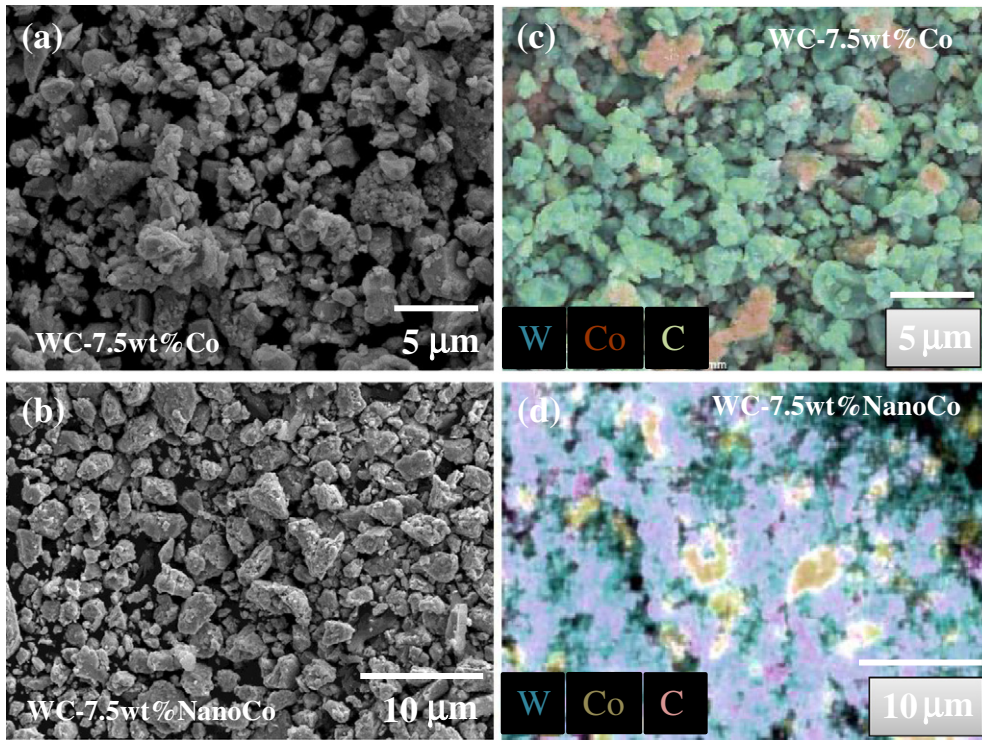| Sample number	Composition	Size of WC particle	Size of Co particle	Milling time (min)	Weight of mixed powder (g)	Compaction pressure (GPa)	Sintering temperature (°C)	Con size (μm)
1	WC–7.5 Co	1–3 μm	1–3 μm	5	2.0	1.5	1400	204.7
2	WC–7.5 Co	1–3 μm	200–300 nm	5	2.0	1.5	1400	202.2
3	WC–7.5 Co	1–3 μm	1–3 μm	5	2.0	1.5	1450	203.6
4	WC–7.5 Co	1–3 μm	200–300 nm	5	2.0	1.5	1450	204.1

Fig. 1. SEM micrographs (SE) of initial (a) WC–7.5 wt.% Co [5] and (b) WC–7.5 wt.% nano-Co powders, and mapping images of initial (c) WC–7.5 wt.% Co and (d) WC–7.5 wt.% nano-Co powders.

the insets. The higher hardness values for WC–7.5 wt.% nano-Co is expected due to its higher density numbers.

For most materials, hardness trends with respect to any parameters like temperature, pressure or grain size can be a strong indication towards the understanding of the toughness, expected under similar experimental conditions. When it comes to cemented carbides, it is already quite well established that there is an inversely proportional relationship between hardness and grain size in sintered condition, irrespective of the process involved. The same can be said about crack length and fracture toughness, as shown in Fig. 4. It is clear that the decrease in crack length can cause the material to display increased fracture toughness. It can be said here also that temperature within this 1400–1450 °C range plays an almost negligible role towards changes in crack length behavior or fracture toughness, while Co particle size still seems to be influential. Previous studies [8,14,21] suggest that it is

unlikely for sintered cemented carbides to have high hardness and fracture toughness at the same time for a specific set of conditions. But an alternative hypothesis [22,23] indicates the possibility of having grain
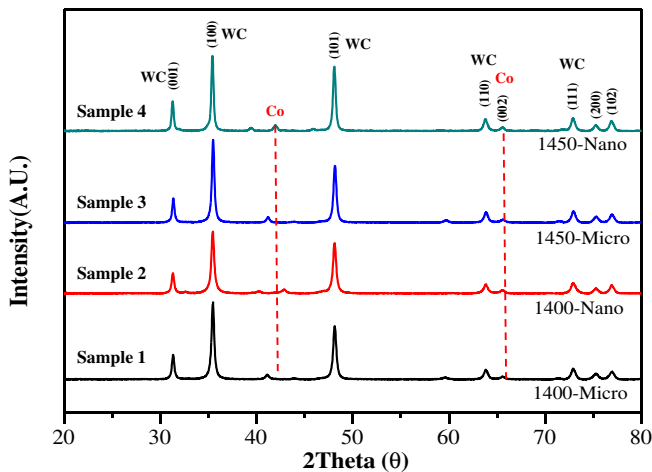

Fig. 2. X-ray diffraction patterns of WC–7.5 wt.% Co and WC–7.5 wt.% nano-Co with respect to varying sintering temperature.
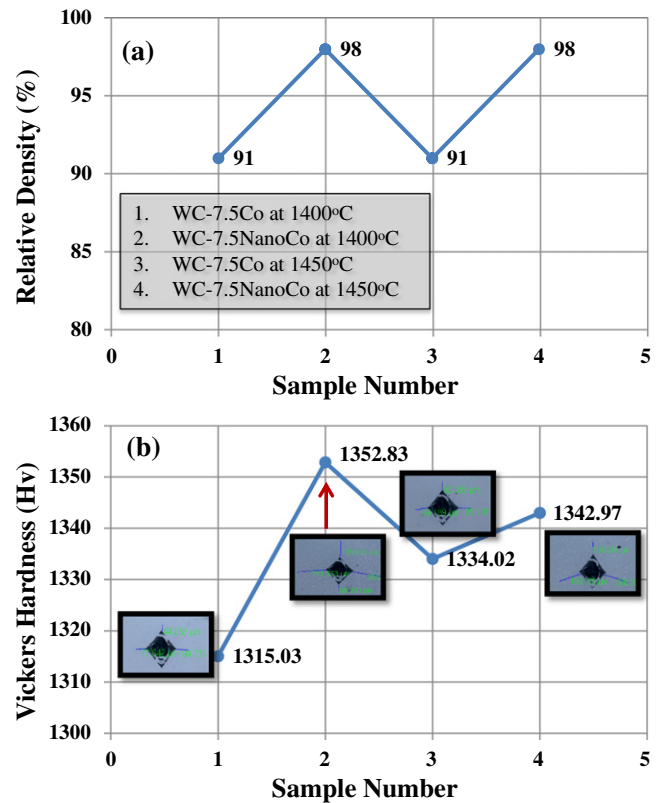

Fig. 3. Changes in a) relative density and b) Vickers hardness of WC–7.5 wt.% Co with respect to varying sintering temperature and initial particle size of Co as part of the composition.
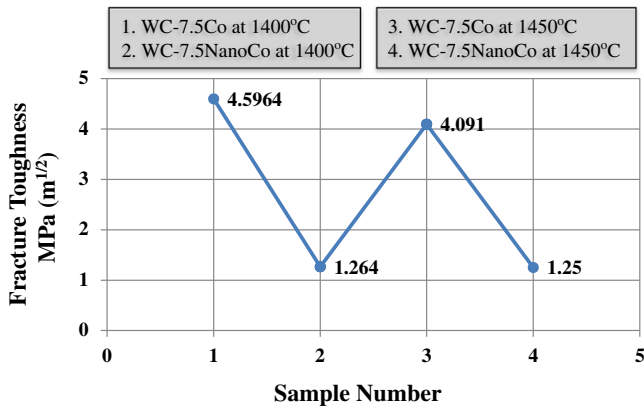
Fig. 4. Changes in fracture toughness of WC–7.5 wt.% Co with respect to varying sintering temperature and initial particle size of Co as part of the composition. It needs to be mentioned that the number of cracks generated along the edges of the indentations can differ without illustrating much microstructural differences.

boundaries with high volume fraction in nanomaterial, resulting in impediments against propagation of cracks, translated into displaying higher fracture toughness and hardness, simultaneously. But the results in this study appear to be opposing that hypothesis. This could be reasoned by saying that the percentage of nanomaterial present in the sample was too small to follow the hypothesis, added to the fact that the size of Co particles was not below 100 nm, the more argued threshold below which materials are to be considered nanostructured [24]. However, it may be argued that the lower fracture toughness values for the WC–7.7 wt.% nano-Co is due to the lack of large Co particles acting as crack arrestor and greater WC–WC particle contact in the nano-Co binder samples facilitated crack propagation. So it might be possible to have a higher volume fraction of grain boundaries through the use of both WC and Co as nanoparticles. The dissimilarity in particle size can be argued to cause an inadequacy in crack arrestors within the composition, which is eventually causing the results to follow one of the hypothesis

mentioned earlier [22,23]. In order to be able to achieve high hardness and fracture toughness in a specific set of samples, a number of factors including but not limited to, similarity in particle size and shape, composition, presence of appropriate amount of binders and WC–Co or other phases through reactive or conventional sintering mechanism need to be considered and monitored carefully. Otherwise, the high brittleness of cemented carbide particles, added to the high percentage of WC present within the composition would easily cause the intergranular or trans-granular cracks to propagate faster in response to hardness indentations, causing it to illustrate an inverse relationship between hardness and fracture toughness.

Fig. 5(a, b) shows SEM micrographs of WC–7.5 Co and WC–7.5 nano-Co, along with their spectrum analysis and quantification. It is clearly visible from the spectrum analysis that both WC and Co are present in the sintered interface, and in right proportions, as confirmed from the quantification. The nature of the grains is quite irregular, which can be resulted from grain agglomeration as well as growth. However, the changes in mechanical properties and other microstructural features including crack analysis suggest against a huge disparity in terms of grain size between and within the samples. The phase within the microstructure is predominantly WC, as the expected liquid binder phase, even if it has not varied enough to affect the solubility behavior of the constituents of the phases, is thought to be channeled towards boundaries and interface between grains. However, it needs further interfacial analysis between grains to confirm the liquid phase formation of Co and its extent. The change in contrast is observed due to the difference in carbon content present in the samples, which could have resulted from either the coating material purposed for creating a conductive pathway, or from the (free/regular) carbon content present within WC. Traces of Ti could be a result of either elemental residues left during coating of samples or milling of initial powders using Ti coated stainless steel balls.

4. Conclusion

The focus of this study was to observe how changes in conventional sintering temperature and binder particle size affect mechanical
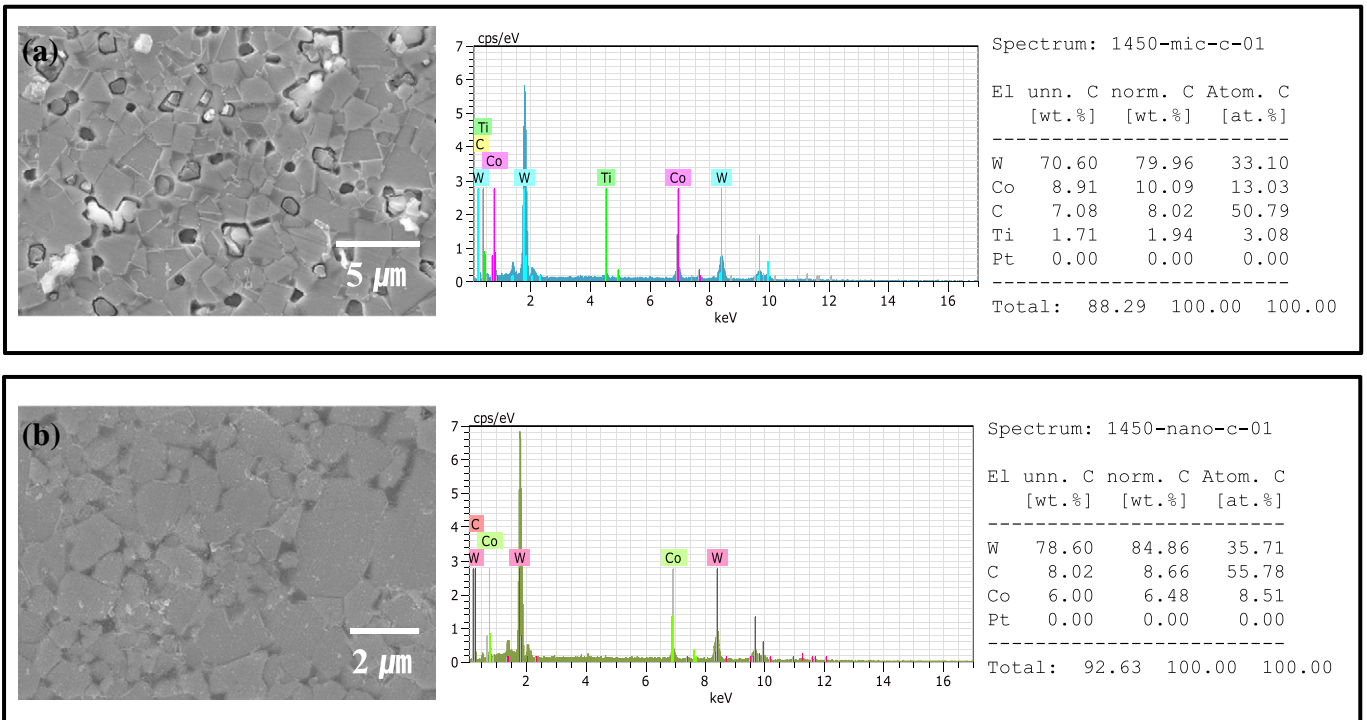

Fig. 5. Cross sectional micrographs of a) WC–7.5 wt.% Co sintered at 1450 °C, and b) WC–7.5 wt.% nano-Co sintered at 1450 °C, along with their spectrum analysis and quantification of elemental presence within selected area.

properties and microstructural behavior of WC–Co. During the process, it was found that the binder (Co) particle size has an inversely proportional relationship with density and hardness, while crack length appeared to have a similar relationship with fracture toughness. The lower fracture toughness values were attributed to lack of large Co particles acting as crack arrestor and also higher percentages of WC–WC contact in the nano-Co binder samples. Sintering temperatures at which the samples were treated for several hours, did not seem to have quite an impact on the properties, and primarily contributed towards stabilizing the homogeneity from a microstructural point of view. WC was found to be the dominant phase in all sintered samples, although Co was homogeneously distributed as a combined result of using high energy ball milling of powders, employing MPC for pre-compaction and several hours of conventional sintering for phase stabilization.

Acknowledgment

References

[1] H. Exner, Analysis of grain-and particle-size distributions in metallic materials, Int. Mater. Rev. 17 (1972) 25–42.

[2] S.I. Cha, S.H. Hong, G.H. Ha, B.K. Kim, Mechanical properties of WC–10Co cemented carbides sintered from nanocrystalline spray conversion processed powders, Int. J. Refract. Met. Hard Mater. 19 (2001) 397–403.

[3] F. Zhang, C. Wang, M. Zhu, Nanostructured WC/Co composite powder prepared by high energy ball milling, Scr. Mater. 49 (2003) 1123–1128.

[4] S. Bhaumik, G. Upadhyaya, M. Vaidya, Full density processing of complex WC-based cemented carbides, J. Mater. Process. Technol. 58 (1996) 45–52.

[5] J.-W. Song, R.M. Raihanuzzaman, S.-J. Hong, Consolidation of WC–Co alloys by magnetic pulsed compaction and evaluation of their mechanical properties, Powder Technol. 235 (2012) 723–727.

[6] R.M. Raihanuzzaman, Z. Xie, S.J. Hong, R. Ghomashchi, Powder refinement, consolidation and mechanical properties of cemented carbides—an overview, Powder Technol. 261 (2014) 1–13.

[7] R.M. Raihanuzzaman, J.-W. Song, S.-J. Hong, Evaluation of mechanical properties and processing conditions of WCCo alloys fabricated by magnetic pulsed compaction, J. Alloys Compd. 536 (2012) S211–S215.

[8] Z.Z. Fang, X. Wang, T. Ryu, K.S. Hwang, H. Sohn, Synthesis, sintering, and mechanical properties of nanocrystalline cemented tungsten carbide—a review, Int. J. Refract. Met. Hard Mater. 27 (2009) 288–299.

[9] T. Chookajorn, H.A. Murdoch, C.A. Schuh, Design of stable nanocrystalline alloys, Science 337 (2012) 951–954.

[10] J.H. Kim, R.Md Raihanuzzaman, C.K. Rhee, J.G. Lee, M.K. Lee, S.-J. Hong, Fabrication and densification behavior analysis of metalizing targets using ZrO2 nanopowders by magnetic pulsed compaction, Mater. Trans. JIM 52 (2011) 1156.

[11] R.M. Raihanuzzaman, J.H. Kim, J.K. Lee, J.S. Yoon, H.-T. Son, S.-J. Hong, Wear behavior of Al–Fe–Cr–Ti alloys fabricated by magnetic pulsed compaction, Powder Technol. 225 (2012) 227–231.

[12] S.-J. Hong, M.R. Rumman, C.K. Rhee, Effect of magnetic pulsed compaction (MPC) on sintering behavior of materials, in: D.A. Lakshmanan (Ed.), , Sintering of Ceramics — New Emerging Techniques, InTech Publishers, Croatia 2012, pp. 159–176.

[13] Z.-H. Xie, M. Hoffman, Y.B. Cheng, Microstructural tailoring and characterization of a calcium α-SiAlON composition, J. Am. Ceram. Soc. 85 (2002) 812–818.

[14] S.I. Cha, S.H. Hong, B.K. Kim, Spark plasma sintering behavior of nanocrystalline WC–10Co cemented carbide powders, Mater. Sci. Eng. A 351 (2003) 31–38.

[15] A. Santhanam, P. Tierney, J. Hunt, Cemented carbides, 10th ed., ASM International, Metals Handbook, 2 1990, pp. 950–977.

[16] S. Coromant, Modern Metal Cutting: A Practical Handbook, Sandvik Coromant, 1994.

[17] M. Xueming, Z. Ling, J. Gang, D. Yuanda, Preparation and structure of bulk nano-structured WC–Co alloy by high energy ball-milling, J. Mater. Sci. Lett. 16 (1997) 968–970.

[18] J. Sun, F. Zhang, J. Shen, Characterizations of ball-milled nanocrystalline WC–Co composite powders and subsequently rapid hot pressing sintered cermets, Mater. Lett. 57 (2003) 3140–3148.

[19] B. Kim, G. Ha, D. Lee, Sintering and microstructure of nanophase WC/Co hardmetals, J. Mater. Process. Technol. 63 (1997) 317–321.

[20] B.G. Butler, L. JUN, Z.Z. Fang, R.K. Rajamani, Production of nanometric tungsten carbide powders by planetary milling, Int. J. Powder Metall. 43 (2007) 35–43.

[21] N. Ingelstrom, H. Nordberg, The fracture toughness of cemented tungsten carbides, Eng. Fract. Mech. 6 (1974) 597–607.

[22] H. Gleiter, Materials with ultrafine microstructures: retrospective and perspectives, Nanostruct. Mater. 1 (1992) 1–19.

[23] R.W. Siegel, Synthesis and properties of nanophase materials, Mater. Sci. Eng. A 168 (1993) 189–197.

[24] L. Hodson, M. Methner, R.D. Zumwalde, Approaches to Safe Nanotechnology: Managing the Health and Safety Concerns Associated with Engineered Nanomaterials, Department of Health and Human Services, Centers for Disease Control and Prevention, National Institute for Occupational Safety and Health, 2009.

Effect of Spark Plasma Sintering Pressure on Mechanical Properties of WC – 7.5 wt. % Nano Co

Md. Raihanuzzaman Rumman[a], Zonghan Xie[a], Soon-Jik Hong[b], Reza Ghomashchi[a*]

[a]School of Mechanical Engineering, The University of Adelaide,
South Australia 5005, Australia
[b]Division of Advanced Materials Engineering, Kongju National University,
Cheonan, Chungnam, 331-717, South Korea

Statement of Authorship

Title of Paper	Effect of Spark Plasma Sintering Pressure on Mechanical Properties of WC–7.5 wt. % Nano Co
Publication Status	☑ Published ☐ Accepted for Publication ☐ Submitted for Publication ☐ Unpublished and Unsubmitted work written in manuscript style
Publication Details	Raihanuzzaman RM, Xie Z, Hong S-J, Ghomashchi R. Effect of Spark Plasma Sintering Pressure on Mechanical Properties of WC–7.5 wt. % Nano Co. Materials & Design. 2015;68:221-7.

Principal Author

| Name of Principal Author (Candidate)	Md Raihanuzzaman Rumman		
Contribution to the Paper	I was responsible for designing the framework for the experimental conditions. I have conducted the sintering experiments, carried out the mechanical property and microstructural behaviour analysis, wrote the first draft of the manuscript and incorporated and addressed all comments and suggestions by other authors in subsequent revisions of the manuscript. Interpretation of data was primarily my responsibility.		
Overall percentage (%)	95%		
Certification:	This paper reports on original research I conducted during the period of my Higher Degree by Research candidature and is not subject to any obligations or contractual agreements with a third party that would constrain its inclusion in this thesis. I am the primary author of this paper.		
Signature		Date	22/12/15

Co-Author Contributions

By signing the Statement of Authorship, each author certifies that:
  i.   the candidate's stated contribution to the publication is accurate (as detailed above);
  ii.   permission is granted for the candidate in include the publication in the thesis; and
  iii.   the sum of all co-author contributions is equal to 100% less the candidate's stated contribution.

Name of Co-Author	Reza Ghomashchi		
Contribution to the Paper	I was supervisor of this work, and contributed to outlining the scope of this work and refining the manuscript.		
Signature		Date	23/12/2015

Name of Co-Author	Zonghan Xie		
Contribution to the Paper	I was joint supervisor for the work, and contributed to refining the manuscript.		
Signature		Date	15/01/2016

Name of Co-Author	Soon Jik Hong		
Contribution to the Paper	I jointly contributed in allowing access to some of the experimental facility in the labs in South Korea, and also helped refine the manuscript.		
Signature		Date	10/02/2016
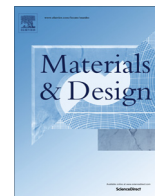
Effect of spark plasma sintering pressure on mechanical properties of WC–7.5 wt% Nano Co

Md. Raihanuzzaman Rumman [a], Zonghan Xie [a], Soon-Jik Hong [b], Reza Ghomashchi [a],*

[a] School of Mechanical Engineering, University of Adelaide, SA 5005, Australia
[b] Division of Advanced Materials Engineering, Kongju National University, 331-717, South Korea

ABSTRACT

In this study, Spark Plasma Sintering (SPS), a relatively fast consolidation method assisted with simultaneous application of heat and pressure, was used to produce bulk carbides from mixed WC–7.5 wt% Nano Co powders. Different pressures ranging from 30 to 80 MPa were applied during sintering to explore its effect on the mechanical properties of resulting carbides. The maximum hardness was found for the samples pressed at 80 MPa, which is ~1925 HV (18.88 GPa), higher than that of the commercially available cemented carbide tools. The marked changes in porosity, hardness, and crack propagation observed in the samples show that the sintering pressure have considerable impact on the mechanical properties of cemented carbides. In particular, the nature of crack initiation and propagation, which is indicative of the fracture toughness of materials, was studied and clarified.

© 2014 Elsevier Ltd. All rights reserved.

1. Introduction

Tungsten carbides (WC), with finely distributed cobalt (Co) acting as a binder, display high hardness, good toughness and moderate stiffness, and have been predominantly used in the manufacture of cutting tools for a variety of machining applications [1,2]. A majority of studies involving cemented carbides in the past few decades have focused on such factors, as composition, powder mixing and consolidation. The incorporation of nano particles in the powders has also gained much interest in recent times [3,4].

For fabrication of hard-to-consolidate nanomaterials, like cemented carbides, Spark Plasma Sintering (SPS), a pressure assisted high temperature consolidation method, has been used. Being able to use both pressure and heat input simultaneously during sintering makes it possible to better control the growth of grains in cemented carbides [5,6], which exhibit superior properties when compared with cemented carbides prepared using conventional consolidation methods. While the effects of sintering temperature have been reported [7,8], the contribution of sintering pressure to the microstructure and mechanical properties of WC–Co remains poorly understood. It is understood that, as with the temperature, pressure is also vital for consolidating the mixed powders during SPS and achieving remarkable mechanical properties, especially high hardness. But the extent to which pressure can

be effectively applied, and how it affects microstructural features of materials need more studies.

In this study, spark plasma sintering was used to prepare hard yet tough carbides from WC–7.5 wt% Nano Co powders without pre-compaction. The purpose of the study is to identify how sintering pressure, as one of the key factors involved in SPS process, affects the microstructural characteristics and mechanical properties of resulting WC–Co, and to elucidate whether the incorporation of nano Co makes any contribution to the final properties. In particular, some aspects, like crack propagation and its interaction within the microstructure, which are believed to be critical to the toughness of cemented carbides, were focused.

2. Experimental procedure

Commercially prepared irregular hexagonal WC particles with an average size of 1–3 μm, with total carbon, free carbon and oxygen content (wt%) of 6.10–6.18, 0.06 and 0.1, respectively, were mixed with nano-sized Co particles. The powder composition and morphology suggested that the powders may have been high energy ball milled for several hours, because of the presence of Zirconium (Zr) traces (from Zr balls bearings used during milling), and the irregular shape of the particles. The Co particles were prepared from Co wires using pulse wire evaporation technique, and were sized within 200–300 nm range. Both WC and Co powders were weighed, and then wet mixed (with ethanol) in a stainless steel jar having zirconium oxide (ZrO₂) liner

---

and stainless steel balls with a ball to powder weight ratio of 10:1. The jar was then rotated at a speed of 1000 rpm for 1 min. The powders were then dried at nearly 100 °C for several hours, and collected for sintering.

Powder mixture (WC–7.5 wt% Nano Co) was consolidated using spark plasma sintering. 2 g of powder mixture was poured into a graphite die, with inner and outer diameters of 10 mm and 40 mm, respectively. Boron nitride (BN), a high temperature lubricant and mold release agent spray were applied on the die inner wall before pouring the powder mixture and placing the upper pin. The outer walls of the dies were drilled horizontally toward the center where an R-type thermocouple was placed to get the actual temperature reading of the die and the powders/compacts. The final sintering temperature was set at 1350 °C, with a heating rate of 100 °C/min and a holding time of 10 min at the sintering temperature. The holding time was chosen to enable the liquid phase to reach equilibrium during sintering. There were no inhibitors such as chromium carbide (Cr_3C_2) or vanadium carbide (VC) or binders used, other than Co. Four different pressures of 30 (Sample A), 45 (Sample B), 60 (Sample C) and 80 (Sample D) MPa were applied on the powder mixtures during SPS, while the other parameters were kept constant. Finally, controlled cooling was carried out (100 °C/min) to bring the samples down to room temperature before they were taken out from the dies. A list of the samples, along with their processing conditions, is given in Table 1. Due to the possibility of having friction between the particles in the powder and between the punch surface and die walls even at high temperature, which may generate density gradients in consolidated samples, sintering was conducted on thin compacts, with a final height of 2 mm [9].

The sintered specimens were mounted, grinded and polished with diamond paste and etched using Murakami reagent for approximately 30 s before optical and electron microscopic analysis. Density of the sintered samples was determined by using Archimedes method. The hardness was measured on polished surfaces using a Vickers hardness tester at 30 kgf load. The results are averages of at least 10 indentations and the standard deviation is given. The equation that was used for Vickers hardness calculation is given below:

$$HV = \frac{2F \sin \frac{136°}{2}}{d^2} \tag{1}$$

where HV is Vickers Hardness, F is applied force and d is the indentation diagonal average length. The values that were mentioned in the study were measured experimentally. During crack length measurement, for each condition, 10–15 indentation marks were analyzed using Field Emission Scanning Electron Microscopy (FE-SEM), and values were averaged. For the porosity measurements and 3D imaging of hardness indentation, Carl Zeiss Axio Image Analyzer was used. The images of the indents were first taken using high magnification optical microscope, which was then processed using image-analyzing software. The shift of focal points from the surface of the samples to the deepest points within the hardness impressions along z-axis generates the 3D images of the indentations, eventually indicating the depth. Fracture toughness values were calculated using the following relationship [10]:

$$K_{1c} = 0.016\sqrt{(E \div H)}(P \div c^{3/2}) \tag{2}$$

where E is Young's modulus, P is the indentation load, c is half of the average indentation crack length, and H is the hardness of the material. There are several ways to measure elastic modulus of WC–7.5%Co. Some of them are listed below:

(a) With the help of an ultrasonic arrangement, elastic modulus can be calculated by measuring the longitudinal wave velocity, transverse wave velocity and density of the sample [11].
(b) Nanoindentation and microindentation reload curves can be used to calculate Young's modulus of a sample experimentally [12].
(c) Stress–strain analysis can be used to find out the elastic modulus of large samples that are easy to machine.

For our work, literature reference was first used [8,13–16] to find out the Young's modulus for WC–7.5 wt%Co, since it varies depending on the fraction of the binder content, which is Co in our study. Nanoindentation tests were also carried out to confirm the values. For fracture toughness calculations, the value of E = 625 GPa was used as the Young's modulus.

Table 1
Mixing and processing conditions of WC–Co powders.

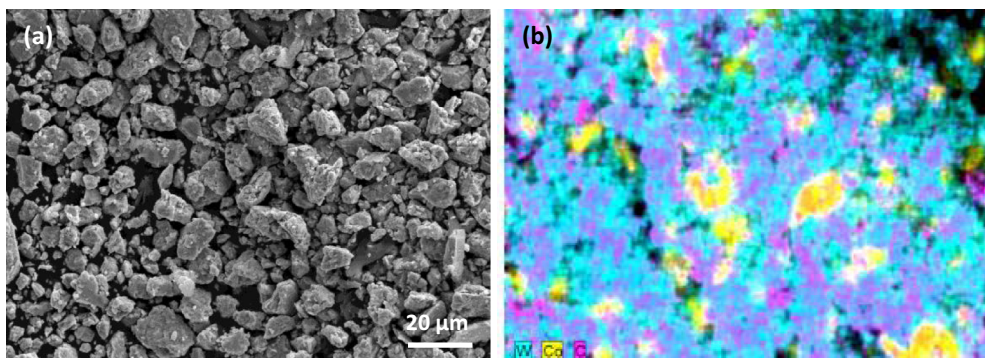| Sample number	Composition	Mixing technique and time	Sintering temp (°C)	Sintering pressure (MPa)	Sample diameter and thickness (mm)
A	WC–7.5 wt% Nano Co	High energy ball milling, 1 min	1350	30	10, 2
B	WC–7.5 wt% Nano Co	High energy ball milling, 1 min	1350	45	10, 2
C	WC–7.5 wt% Nano Co	High energy ball milling, 1 min	1350	60	10, 2
D	WC–7.5 wt% Nano Co	High energy ball milling, 1 min	1350	80	10, 2

Fig. 1. (a) SEM image and (b) EDS mapping of mixed WC–7.5 wt% Nano Co powders.
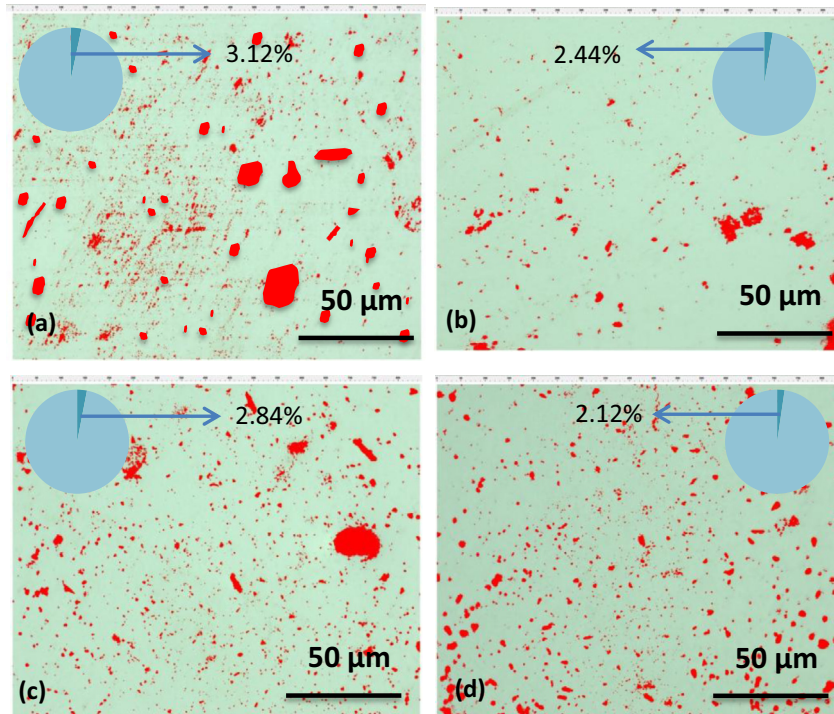
Fig. 3. Porosity analysis of SPS-ed samples sintered at (a) 30 MPa, (b) 45 MPa, (c) 60 MPa and (d) 80 MPa.

3. Results and discussion

The SEM micrograph of the mixed WC–7.5 wt% Nano Co powder samples is given in Fig. 1, along with the EDS (energy dispersive spectroscopy) X-ray mapping of W, C and Co. It shows a nearly homogeneous distribution of both WC and Co. As cobalt serves as binder for WC particles, it is important to have homogeneously distributed WC–Co powders. The coarse WC particles appear to have agglomerated with fine Co particles distributed almost uniformly, in addition to Co agglomerations. Co particles have finer shape in general and could mostly be identified along the periphery of WC particles. The irregularity in shape of the particles suggests that the WC powders have been fabricated using mechanical milling. Unlike spray conversion [4,17], or other thermochemical processes, mechanical milling [18,19] would result in the particle shape being irregular with sharp corners as shown in Fig. 1.

Fig. 2(a) and (b) shows SEM micrographs of WC–7.5 wt% Nano Co samples sintered at 30 (A) and 60 MPa (C) pressure. Although the microstructure is fairly simple with WC as the predominant phase, a change in the size and distribution of pores with sintering pressure is apparent within the microstructure. It can be seen from low pressure sintered sample (30 MPa) that the pores are larger in dimension, and appear frequent. On the other hand, the high pressure sintered sample showed relatively smaller pores with less frequent appearance within the microstructure. This observation suggests that these pores tend to decrease in size with increasing pressure. Fig. 2(c) shows a back-scattered SEM image of an 80 MPa (D) pressure sintered sample, which shows the WC phase. It is clear that both the size and shape of the WC grains are varied, however, most of the grains are within the 1–5 μm range.

Porosity is a critical parameter that affects density and hardness of sintered carbides. However, quantitative measurement of porosity is extremely difficult [20,21] due to the fact that cobalt or other binder phase in WC comes in low quantities in the compositions, making it difficult to differentiate the presence of pores between
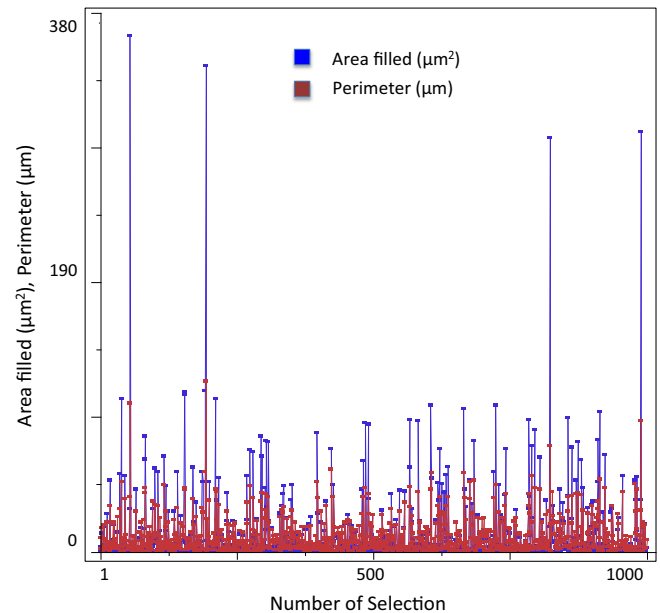

Fig. 4. Selection of porous content and their size distribution for SPS-ed sample sintered at 80 MPa (Sample D).

different phases. Fig. 3 shows the polished surface and porosity measurement of samples prepared with increasing pressure. The image representing each sample is an average of 30 images with variable focal points, reconfirmed against regular and polarized lighting, in an attempt to identify the pore features. Excessively large sizes of pores, although very few in number, that may have resulted from particles being chipped away during grinding and polishing, were excluded from consideration [20]. In addition to the SEM images discussed in Fig. 2, it can be seen from Fig. 3 that there is a slight declining pattern in porosity with increasing
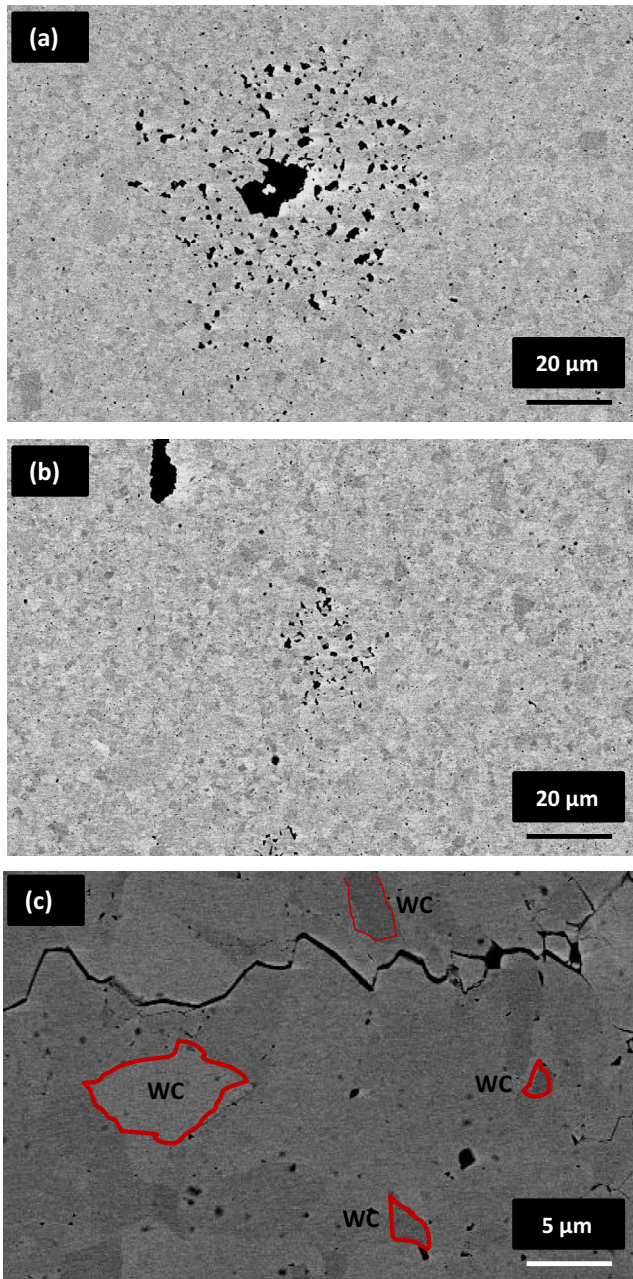
Fig. 2. SEM secondary electron images of WC–7.5 wt% Nano Co samples sintered at (a) 30 MPa, (b) 60 MPa showing overall microstructure and porosity. Back scattered electron image (c) shows WC as the predominant phase present in the sample sintered at 80 MPa. Note the crack in (c) is extrinsic, resulting from the indentation that was made during hardness measurements. The image focuses on the primary phase observed as part of the microstructure.

pressure from 30 to 80 MPa, suggesting an increase in density. Moreover, the pores found on the low pressure samples are relatively big and less homogenously distributed as opposed to the high pressure sintered ones. The lowest porosity content was recorded for the 80 MPa sample, which was 2.14% of the total area. A selection of 1000 porous content along with their size distribution (area and perimeter) for Sample D is illustrated in Fig. 4, which shows good homogeneity in size for these pores under such high pressure condition.

The changes in average crack length in the SPS-ed samples as a function of pressure were measured and are illustrated in Fig. 5. Crack length reduced to an average of 116 μm for Sample D from

an initial 208 μm for Sample A. The apparent homogeneous distribution of pores on Sample C may have contributed to the relatively higher crack length by allowing cracks to propagate through and around them. It is also a matter of consideration that large pores can also influence the presence of relatively longer cracks. Another way of considering the behavior would be to say that the lack of a softer binder phase, which is Co in this study, along the path of a generated crack could result into having longer cracks due to the influence of brittle WC. It is possible that for the high-pressure sample (D), the inability in having a proper hardness impression is indicative of high hardness. The shock or damage during indentation on the surface of the 80 MPa sample can possibly dissipate both radially and laterally to the pressing direction, resulting in reduced crack length as opposed to the low pressure sintered samples. It is important to mention that the samples in this study did not show signs of secondary cracks usually branching out from primary cracks otherwise. From Fig. 5, it would first appear that Sample D had low hardness. When hardness tests were carried out, and the surfaces was analyzed, it was repeatedly found that Sample D had some material chipping off around the edges of the indentation, which may or may not have been part of the contact area. In order to clarify that, a magnified image of Sample D around the indentation mark has been shown in Fig. 5d, which suggest that the contact area to be taken into consideration is smaller than the total worn out area observed. Now in order to be able to find out the contact area, the contact depth of the indentations of all samples were also analyzed. The z stack analysis helped develop a 3D image layout by varying the focal lengths at the two farthest most points of the indentation marks, which clearly indicates (later discussed in Fig. 8) that there is a gradual decrease in depth with increasing sintering pressure, with Sample D being the lowest.

Fig. 6 shows SEM micrographs of Sample C, having longer cracks, sintered at 60 MPa pressure. The images suggest that the cracks, generated along the edges of the indentation, are fairly straight in nature, without much curving or deflection. The cracks were mostly found to be intergranular, although it was difficult to see the presence and positioning of the binder phase integrated into or separated from the dominant WC grains. The change in color of WC phase is due to the difference in carbon content, with darker contrast confirming higher percentage. It is understood that the sintered structure of WC/Co, be it Spark Plasma Sintering (SPS) or Hot Isostatic Press (HIP), comprises of some of the WC dissolving into the cobalt binder phase on the surface of the original WC [1]; an idea that was established based on several fundamental studies [22–24] that suggested an analytical expression describing several factors, namely, pressure, liquid volume fraction, solid particle size and so on. However, the derivation was based on several assumptions, including that the particles are of same size, shape and are uniformly distributed in the final liquid phase matrix, which are often far from real when these are observed experimentally. It is argued [25] that although it may be principally possible to quantitatively predict the distributions in particle size and shape, the mathematical complexity and difficulty are expected to be too large to be feasible. Therefore, a more practical way to explain the microstructure is to focus on the grains and phases and observe the changes experimentally.

When mechanical properties of cemented carbides are considered, hardness is one of the most important factors that determine how well the carbide tools or inserts will withstand extreme cutting conditions. The changes in hardness for the SPS-ed samples as a function of pressure applied during the process is shown in Fig. 7. The values indicate an almost gradual increase in hardness with increasing pressure, reaching a maximum of 1925 HV (18.88 GPa) at 80 MPa pressure. Hardness values were found to be similar on both surfaces of the samples and along the cross sections. The minimum hardness recorded for the series of samples
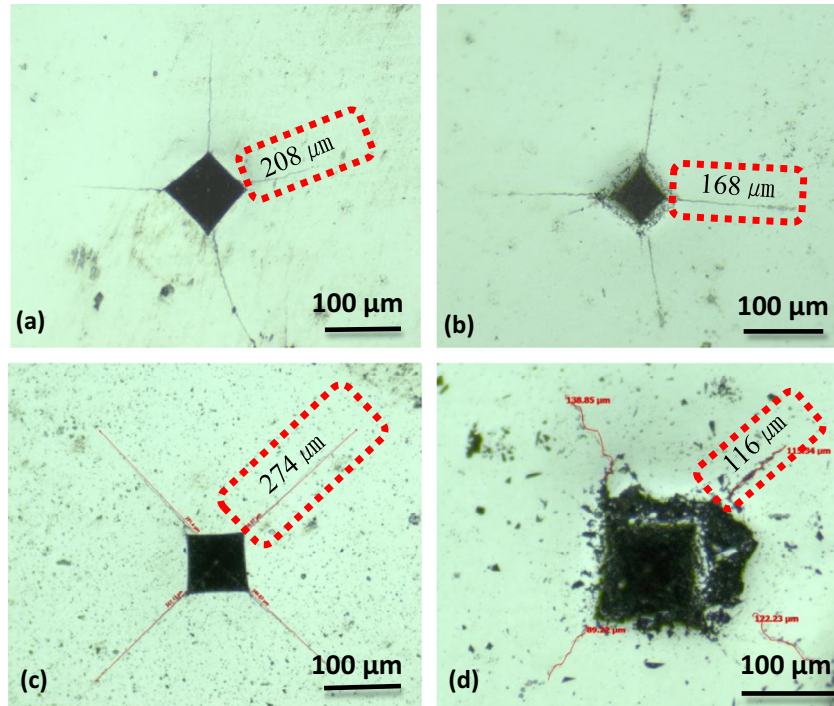
Fig. 5. Hardness impression and crack length of spark plasma sintered samples (a) A, (b) B, (c) C and (d) D.
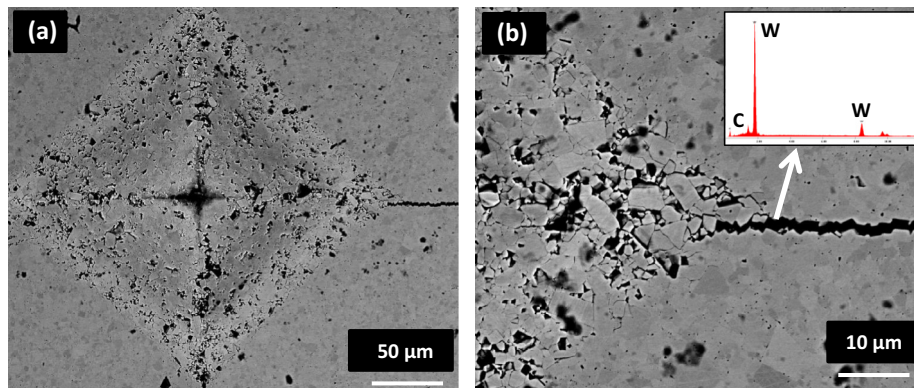

Fig. 6. SEM images showing (a) hardness impression and (b) magnified crack initiation and propagation in sintered WC–7.5 wt% Nano Co at 60 MPa. Image (b) shows WC phases around the crack propagation path. The darker grains contain higher percentage of carbon. The presence of cobalt along the crack is hardly identifiable. The WC–7.5 wt% Nano Co sample was spark plasma sintered at 1350 °C at 60 MPa pressure.
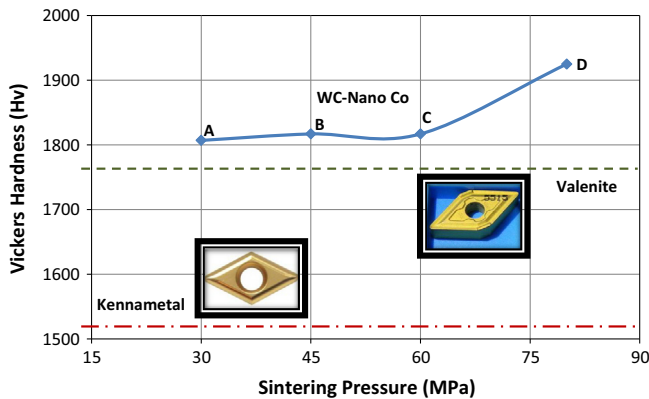

Fig. 7. Changes in Vickers hardness with respect to SPS-ed pressure (a) 30 MPa, (b) 45 MPa, (c) 60 MPa and (d) 80 MPa. The dashed lines represent two reference commercial cutting inserts' (Valenite VP 5515 and Kennametal KC 850) hardness.

was 1807 HV, which is well above some commercially available cutting inserts' hardness, and the values suggested for coarse grain WC cutting tools in Ref. [26]. As for comparison, the hardness values in this study were tested against commercial carbide inserts, whose hardness was found to be near the 1800 and 1500 HV mark, respectively. It is important to notice that the SPS-ed samples were prepared at a lower temperature than what is generally used during most conventional which is around 1450–1550 °C. There has been reports [8] of hardness values of SPS-ed samples prepared at pressures as high as 100 MPa and temperature around 1100 °C, reaching nearly 1600 HV (15.69 GPa). It is understood that there is room for optimization of hardness by controlling sintering pressure, temperature and will be pursued in the future work.

The hardness tests generated indentations on the samples resulting in initiation and propagation of cracks along all corners of the indents, which can be analyzed to validate the hardness and fracture toughness behavior of the samples and the microstructural characteristics (Fig 6) discussed before. Fig. 8 shows
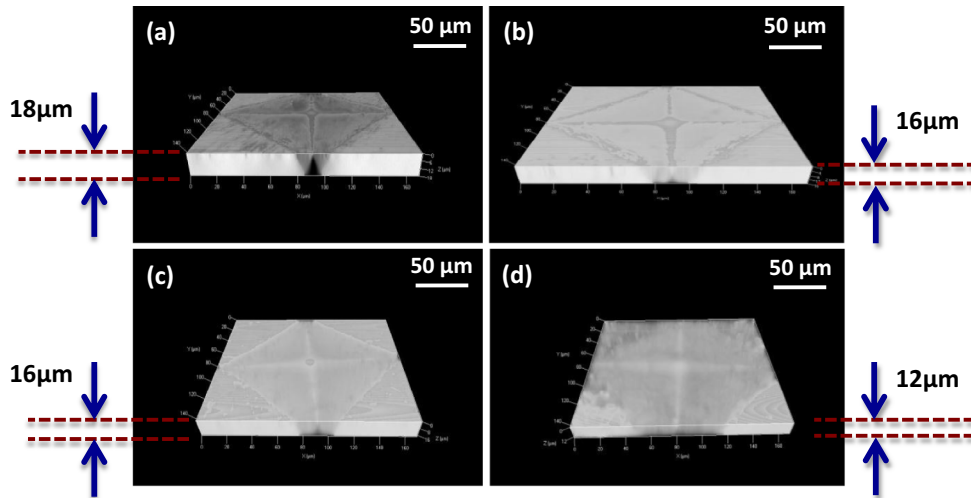
Fig. 8. 3D images of surface hardness indentations of SPS-ed samples sintered at (a) 30 MPa, (b) 45 MPa, (c) 60 MPa and (d) 80 MPa.
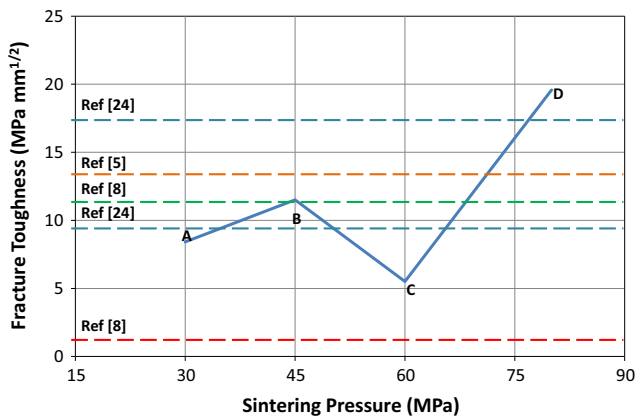

Fig. 9. Changes in fracture toughness with respect to SPS-ed pressure (a) 30 MPa, (b) 45 MPa, (c) 60 MPa and (d) 80 MPa. The dashed lines represent reference fracture toughness from a number of studies in the literature.

3D images of the indentation sites on the surface of the SPS-ed samples with changing pressure. It was found that the depth for the 30 MPa sample (Sample A) was around 18 μm which gradually decreased with increasing pressure, meaning increasing hardness (Fig 7), reaching a minimum of 12 μm for 80 MPa sample (Sample D). The changes in indentation depth along the cross sections, however, were pretty similar due to the low thickness of the samples, and resulted the cracks to always propagate toward the closest edge along the height. The cross sectional crack length values may have been different if sample size was varied, which is why they are not included in this study and requires further observation. Overall, the patterns displayed through the changes in indentation depth in the SPS-ed samples with respect to pressure conform to the aforementioned hardness behavior and microstructural observations.

The changes in fracture toughness of the samples are shown in Fig. 9. The values are calculated using the average crack lengths for each sample generated from the hardness impressions on the surface from Eq. (2). The fracture toughness results were compared against some other studies reported in the literature [5,8,27]. Although there are several other fracture toughness values that can be compared with the results of this study, the values that were chosen from the literature are close enough in terms of

processes applied and particle or grain size of cemented carbides, with minor differences in terms of compositions and sintering temperature. It has been discussed earlier that there is a gradually increasing relationship between pressure applied during sintering and hardness that has been observed on the sintered samples. Now, if that is the case, it is also possible to draw a conclusion based on Eq. (2) that there might be an inversely proportional relationship between crack length and fracture toughness, although the results from this study is far from a generalized comment in this regard. The individual cracks that were generated along the edges of the indentations were not always consistent or suggesting a pattern, but the overall crack length measurements suggest an almost gradual decrease with increasing pressure, eventually leading the fracture toughness to increase.

4. Conclusions

The study has focused on the effects of pressure that was employed during spark plasma sintering, on mechanical properties, namely hardness and fracture toughness of WC–7.5 wt% Nano Co. In addition, the changes in crack length, propagation, porosity and microstructure have been discussed. It was found that hardness increases in the samples with increasing SPS pressure reaching a maximum of 1925 HV (18.88 GPa). Porosity also reduced in the samples with increased homogeneity in terms of size and distribution, both on the surface and along cross section, with incremental sintering pressure. While the decrease in crack length showed an increase in hardness and fracture toughness, it was difficult to identify the contribution of binder phase (nano cobalt) in terms of limiting crack propagation, as WC was the dominant phase around the cracks and throughout the microstructure.

References

[1] Schwarzkopf P, Kiefer R. Cemented carbides, vol. 71. New York: The Macmillan Company; 1960. p. 140–55.
[2] Mohan K, Strutt P. Observation of Co nanoparticle dispersions in WC nanograins in WC–Co cermets consolidated from chemically synthesized powders. Nanostruct Mater 1996;7:547–55.
[3] Xueming M, Gang J. Nanostructured WC–Co alloy prepared by mechanical alloying. J Alloy Compd 1996;245:L30–2.
[4] Cha SI, Hong SH, Ha GH, Kim BK. Mechanical properties of WC–10Co cemented carbides sintered from nanocrystalline spray conversion processed powders. Int J Refract Metal Hard Mater 2001;19:397–403.
[5] Fang ZZ, Wang X, Ryu T, Hwang KS, Sohn H. Synthesis, sintering, and mechanical properties of nanocrystalline cemented tungsten carbide – a review. Int J Refract Metal Hard Mater 2009;27:288–99.

[6] Jia K, Fischer T, Gallois B. Microstructure, hardness and toughness of nanostructured and conventional WC–Co composites. Nanostruct Mater 1998;10:875–91.

[7] Jia C-C, Tang H, Mei X-Z, Yin F-Z, Qu X-H. Spark plasma sintering on nanometer scale WC–Co powder. Mater Lett 2005;59:2566–9.

[8] Cha SI, Hong SH, Kim BK. Spark plasma sintering behavior of nanocrystalline WC–10Co cemented carbide powders. Mater Sci Eng, A 2003;351:31–8.

[9] Favrot N, Besson J, Colin C, Delannay F. Cold compaction and solid-state sintering of WC–Co-based structures: experiments and modeling. J Am Ceram Soc 1999;82:1153–61.

[10] Xie Z-H, Hoffman M, Cheng YB. Microstructural tailoring and characterization of a calcium α-SiAlON composition. J Am Ceram Soc 2002;85:812–8.

[11] Kono Y, Nakamoto M, Irifune T. Elastic properties of sintered diamonds with and without Co binder. In: Journal of physics: conference series, IOP Publishing; 2010. p. 012134.

[12] Shuman DJ, Costa AL, Andrade MS. Calculating the elastic modulus from nanoindentation and microindentation reload curves. Mater Charact 2007;58:380–9.

[13] Doi H, Fujiwara Y, Miyake K, Oosawa Y. A systematic investigation of elastic moduli of WC–Co alloys. Metall Mater Trans 1970;1:1417–25.

[14] Upadhyaya G. Materials science of cemented carbides – an overview. Mater Des 2001;22:483–9.

[15] Santhanam A, Tierney P, Hunt J. Cemented carbides. In: Metals Handbook, vol. 2. New Jersey: ASM International; 1990. p. 950–77.

[16] Coromant S. Modern metal cutting: a practical handbook. Sandvik Coromant; 1994.

[17] Kim B, Ha G, Lee D. Sintering and microstructure of nanophase WC/Co hardmetals. J Mater Process Technol 1997;63:317–21.

[18] Xueming M, Ling Z, Gang J, Yuanda D. Preparation and structure of bulk nanostructured WC–Co alloy by high energy ball-milling. J Mater Sci Lett 1997;16:968–70.

[19] Sun J, Zhang F, Shen J. Characterizations of ball-milled nanocrystalline WC–Co composite powders and subsequently rapid hot pressing sintered cermets. Mater Lett 2003;57:3140–8.

[20] Martínez V, Echeberria J. Hot isostatic pressing of cubic boron nitride–tungsten carbide/cobalt (cBN–WC/Co) composites: effect of cBN particle size and some processing parameters on their microstructure and properties. J Am Ceram Soc 2007;90:415–24.

[21] Amberg S, Doxner H. Porosity in cemented carbide. Powder Metall 1977;20:1–10.

[22] Beere W. A unifying theory of the stability of penetrating liquid phases and sintering pores. Acta Metall 1975;23:131–8.

[23] Park H-H, Yoon DN. Effect of dihedral angle on the morphology of grains in a matrix phase. Metall Trans A 1985;16:923–8.

[24] Delannay F, Pardoen D, Colin C. Equilibrium distribution of liquid during liquid phase sintering of composition gradient materials. Acta Mater 2005;53:1655–64.

[25] Raihanuzzaman RM, Song J-W, Hong S-J. Evaluation of mechanical properties and processing conditions of WCCo alloys fabricated by magnetic pulsed compaction. J Alloy Compd 2012;536:S211–5.

[26] Ettmayer P. Hardmetals and cermets. Annu Rev Mater Sci 1989;19:145–64.

[27] Ingelstrom N, Nordberg H. The fracture toughness of cemented tungsten carbides. Eng Fract Mech 1974;6:597–607.

Mechanical Properties and Microstructural Behavior of Microwave Sintered WC - Co

Rumman Md Raihanuzzaman*, Lee Chang Chuan[1], Zonghan Xie, Reza Ghomashchi*

School of Mechanical Engineering, The University of Adelaide,
South Australia 5005, Australia
[1]School of Manufacturing Engineering, University Malaysia Perlis,
Malaysia

Statement of Authorship

Title of Paper	Mechanical Properties and Microstructural Behavior of Microwave Sintered WC - Co
Publication Status	☐ Published ☐ Accepted for Publication ☑ Submitted for Publication ☐ Unpublished and Unsubmitted work written in manuscript style
Publication Details	Raihanuzzaman RM, Lee Chang Chuan, Zonghan Xie, Reza Ghomashchi Mechanical Properties and Microstructural Behaviour of Microwave Sintered WC – Co, International Journal of Refractory Metals and Hard Materials (Under Review)

Principal Author

Name of Principal Author (Candidate)	Md Raihanuzzaman Rumman		
Contribution to the Paper	I was responsible for the literature review required for this work, and designed the framework for the experimental conditions. I carried out the mechanical property and microstructural behaviour analysis, wrote the first draft of the manuscript and incorporated and addressed all comments and suggestions by other authors in subsequent revisions of the manuscript. Interpretation of data was primarily my responsibility.		
Overall percentage (%)	85%		
Certification:	This paper reports on original research I conducted during the period of my Higher Degree by Research candidature and is not subject to any obligations or contractual agreements with a third party that would constrain its inclusion in this thesis. I am the primary author of this paper.		
Signature		Date	22/12/15

Co-Author Contributions

By signing the Statement of Authorship, each author certifies that:
  i.   the candidate's stated contribution to the publication is accurate (as detailed above);
  ii.   permission is granted for the candidate in include the publication in the thesis; and
  iii.   the sum of all co-author contributions is equal to 100% less the candidate's stated contribution.

Name of Co-Author	Reza Ghomashchi		
Contribution to the Paper	I was supervisor of this work, and contributed to outlining the scope of this work and refining the manuscript.		
Signature		Date	23/12/2015

Name of Co-Author	Zonghan Xie		
Contribution to the Paper	I was joint supervisor for the work, and contributed to refining the manuscript.		
Signature		Date	15/01/2016

Name of Co-Author	Lee Chang Chuan		
Contribution to the Paper	I have conducted the microwave sintering of the powder samples, and jointly contributed in refining the manuscript.		
Signature		Date	08/02/2016

Manuscript details

Manuscript number	IJRMHM_2016_82
Title	Mechanical Properties and Microstructural Behavior of Microwave Sintered WC - Co
Article type	Research Paper

Abstract

Tungsten or in general cemented carbides have been of great interest within industrially manufacturable hard materials for their excellent mechanical properties, especially in the last few decades, with a number of new and revamped processing techniques emerging in order to develop high performance carbide tools. Microwave sintering or heating is known for its application on a range of materials, which includes ceramics as well. Although it has been widely used, its effect however on grain growth of materials still requires clear understanding. Furthermore, the effect of sintering temperature and initial particle size and how they influence microwave behaviour for such range of materials is another area that requires clear understanding. This article focuses on microwave sintering being used on cemented carbides using a range of final sintering temperatures and initial particle sizes, which sheds light on the entire process and its effectiveness on ceramic processing. The microstructural features associated to the sintering process have also been focused as part of the study, addressing

some of the key issues and challenges faced in the research.

Keywords   Tungsten Carbide; Compaction; Microwave Sintering, Microstructure, Mechanical Properties

Corresponding Author   Md. Raihanuzzaman Rumman

Corresponding Author's Institution The University of Adelaide

Order of Authors   Md. Raihanuzzaman Rumman, Lee Chang Chuan, Zonghan Xie, Reza Ghomashchi

Submission files included in this PDF

File Type	**File Name**
Cover Letter	Cover Letter.docx
Highlights	Research Highlights.docx
Manuscript File	Manuscript.docx
Figure	Figures.pptx
Table	Tables.pptx

To view all the submission files, including those not included in the PDF, click on the manuscript title on your EVISE Homepage, then click 'Download zip file'.

Request for Publication

Tuesday, Feb 09, 2016

Editor
International Journal of Refractory Metals and Hard Materials

Title: **"Mechanical Properties and Microstructural Behavior of Microwave Sintered WC – Co"** by Rumman

Md Raihanuzzaman, Lee Chang Chuan, Zonghan Xie and Reza Ghomashchi

Dear Editor

I am pleased to submit an article entitled **"Mechanical Properties and Microstructural Behavior of Microwave Sintered WC – Co"** by Rumman Md Raihanuzzaman, Lee Chang Chuan, Zonghan Xie and Reza Ghomashchi for publication in your journal. Please find enclosed a copy of the manuscript. The manuscript has not been previously published, is not currently submitted for review to any other journal, and will not be submitted elsewhere before one decision is made. All authors are fully aware of the progress and state of this paper.

I would appreciate if it is kindly considered and processed for publication on the journal.

Sincerely yours,

Rumman Md Raihanuzzaman
School of Mechanical Engineering, The University of Adelaide, Adelaide, Australia 5000
E-mail: raihan.rumman@adelaide.edu.au
Tel: +61 (08) 8313 4185, Fax: +61 (08) 8313 4367

Research Highlights

- Effect of microwave sintering temperature and particle size on mechanical properties was studied.
- Crack initiation, propagation and grain size were analyzed to discuss mechanical properties.
- Quantitative measurement of porosity was carried out in reconfirming density and hardness behavior.
- Overall, microstructural characteristics were analyzed to explain hardness and fracture toughness.

Mechanical Properties and Microstructural Behavior of Microwave Sintered WC - Co

Rumman Md Raihanuzzaman*, Lee Chang Chuan[1], Zonghan Xie, Reza Ghomashchi*

School of Mechanical Engineering, University of Adelaide, South Australia

[1]School of Manufacturing Engineering, University Malaysia Perlis, Malaysia

Phone: +61 (0) 8 8313 4185, Email: raihan.rumman@adelaide.edu.au, reza.ghomashchi@adelaide.edu.au

Abstract

Tungsten or in general cemented carbides have been of great interest within industrially manufacturable hard materials for their excellent mechanical properties, especially in the last few decades, with a number of new and revamped processing techniques emerging in order to develop high performance carbide tools. Microwave sintering or heating is known for its application on a range of materials, which includes ceramics as well. Although it has been widely used, its effect however on grain growth of materials still requires clear understanding. Furthermore, the effect of sintering temperature and initial particle size and how they influence microwave behaviour for such range of materials is another area that requires clear understanding. This article focuses on microwave sintering being used on cemented carbides using a range of final sintering temperatures and initial particle sizes, which sheds light on the entire process and its effectiveness on ceramic processing. The microstructural features associated to the sintering process have also been focused as part of the study, addressing some of the key issues and challenges faced in the research.

Keywords: Tungsten Carbide; Compaction; Microwave Sintering, Microstructure, Mechanical Properties

1. Introduction

For industrial applications, materials can be processed in a number of ways, and powder metallurgy is one that has been of great interest in recent times. The process includes several stages, one of which is the compaction of powders into green samples, which would then be sintered or further consolidated at high temperatures to convert the green samples into a robust finished product with desirable mechanical properties. During the sintering process which is a critical part of the manufacturing chain, the particles, initially compacted into green bodies, go through a process of fusing together which could involve high degree of growth in terms of grain size; a phenomenon that is undesirable, and needs to be controlled to an extent that is experimentally feasible. A number of techniques have been used in an attempt to reduce the degree of grain size coarsening, including some innovative approaches taken in response to this emerging challenge faced in PM industry [1, 2].

Microwave sintering is one of the processes that essentially became quite influential in ensuring some of the unique microstructural features and mechanical properties, as well as energy consumption and manufacturing cost for a wide range of materials including metals, ceramics and composites [3]. The way microwave sintering works is inherently different from how conventional sintering functions. When it comes to conventional sintering which is still being used in most manufacturing industries for production of engineering components, thermal energy is directed to the surface of the material through either radiation or convection process, which is then carried to the rest of the material via a relatively slow conduction method. In microwave sintering, the energy that is delivered however penetrates through the material using molecular interaction, capitalizing on the electromagnetic field, and making sure that it is transferring the energy faster than the conventional process. The concept of reheating during microwave sintering is not a mere heat transfer between the heating source and the green compact but it is considered to be a conversion of electromagnetic energy to thermal energy. The use of microwave sintering ensures that the generated heat covers the entire volume of the material, which will eventually lead to the material experiencing rapid heating, making it a major differentiating factor between several sintering processes. In addition, unlike conventional sintering, which is known to over-cure the surface than the interior and leaves traces of temperature gradients, microwave sintering ensures uniform heating of green samples with no thermal gradient present. Therefore, defects in materials caused due to thermal gradients can be treated and removed, and the need for additional manufacturing stages to cater for the imperfections becomes redundant.

Rodiger et al. [4] did some extensive work in order to determine the difference in time between microwave sintering and conventional heating for a number of hard materials that were initially compacted and then sintered. It was found that microwave heating was able to shorten the sintering cycle, which excludes the cooling phase, by a factor of 3 in comparison with conventional sintering. The significant difference in heating time between conventional and microwave sintering evidently led to the understanding that microwave heating doesn't only allow a faster path for sintering of materials, but also consumes much less electricity or energy due to a shorter processing cycle as opposed to conventional heating. By taking advantage of the features of microwave sintering, it is possible to sinter hardmetals as well as other materials with presence of metallic binders at temperatures that are at least 50-100K lower than the temperatures required for conventional sintering. This, in effect changes the entire dynamics of the heating pattern as materials will be able to reach their desired sintering state well below the solidus (e.g. eutectic temperatures). For the same set of reasons, added to the fact that a lower temperature achieves the desired sintering state, grain growth within particles will be limited to a great extent. Grain growth inhibition is one of the critical challenges during such sintering steps since it is almost directly proportional to the temperature used in the process, meaning a higher temperature would lead the material in having larger average grain size, as opposed to low temperature results. Fine grain size is a strong indicator of how well the product performs in terms of mechanical properties, and is expected to not deviate much from its original size, be it in grain or particle form. While this deviation is more in conventional sintering than microwave heating, it is easier for the latter to provide better balance in terms of mechanical properties, operational requirements and cost. Even in terms of densification, the reduction in final temperature and duration of the process while achieving enhanced mechanical properties, suggest that densification starts and reaches its final state faster than any other processes; a behaviour that can be attributed to the simultaneous reduction of open and closed porosity during microwave sintering.

This paper focuses on WC - 7.5 wt. % Co samples with varied initial particle size and final microwave sintering temperatures based on the changes in mechanical behaviour and microstructural features.

2. Microwave Sintering: Advantages and Applications:

The heating mechanism in microwave sintering is the main differentiating factor from other conventional heating methods when it comes to sintering materials. A list of tangible advantages of using microwave heating includes, but not limited to the following [1, 5]:

- Faster diffusion process,
- Less energy consumption,
- Faster heating and cooling rate,
- Reduced operating time,
- Reduced sintering temperature,
- Enhanced mechanical properties,
- Improved physical properties,
- Simplicity of operation,
- Reduced operational costs,
- Better quality control,
- Production of innovative and advanced materials,
- Health and environmental benefits

The understanding and control of microwave sintering are critical for many industrially manufacturable materials and products. While the feature that ensures proper penetration of heat through materials, eventually leading to rapid heating, processes used on samples prior to microwave heating is of importance as well. The nature of the green sample may also indicate the level of precision or dimensional changes and quality to be expected from microwave sintering. It used to be thought that all metals are prone to radiating microwave or could generate plasma formation, which is why they are not safe to be considered for microwave heating [6]. It was later clarified that this idea was only applicable to sintered metals or those in bulk condition, at ambient temperature, and would not affect particles being heated at an elevated temperature range. This clarification then opened windows for microwave heating as a possible and rapidly growing tool for materials sintering.

2.1 Low temperature microwave applications

The applications of microwave sintering are quite varied, as it has been used by a number of industries over the last few decades. However, based on temperature, applications of microwave sintering can be classified into two main groups, low and high temperature [6]. Low temperature (less than 500ºC) microwave applications cover the following areas:

- Communication (Used in cellular devices for establishing long distance communicative route)
- Food processing
- Rubber industry (Preheating and vulcanization)
- Drying of wood based materials/products
- Ceramic drying
- Pharmaceutical products (Manufacture and preservation)

- Polymer
- Printing material
- Biomedical work

2.2 High temperature microwave applications

Involvement of microwave heating at elevated temperatures, exceeding 500 º C is rather relatively new, and has been observed only in the past couple of decades. High temperature applications of microwave sintering have primarily been focused on the following areas [7-10]:

- Ceramics
- Composites
- Metallic materials
- Aerospace defence

Microwave sintering furnaces can be of different size, shape and capacity and depend primarily on the manufacturing requirement of the products.

3. Experimental Procedure

Three types of irregular hexagonal shaped WC particles, sized at 1~3 µm, 500 nm and 100nm, with an average of 0.1 (wt. %) total oxygen, 0.06 (wt.%) free carbon and 6.10–6.18 (wt.%) carbon content were mixed with three types of cobalt particles sized within the same range, while a fixed composition of WC-7.5wt.% Co was used. The details of the samples are given in Table 1. Powders were mixed using a high-energy ball mill. The process started by first placing the powders in a stainless steel container with WC inner lining and then mixing them with 10 mm diameter Ti coated WC ball bearings with a ball to powder weight ratio of 5:1. The speed of rotation was set at 500 rpm and was used for 5 minutes to mix the powders under dry conditions. Powders were first compacted using a conventional single action press with a pressure set at 50 MPa for all samples. The green compacts were microwave sintered at three different temperatures ranging between 1000 and 1400 º C. Specifications of the furnace used for this work is given in Table 2. Details on heating rate and holding time are given in Table 1. Figure 1 shows a schematic diagram of a microwave sintering assembly [11, 12]. The microwave energy is generated by a generator, or sometimes called magnetrons. The actual chamber where the heating takes place is insulated to avoid temperature gradient radiating inside and outside of the heating zone.

The resistance heating tuner (R-H Tuner) helps with the heating while preventing rapid fluctuations in temperatures.

The samples were sectioned longitudinally after sintering, mounted and conventionally prepared (down to 1 µm diamond paste) for metallographic analysis. For etching, a batch of Murakami reagent (10 g potassium ferricyanide K_3Fe (CN)$_6$, sodium hydroxide (NaOH), and 100 mL water) was prepared. Density of the WC-Co samples was measured by Archimedes method, weighing them in water and air. The hardness was measured on polished surfaces using a Vickers hardness tester at 30 kgf load. The results are averages of at least 10 indentations. The equation that was used for Vickers hardness calculation is given below:

$$HV = \frac{2F\sin\frac{136°}{2}}{d^2}$$ ....

.. (1)

Here,

HV = Vickers Hardness,

F = Force applied during the test and

d = Diagonal average length of the indentation.

For microstructural analysis including crack length measurements, a QUANTA 450 FE-SEM was used, while porosity measurements were carried out using optical microscopy (AxioVision Software). Since the sintered samples were quite small in size (100 mm diameter, 3 mm long), fracture toughness values were calculated using the following equation [13]:

$$K_{1c} = 0.016\sqrt{(E \div H)}\left(P \div c^{3/2}\right)$$ .... (2)

Where E is Young's modulus [14-18], H is the hardness of the material measured using a Vickers Hardness tester, P is the indentation load, and c is half of the average indentation crack length. The crack lengths are measured from the initiation points, which are along the edges of the indentation marks, till the end of the propagation.

The elastic modulus of a ceramic sample can be measured in more than just one way. Some of the more used methods are briefly mentioned below:

a) Ultrasonic Measurement: Elastic modulus of a ceramic can be calculated through the employment of an ultrasonic arrangement, which measures the wave velocities, namely longitudinal and transverse, and density [19]

b) Nano-Indentation: A series of nano-indentation tests can be carried out on polished sintered samples, which provide information that can be presented in the form of reload curves. The reload curves can then be used to find out the elastic behaviour of the material, experimentally. [20]

c) Stress Analysis: For samples that are big enough to be tested for tensile and compressive strength, stress analysis can be used, which will illustrate the elastic behaviour of the tested material.

In order to find out the Young's Modulus (E) of WC-Co, we first looked into references from the literature [14-18]. In addition, nano-indentation test was carried out. For the K_{IC} calculations, E= 625 GPa was used.

4. Results and Discussion

Fig 2 shows the SEM micrographs of both WC and Co initial particles. WC and Co, sized at 1~3 µm are shown in figure 2 (a) and 2 (b) respectively. The reason for the initial observation was to check the size and shape of the particles. It is important to see the initial state of the particles, not only to predict the expected behavioural change with respect to processing, but also to confirm if there is any defect or deviation in terms of particle characteristics. Since three different sizes of particles were used in this study, it was of interest to clearly identify and observe the difference in terms of size and shape before further processing was employed. All batches of particles were found to have complied with the requirements of the work, i.e. the desired size limits. Particles shapes were mostly found to be spherical in nature, for both WC and Co, irrespective of their size. Figure (2c) shows the WC – 7.5 wt. % Co particles after being mixed using a high energy ball mill. A number of studies [21-23] have focused on ball milling of WC-Co particles that essentially leads to the idea that it takes a considerable amount of time for WC-Co particles to break and get refined, even when high energy ball milling is used. Another way to look at it would be to say that these studies have presented the idea that high energy ball milling can now be used for mixing of WC-Co without further refinement of particles, if carried out during a short period of time and at a relatively low rotational speed. The initial particles were only milled for 5 minutes,

resulting in a homogenous mixture of WC and Co, which is critical as it can ensure enhanced mechanical properties and microstructural features in sintered WC-Co samples. Since Co is a softer material in nature as opposed to WC and acts as a binder, either in solid or liquid state within the WC matrix, it is essential that Co is dispersed homogeneously in the composition. This will not only facilitate the compaction of the particles into green samples, but can also enhance the performance during sintering by channelling a continuous Co bridge between WC. In addition, since industrial grain growth inhibitors [24-26] were not used in this study as part of the compositions, it was vital that a homogenous mixture of WC-Co was used. The EDX image in Fig 2 (d) also confirms the homogeneity of WC and Co particles within the composition. The brownish/reddish coloured sections represent the areas where Co is present. It is possible that some of the Co particles may have gone through initial agglomeration since they are soft in nature and have gone through a milling stage in presence of harder WC particles. Although a little shift in shape was observed from the initial particles to the final mixture, the average size remained the same.

The XRD pattern of the used WC - 7.5 Co powder is shown in Fig 3. The diffraction peaks of the mixed WC-Co powders were identified where the main WC and Co reflections were used to figure out the crystallite size, using Scherrer's equation. In order to be able to find accurate FWHM values, Co peaks were enlarged since intensity was quite low. It was concluded, while also conforming to expectation, that WC was the dominant peak. Although Co peaks are extremely difficult to identify, especially for compositions with low Co content, traces are usually seen at 37, 44, 52, 65 and 75 2theta (2θ) degree angles, illustrating reasonably low intensities. It is worth mentioning that this behaviour is often mirrored in sintered WC-Co samples with low Co content as well. Beyond a specific proportion of Co, it is difficult to clearly identify the positioning or the distribution of Co in such samples regardless of their forms. XRD, as well as SEM analysis which will be discussed later in this paper, however do show evidence of Co being present and well dispersed within the sample.

The changes in relative density for all WC-7.5wt% Co sintered samples with respect to sintering temperature and initial particle size are illustrated in Fig. 4. The final density of the samples is a result of two separate stages that was sequentially carried out, compaction and sintering. Since microwave sintering is a pressure less heating or sintering process, a pre-compaction stage is required to initially form the powders into green samples. While the compaction is at play, it is vital to ensure that consolidation occurs evenly and in all directions of the samples. For WC particles or grains, the homogeneous sedimentation in solid or liquid cobalt phase, either during the compaction or sintering stage, eventually contributes to the enhanced density of WC-Co samples. The

way compaction process works on particles has been discussed as part of many studies [27-30]. At the start of the compaction process the mixed powder with a certain distribution of particle size and shape along with its pore distribution is inserted into a die. In most cases, frictional force is observed between particles, and between particles and the inner wall of the die. In order to reduce the friction between particles and die wall, a boron nitride or similar spray is often used. Even after that, it is often seen that the exact applied pressure is not translated within the particles due to the difference in nature of frictional forces. Hence it is possible that a pressure gradient is present along the length of the consolidated green sample. During the compaction stage, most particles go through two different phases that can also be observed simultaneously, rearrangement and deformation. While some particles may experience only deformation, others may go through both deformation and rearrangement either sequentially or simultaneously, depending on the shape and orientation of the particle with respect to the adjacent particles. Irrespective of the nature of particles or amount of pressure applied, it is safe to assume that rearrangement is a dominant mechanism within the compaction stage. Having said that, there is a level of unpredictability in determining what mechanism a particle may go through, and more importantly, when. This effect may cause a difference in density in compacted or even sintered samples. The presence of a liquid phase may eliminate the defects within a sample to an extent, or even generate some pores when infiltrates through the bulk due to capillary effect and therefore can't be considered as a completely effective method in case of pressure less sintering. It can be seen from the figure that density shows an incremental pattern for all three samples with respect to increasing temperature, reaching almost a fully dense state at 1400 $^{\circ}$ C. The significant elevation in density between samples sintered at 1000 $^{\circ}$ C and 1250 $^{\circ}$ C, and beyond can be attributed to the presence of a liquid phase that essentially helps improve the density profile through gradual decrease of pores [14, 31-34]. It is also worth noting that it was possible to reach a reasonably high density in samples sintered at 1250 $^{\circ}$ C, which is around the liquid phase initiation point (Liquid Co + WC) [35] indicating how effectively a binder phase in liquid state can result in the sample having a high density without requiring an enormous amount of pressure or high temperature. It is understood that binder mobility can cause agglomerates to form. The binder is initially found being spread on WC particles in the form of a thin layer. The bulk of the binder then spreads on this layer and forms the WC-Co agglomerates. Densification can even be observed prior to liquid formation, depending on how the process has been carried out, although mostly it happens after liquid phase has been formed [36].

The changes in hardness of the WC-Co samples with respect to sintering temperature and initial particle size are shown in Figure 5. For all three different types of particles, an incremental pattern in hardness was observed as a function of temperature, reaching a maximum at 1400 $^{\circ}$ C. It was also found out that samples that started with submicron size particles ended up having the highest hardness while samples with initial nano particles displayed the lowest. The apparent low hardness of nano particle samples after sintering conforms to our previous work [37] as well, which focuses on conventional sintering of WC-Co. When nano particles are employed, it does illustrate a higher amount of exposed surface area as opposed to particles that are larger in size, making them more prone to grain growth as a function of temperature during the sintering process, resulting in low hardness. While there are a number of parameters that can affect the hardness behaviour of sintered samples, three are considered to be the most influential; pressure, temperature and particle size. Since microwave sintering is a pressure less heating process and an initial pre-compaction was carried out on all samples with a constant pressure, temperature and particle size are the only parameters that can essentially factor in for the hardness behaviour displayed for these set of samples. It has been established before [14] that the absence of a liquid phase in sintered carbides can result in low density and hardness as it is difficult for the low concentration binder material to ensure proper solubility within a hard matrix that is in solid form as well, on top of the fact that pressure is not influencing the process. This explains the low hardness observed around 1000 $^{\circ}$ C irrespective of the type of carbide samples. When temperature was raised to 1250 $^{\circ}$ C, which is capable of generating a liquid phase [38, 39] within the microstructure, a rather wide spectrum of hardness values were noted, submicron samples being the hardest. It is possible that at the beginning of the liquid phase formation process for the primary binder, the wettability status as well as the solubility of Co matrix and WC are quite uncontrolled without the presence of applied pressure [40]. In addition, the fact that the binder might not reach a complete liquid phase and that there is a partial presence of semi liquid or solid phase present may cause further uncertainly to the hardness behaviour. Also in terms of microstructure, grain growth is a critical factor in understanding hardness behaviour of carbides under such conditions, which will be further elaborated in the microstructural analysis part of this paper. So, it is understandable to a certain extent that WC-Co particles can end up displaying a rather wide range of hardness values after being sintered around that temperature bracket. In contrast, when there is clear presence of a liquid phase which is typically observed at higher temperatures ranging between 1350-1500 $^{\circ}$ C [32], hardness behaviour is more controlled and predictable due to a higher level of solubility of binder within the matrix [38], irrespective of the initial particle size.

Fracture toughness of a material is an indication of how resistant a material is against crack propagation or brittle failure. It has been of interest to moderate the fracture toughness behaviour for cemented carbides since a combination of high hardness and reasonable fracture toughness is much desired for industrial applications. The fracture toughness behaviour of the WC-Co samples microwave sintered at different temperatures is illustrated in Figure 6, which shows an increasing pattern for all three types of samples with respect to varying temperatures. Similar to the hardness behaviour, fracture toughness as well seems to have the lowest values for samples that started with initial nanosized particles. The values were also found to be quite low for low temperature tests regardless of the initial particle size as it was not adequate to generate the minimum interfacial energy between different phases or grains that would ideally allow them to join together and form a strong bond, eventually leading to displaying high strength. For tests involving temperatures towards the higher limit, fracture toughness values were found to be improved, which indicates the likelihood of WC and Co having a cohesive bonding resulting in higher strength, both in terms of hardness and fracture toughness. The fact that samples that started with nano particles are prone to fracture more than the other samples even at the highest temperature suggest that microstructural feature like grain growth may have a contribution to it. It is well established that grain growth can have adverse effects on fracture toughness in brittle materials [41-43]. Although several studies have introduced ideas of controlling grain growth [44-49] that would help increase fracture toughness in materials, most of them, as opposed to our work, employed additional commercial grain growth inhibitors as part of the composition. Another way to explain the low fracture toughness along with the hardness behaviour of the nano samples is to indicate that nano particles are more prone to agglomeration than micron size particles. Since there is larger amount of surface area available as well, the binder might not be uniformly distributed between the WC particles for nano particles when compared to micron. This would essentially refer to the idea that there is a possibility of more WC-WC contact in nano Co than in micron. In addition since WC-WC bond formation requires high temperature, the bond is not as well established as the bond for WC-Co-WC since WC dissolves in Co at around 1300 °C to generate a strong bond.

Based on the understanding we have on fracture toughness, it is safe to assume that it is more likely to be influenced by factors like final sintering temperature and grain growth than initial particle size, unless final grain size is found to be almost within the identical range with the initial particle size. Having said that, it is important to know that particle size is also critical in the understanding of grain growth behaviour. Due to the constraints on sample size, the conventional fracture toughness tests could not to be carried out. Using eq. (2), and the hardness and crack length measurements, fracture toughness values were obtained. A typical optical image of a

hardness impression on sintered WC- Co sample is given in Figure 7. As it can be seen from Figure 7 (a), clean cracks are expected to generate along the edges of the indentation points. Since the nature of the material is still brittle, cracks tend to propagate in an almost straight manner without presence of much deflection. In some cases however, as seen in Figure 7 (b), for samples sintered at 1400 º C, multiple cracks along the edges can generate. It can also be seen that some cracks will initiate secondary cracking along the minor deflection points of propagation which essentially shortens the length of the primary crack by partially offering additional resistance against propagation. In cases like this, fracture toughness values are expected to be higher, which is also reconfirmed from the pattern and values observed in Figure 6.

Figure 8 shows the SEM micrograph of a WC – 7.5 wt. % Co sample sintered at 1400 º C with an initial particle size of around 100 nm. The first thing to notice is the average grain size which seems to have increased by a significant amount during the sintering process. This increase in grain size was not observed for other samples that had larger initial particle size. Several studies [11, 50, 51] suggest that microwave sintering has been pretty effective in preventing grain growth for cemented carbides, with or without the presence of commercial grain growth inhibitors as part of the composition. But it is unclear whether this behaviour is a general understanding for all cemented carbides taking into account that they may vary in terms of particle size and processing conditions. In order to be able to clarify this behaviour, three aspects that are quite important need to be considered. First the initial particle size of the composition that is used for microwave sintering needs to be factored in. Assuming that pre-compaction or pre-milling doesn't cause the particles to go through major deformation or refinement, it has been mostly seen that grain growth is generally absent or of a minimal amount when it comes to submicron or larger particles [52]. Secondly, for nanoparticles, grain growth is something that is considered almost obvious unless one or more grain growth inhibitors are used, which hints at the idea that they may be contributing to limiting growth as an added tool to the already employed microwave sintering process. In other words, the use of microwave sintering alone might not be sufficient for a specific range of particle size when it comes to the controlling grain growth, and can be more effective if more influential catalysts are incorporated. Finally, sintering temperature is also a matter of concern when grain growth needs controlling. Microwave sintering for cemented carbides is thought to be most effective in terms of grain size when sintering temperature doesn't exceed the liquid phase initiation point by a large margin [52]. As temperatures beyond that limit was also employed in this study, a level of grain growth was expected and seen in most samples, although submicron and micron samples only showed minor changes.

For sintered samples, the understanding of density and porosity are quite important. While both of these are essentially the same property, density tends to be more of a physical feature where porosity provides a better reflection from a microstructural perspective. Porosity as a microstructural feature is difficult to measure since it needs to be a quantitative measurement [53, 54], considering the low concentration of the binder phase which can also be overlapped with the pores or the dominant WC phase present within the microstructure. Porosity measurements were carried out on all samples as part of the study using the image analyser mentioned in the experimental section. Figure 9 shows the porosity profiles of two WC (1-3 µm) -7.5 wt. % Co (1-3 µm) samples sintered at 1000 $^{\circ}$ C (a) and 1400 $^{\circ}$ C (b). The dark blue areas in the images are identified as pores which may partially contain some binders as well, while the red areas were identified as Cobalt phases. The remaining sections are representing the more dominant WC phase. The change in colour between different WC phases can be attributed to the difference in carbon content, which was also seen during SEM analysis [31]. During the porosity analysis, two observations were considered quite clear, managing to indicate a shift in pattern with changing sintering conditions. First was the porosity content which was found to be quite high for samples that were sintered at 1000 $^{\circ}$ C, which then showed a declining trend with increasing sintering temperature. This behaviour also conforms to the density and hardness patterns displayed under such sintering conditions, as well as the idea that there may have been a major shift from purely solid phase to a solid-liquid or a liquid phase during the increase of sintering temperature. The dispersion and homogeneity of porosity and the binder phase also seemed to have changed with increasing sintering temperature. The idea that there might be partial dissolution of WC into low concentration liquid Co matrix supports the experimental observation that shows a diminishing behaviour for the binder content. It has been discussed on several occasions, with a reasonable level of understanding that irrespective of the nature of the sintering process, sintered WC-Co does experience WC grains being embedded in a Co matrix [55], which can be thought of as quite conclusive since it came out as a concluding remark from a number of fundamental studies [56-58] that had focused on developing an analytical expression including factors like pressure, temperature, volume fraction of the liquid phase, grain size and so on.

Figure 10 shows the SEM micrographs of all three types of WC-Co samples sintered at three different temperatures, ranging between 1000 and 1400 $^{\circ}$ C. It was observed that particles were not joined very well with each other in samples that were sintered at 1000 $^{\circ}$ C regardless of the initial particle size of the samples, indicating a wide presence of solid WC and Co phases as part of the microstructure. When sintering temperature

was increased to 1250 º C, micron and submicron samples were showing evidence of a liquid phase, as grain shapes were quite irregular in nature, and had deviated from the initial particle size by a reasonable margin. For nano WC-Co samples, there was not much of a difference in microstructural behaviour between 1000 and 1250 º C, suggesting that a higher temperature would be required for the particles to initiate and enhance bonding mechanism. At the highest temperature, all three different types of samples were seen to have irregular shaped grains present. It was also observed that nano particles went through a higher magnitude of grain growth as opposed to the rest of the samples, suggesting that they may be more prone to growth due to the higher percentage of exposed surface area. This result also confirms why they have the least amount of fracture toughness and hardness among the three different types of WC-Co samples, sintered at high temperature. The observation that both micron and submicron particles displayed a proper sintered microstructure even at a temperature as low as 1250 º C not only confirms the high mechanical properties within that temperature bracket, but also indicates the effectiveness of microwave sintering at low temperatures, ensuring possible greater diffusion, faster necking between grains and penetration of heat throughout the material and not just the surface.

It has been mentioned earlier in this paper and in other studies [34, 36] that the importance of binder in cemented carbides is paramount. The facts that it can facilitate the densification process, exhibit more sensitivity to temperature than carbide in both solid and liquid phase, and accelerate the process make it all the more critical in terms of selection and compositional concentration. When microwave sintering is used, which is essentially a pressure less process, pre-compaction is necessary, which yields green samples that are quite porous in nature. Co, which is the primary binder in the composition, along with the sintering temperature, work together in an attempt to reduce porosity through creating a series of faceted WC grains that are embedded in a Co matrix. In order to be able to separate the WC grains from each other, Co should ideally be dispersed and positioned between them. According to several studies, it is also believed that Co doesn't only get wet and spread out, but can also pull WC particles closer after agglomeration [59-61]. Since it is usually difficult to find traces of Cobalt in sintered WC-Co samples, a line scanning was carried out (Figure 11) between several WC grains to observe whether there is presence of the binder that can also help explain the improved mechanical behaviour at elevated sintering temperature. It was seen that Co, although in limited concentration, was present between WC grains, which indicates that liquid phase sintering allowed room for Co migration and channelling between irregular shaped hard WC grains.

5. Conclusion

Three different types of initial WC - Co samples were microwave sintered with varying sintering temperatures. Based on the characteristics, microstructural features and mechanical properties of the sintered samples, it has been suggested that microwave sintering can effectively help improve the quality of a product by transferring energy at an atomic level, throughout an entire volume of a material as opposed to a particular surface or a layer of particles. Density, hardness and fracture toughness all illustrated an incremental behaviour in response to increasing sintering temperature, although mid-range temperature (1250 $^\circ$ C) demonstrated promising results for both micron and submicron samples. The advantages of using this process are many, including but not limited to grain growth inhibition, faster heating, low temperature sintering, reduction in energy consumption and less precipitation of selective phases.

References

[1] Oghbaei M, Mirzaee O. Microwave versus conventional sintering: A review of fundamentals, advantages and applications. Journal of Alloys and Compounds. 2010;494:175-89.

[2] Raihanuzzaman RM, Jeong TS, Ghomashchi R, Xie Z, Hong S-J. Characterization of short-duration high-energy ball milled WC–Co powders and subsequent consolidations. Journal of Alloys and Compounds. 2014;615:S564-S8.

[3] Clark DE, Sutton WH. Microwave processing of materials. Annual Review of Materials Science. 1996;26:299-331.

[4] Ro K, Dreyer K, Gerdes T, Willert-Porada M. Microwave sintering of hardmetals. International Journal of Refractory Metals and Hard Materials. 1998;16:409-16.

[5] Clark DE, Folz DC, West JK. Processing materials with microwave energy. Materials Science and Engineering: A. 2000;287:153-8.

[6] Agrawal D. Microwave sintering, brazing and melting of metallic materials. Sohn International Symposium; Advanced Processing of Metals and Materials Volume 4: New, Improved and Existing Technologies: Non-Ferrous Materials Extraction and Processing2006. p. 183-92.

[7] Bykov YV, Rybakov K, Semenov V. High-temperature microwave processing of materials. Journal of Physics D: Applied Physics. 2001;34:R55.

[8] Holcombe CE, Dykes NL, Morrow MS. Thermal insulation for high temperature microwave sintering operations and method thereof. Google Patents; 1995.

[9] Katz JD. Microwave sintering of ceramics. Annual Review of Materials Science. 1992;22:153-70.

[10] Holcombe C, Dykes N. 'Ultra'High-Temperature Microwave Sintering. DTIC Document; 1992.

[11] Agrawal DK. Microwave processing of ceramics. Current Opinion in Solid State and Materials Science. 1998;3:480-5.

[12] Raihanuzzaman RM, Chuan LC, Xie Z, Ghomashchi R. Microwave Sintering and Its Application on Cemented Carbides. World Academy of Science, Engineering and Technology, International Journal of Chemical, Molecular, Nuclear, Materials and Metallurgical Engineering. 2015;9:930-3.

[13] Xie Z-H, Hoffman M, Cheng YB. Microstructural Tailoring and Characterization of a Calcium α-SiAlON Composition. Journal of the American Ceramic Society. 2002;85:812-8.

[14] Cha SI, Hong SH, Kim BK. Spark plasma sintering behavior of nanocrystalline WC–10Co cemented carbide powders. Materials Science and Engineering: A. 2003;351:31-8.

[15] Doi H, Fujiwara Y, Miyake K, Oosawa Y. A systematic investigation of elastic moduli of WC-Co alloys. Metallurgical and Materials Transactions. 1970;1:1417-25.

[16] Upadhyaya G. Materials science of cemented carbides—an overview. Materials & Design. 2001;22:483-9.

[17] Santhanam A, Tierney P, Hunt J. Cemented carbides. ASM International, Metals Handbook, Tenth Edition. 1990;2:950-77.

[18] Coromant S. Modern metal cutting: a practical handbook: Sandvik Coromant; 1994.

[19] Kono Y, Nakamoto M, Irifune T. Elastic properties of sintered diamonds with and without Co binder. Journal of Physics: Conference Series: IOP Publishing; 2010. p. 012134.

[20] Shuman DJ, Costa AL, Andrade MS. Calculating the elastic modulus from nanoindentation and microindentation reload curves. Materials characterization. 2007;58:380-9.

[21] Xueming M, Ling Z, Gang J, Yuanda D. Preparation and structure of bulk nanostructured WC-Co alloy by high energy ball-milling. Journal of materials science letters. 1997;16:968-70.

[22] Kimmel ER, Shaffer ME, Pinkowski TR, Harris GL. Method of producing monotungsten carbide powder. Google Patents; 1987.

[23] Butler BG, JUN L, Fang ZZ, Rajamani RK. Production of nanometric tungsten carbide powders by planetary milling. International journal of powder metallurgy. 2007;43:35-43.

[24] Morton C, Wills D, Stjernberg K. The temperature ranges for maximum effectiveness of grain growth inhibitors in WC–Co alloys. International Journal of Refractory Metals and Hard Materials. 2005;23:287-93.

[25] Fang Z, Eason JW. Study of nanostructured WC-Co composites. International Journal of Refractory Metals and Hard Materials. 1995;13:297-303.

[26] Choi K, Hwang N. Effect of VC addition on microstructural evolution of WC–Co alloy: mechanism of grain growth inhibition. Powder Metallurgy. 2000;43:168-72.

[27] Chandler H, Sands C, Song J, Withers P, McDonald S. A plasticity model for powder compaction processes incorporating particle deformation and rearrangement. International Journal of Solids and Structures. 2008;45:2056-76.

[28] Martin C, Bouvard D, Shima S. Study of particle rearrangement during powder compaction by the discrete element method. Journal of the Mechanics and Physics of Solids. 2003;51:667-93.

[29] Lamy P, Brunet L, Thomas G. Modeling the porosity evolution of a powder under uniaxial compression. Propellants, Explosives, Pyrotechnics. 2005;30:397-403.

[30] Aryanpour G, Farzaneh M. Application of a piston equation to describe die compaction of powders. Powder Technology. 2015;277:120-5.

[31] Rumman MR, Xie Z, Hong S-J, Ghomashchi R. Effect of spark plasma sintering pressure on mechanical properties of WC–7.5 wt% Nano Co. Materials & Design. 2015;68:221-7.

[32] Song J-W, Raihanuzzaman RM, Hong S-J. Consolidation of WC-Co Alloys by Magnetic Pulsed Compaction and Evaluation of their Mechanical Properties. Powder Technology. 2012;235: 723–7.

[33] Hong S-J, Rumman MR, Rhee CK. Effect of Magnetic Pulsed Compaction (MPC) on Sintering Behavior of Materials. In: Lakshmanan DA, editor. Sintering of Ceramics - New Emerging Techniques. Croatia: InTech Publication; 2012. p. 159-76.

[34] Shao G, Duan X, Xie J, Yu X, Zhang W, Yuan R. Sintering of nanocrystalline WC-Co composite powder. Reviews on Advanced Materials Science. 2003;5:281-6.

[35] Sun L, Jia C, Cao R, Lin C. Effects of Cr 3 C 2 additions on the densification, grain growth and properties of ultrafine WC–11Co composites by spark plasma sintering. International Journal of Refractory Metals and Hard Materials. 2008;26:357-61.

[36] Da Silva A, Schubert W, Lux B. The role of the binder phase in the WC-Co sintering. Materials Research. 2001;4:59-62.

[37] Raihanuzzaman RM, Han S-T, Ghomashchi R, Kim H-S, Hong S-J. Conventional sintering of WC with nano-sized Co binder: Characterization and mechanical behavior. International Journal of Refractory Metals and Hard Materials. 2015.

[38] Jia C-C, Tang H, Mei X-Z, Yin F-Z, Qu X-H. Spark plasma sintering on nanometer scale WC–Co powder. Materials Letters. 2005;59:2566-9.

[39] Jia K, Fischer T, Gallois B. Microstructure, hardness and toughness of nanostructured and conventional WC-Co composites. Nanostructured Materials. 1998;10:875-91.

[40] Bhaumik S, Upadhyaya G, Vaidya M. Full density processing of complex WC-based cemented carbides. Journal of materials processing technology. 1996;58:45-52.

[41] Kenny P. Application of fracture mechanics to cemented tungsten carbides. Powder Met. 1971;14:22-38.

[42] Yen SS. Fracture toughness of cemented carbides: Lehigh University; 1971.

[43] Ingelstrom N, Nordberg H. The fracture toughness of cemented tungsten carbides. Engineering Fracture Mechanics. 1974;6:597-607.

[44] Sivaprahasam D, Chandrasekar S, Sundaresan R. Microstructure and mechanical properties of nanocrystalline WC–12Co consolidated by spark plasma sintering. International Journal of Refractory Metals and Hard Materials. 2007;25:144-52.

[45] Zhao H, Zhu L, Huang Q. Nanocrystalline WC-10% Co-0.8% VC cemented carbides prepared by spark plasma sintering. Rare Met Mat Eng. 2005;34:82-5.

[46] Yingfang X, Xingqing W, Lidong C, Xiaodong L, Hailiang G. Preparation of superfine-cemented carbide by spark plasma sintering. Journal of Wuhan University of Technology--Materials Science Edition. 2006;21:42-5.

[47] Maizza G, Grasso S, Sakka Y, Noda T, Ohashi O. Relation between microstructure, properties and spark plasma sintering (SPS) parameters of pure ultrafine WC powder. Science and Technology of Advanced Materials. 2007;8:644-54.

[48] Michalski A, Siemiaszko D. Nanocrystalline cemented carbides sintered by the pulse plasma method. International Journal of Refractory Metals and Hard Materials. 2007;25:153-8.

[49] Raihanuzzaman RM, Kim JH, Lee JK, Yoon JS, Son H-T, Hong S-J. Wear Behavior of Al-Fe-Cr-Ti Alloys fabricated by Magnetic Pulsed Compaction. Powder Technology. 2012;225:227–31.

[50] Das S, Mukhopadhyay A, Datta S, Basu D. Prospects of microwave processing: An overview. Bulletin of Materials Science. 2009;32:1-13.

[51] Demirskyi D, Borodianska H, Agrawal D, Ragulya A, Sakka Y, Vasylkiv O. Peculiarities of the neck growth process during initial stage of spark-plasma, microwave and conventional sintering of WC spheres. Journal of Alloys and Compounds. 2012;523:1-10.

[52] Breval E, Cheng J, Agrawal D, Gigl P, Dennis M, Roy R, et al. Comparison between microwave and conventional sintering of WC/Co composites. Materials Science and Engineering: A. 2005;391:285-95.

[53] Martínez V, Echeberria J. Hot isostatic pressing of cubic boron nitride–tungsten carbide/cobalt (cBN–WC/Co) composites: effect of cBN particle size and some processing parameters on their microstructure and properties. Journal of the American Ceramic Society. 2007;90:415-24.

[54] Amberg S, Doxner H. Porosity in cemented carbide. Powder Metallurgy. 1977;20:1-10.

[55] Schwarzkopf P, Kiefer R. Cemented Carbides, 1960. The Macmillan Company, New York.71:140-55.

[56] Beere W. A unifying theory of the stability of penetrating liquid phases and sintering pores. Acta Metallurgica. 1975;23:131-8.

[57] Park H-H, Yoon DN. Effect of dihedral angle on the morphology of grains in a matrix phase. Metallurgical Transactions A. 1985;16:923-8.

[58] Delannay F, Pardoen D, Colin C. Equilibrium distribution of liquid during liquid phase sintering of composition gradient materials. Acta materialia. 2005;53:1655-64.

[59] Meredith B, Milner D. Densification Mechanisms in the Tungsten Carbide—Cobalt System. Powder Metallurgy. 1976;19:38-45.

[60] Snowball R, Milner D. Densification processes in the Tungsten Carbide-Cobalt system. Powder Metallurgy. 1968;11:23-40.

[61] Nelson R, Milner D. Liquid-flow densification Mechanisms in the Tungsten Carbide—Copper System. Powder Metallurgy. 1971;14:39-63.

[62] Raihanuzzaman RM, Chuan LC, Xie Z, Ghomashchi R. Microwave Sintering and Its Application on Cemented Carbides.

List of Tables

Table 1: Mixing and processing conditions of WC-Co powders

Table 2: Features of the microwave furnace
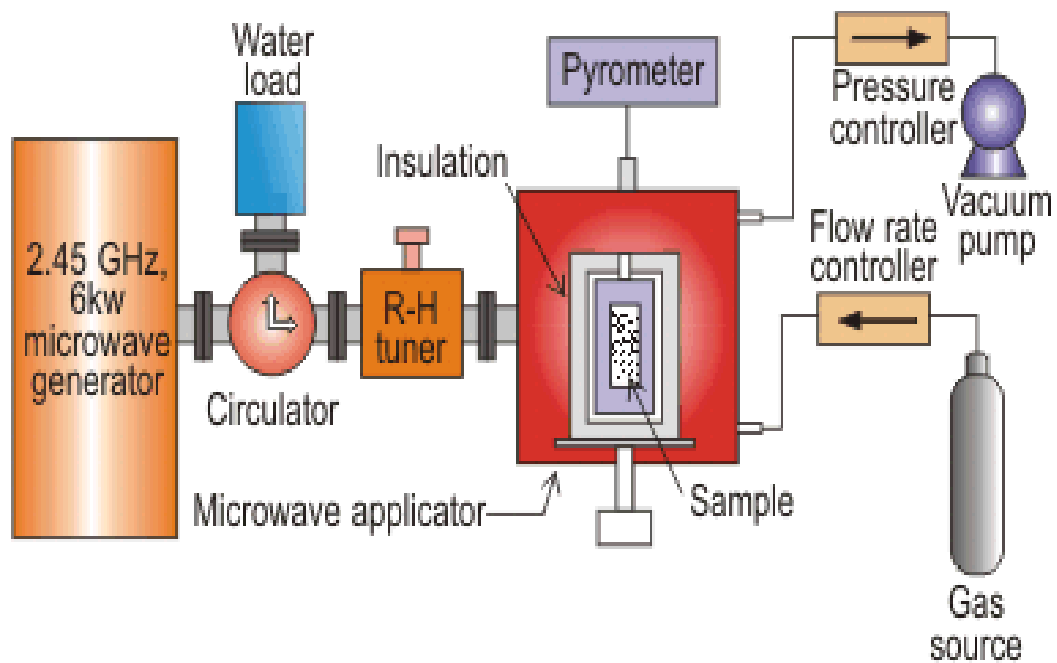
List of Figures

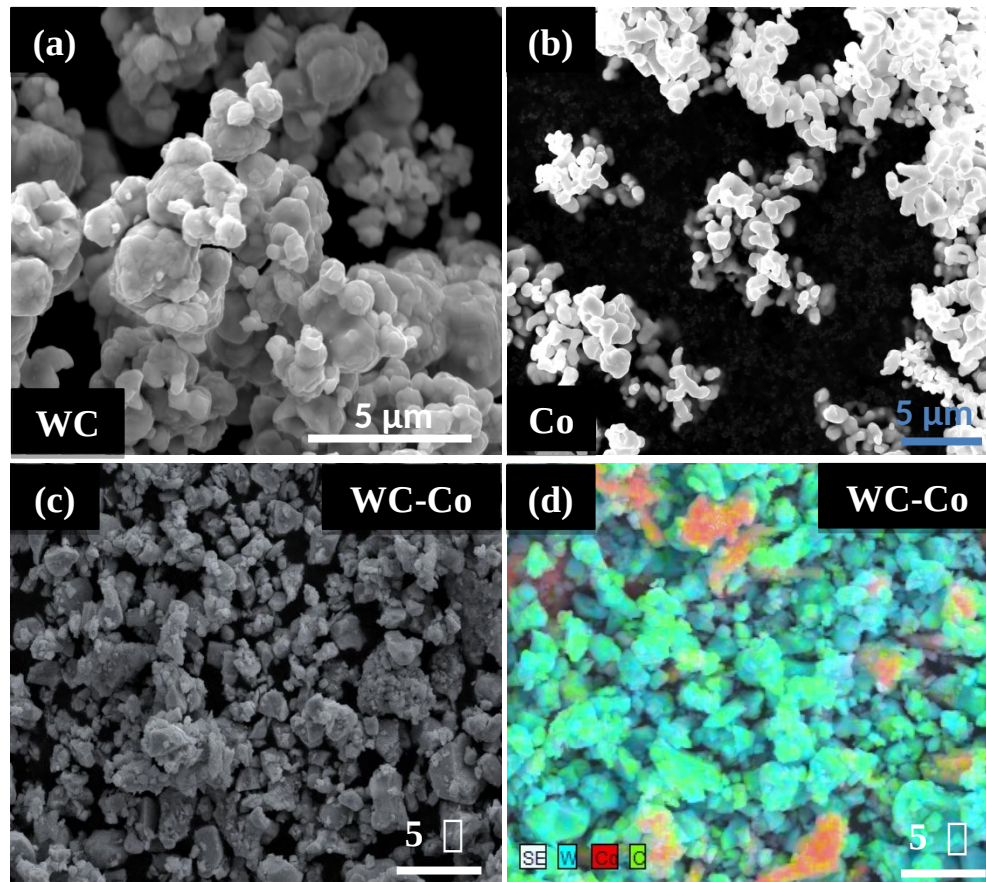Fig 1: Schematic diagram of a microwave furnace assembly

Fig 2: SEM micrographs (SE) of (a) initial WC powders (b) initial Co powders (c) mixed WC-7.5 wt.% Co powders and (d) EDX image of mixed WC-7.5 wt. % Co powders
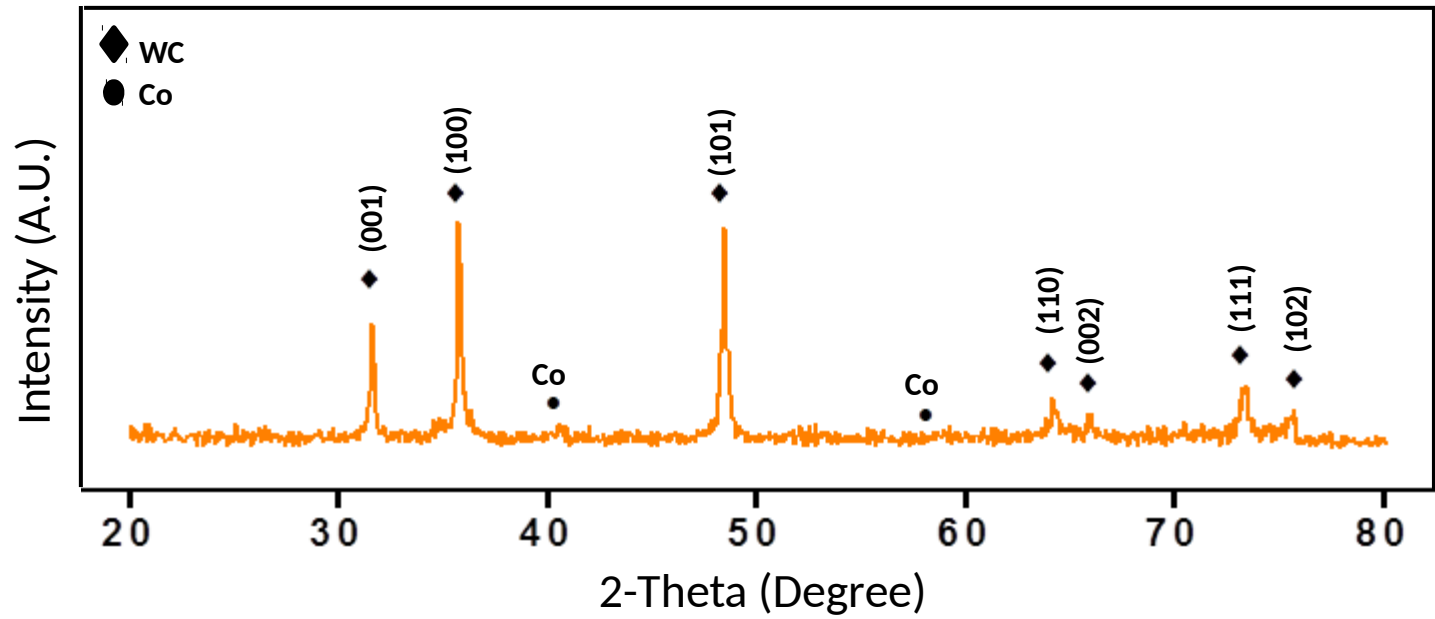
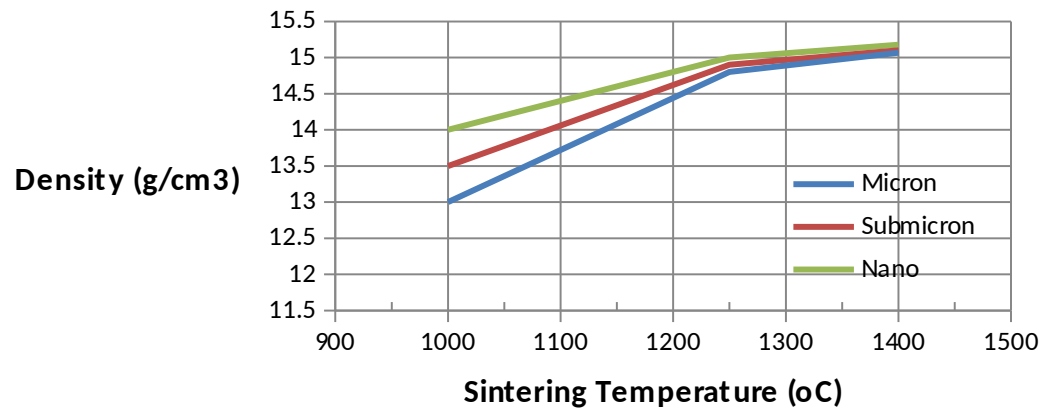Fig 3: XRD pattern of WC - 7.5 wt. % Co Powders

Fig 4: Changes in density of sintered WC - 7.5 wt. % Co with varying sintering temperature and initial particle size.
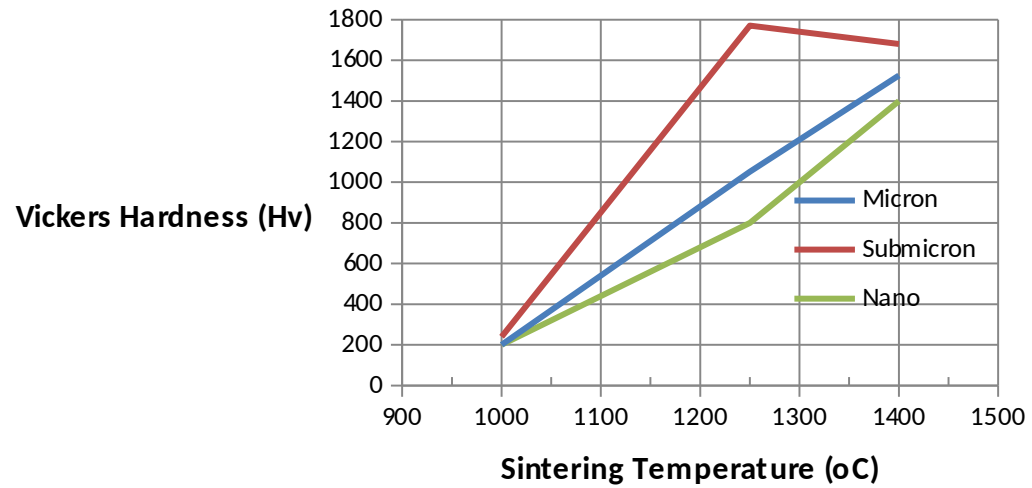
Fig 5: Changes in hardness behavior of sintered WC - 7.5 wt. % Co with varying sintering temperature and initial particle size.
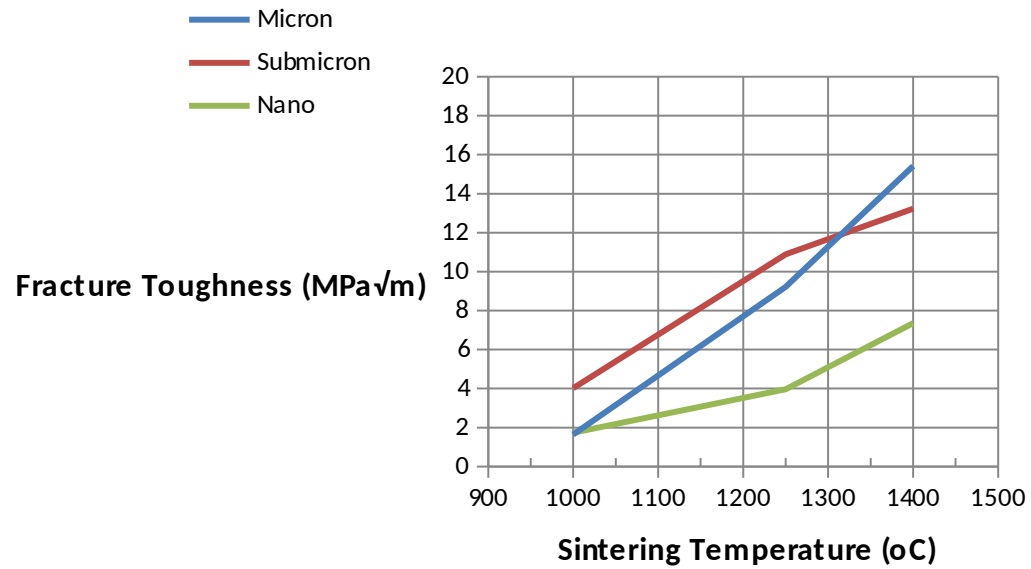
Fig 6: Changes in fracture toughness of sintered WC - 7.5 wt. % Co with varying sintering temperature and initial particle size.
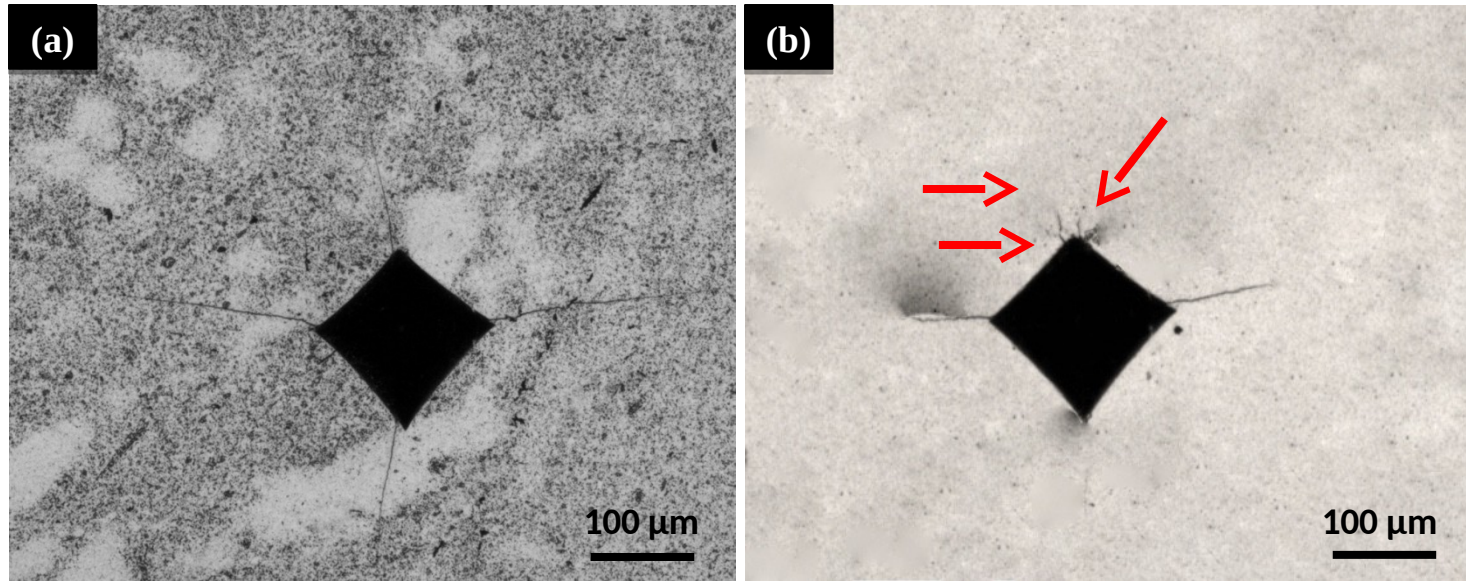
Fig 7: Optical micrographs of WC-Co samples sintered at a) 1250 ^{o}C and b) 1400 ^{o}C. The initial particle size of both WC and Co were around 500 nm. The cracks observed in the first figure are representative of how cracks usually generated along the edges in response of hardness indentations. However, in some cases, multiple, but smaller cracks were found to be present around a single edge, as seen in (b)
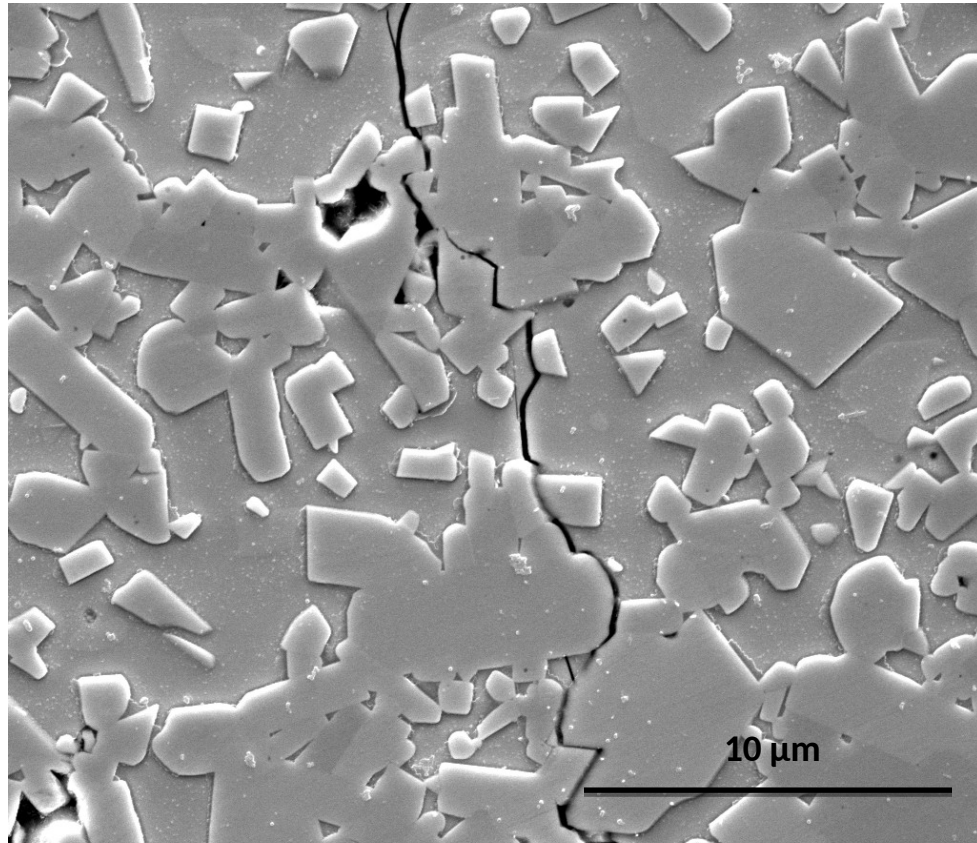
Fig 8: WC (100 nm) - 7.5 wt. % Co (100 nm) microwave sintered at 1400 ^{o} C
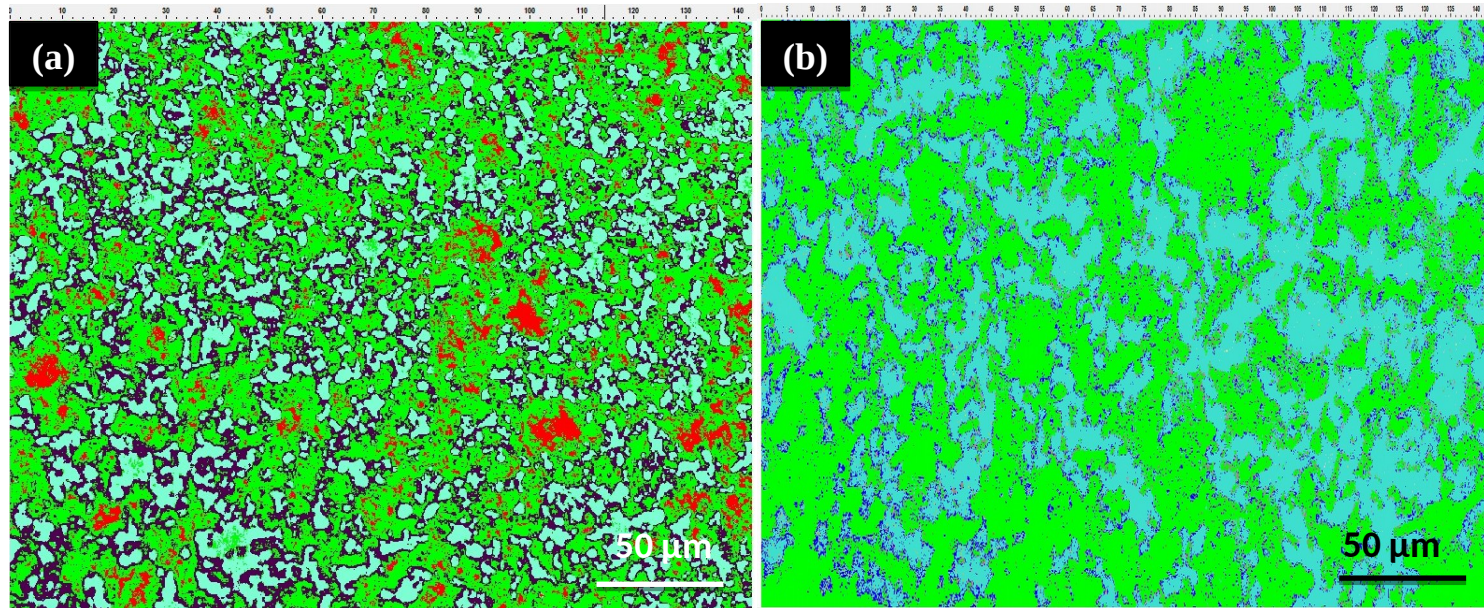
Fig 9: Porosity analysis of spark plasma sintered samples (a) WC (1-3 µm) -7.5 wt.% Co (1-3 µm) at 1000 $^{\circ}$ C (b) WC (100 nm) - 7.5 wt. % Co (100 nm) at 1400 $^{\circ}$ C

	1000 °C	1250 °C	1400 °C
Micron	(a)	(b)	(c)
Sub Micron	(d)	(e)	(f)
Nano	(g)	(h)	(i)

Fig 10: SEM secondary electron images of WC-7.5wt. % Co samples sintered at different temperatures.
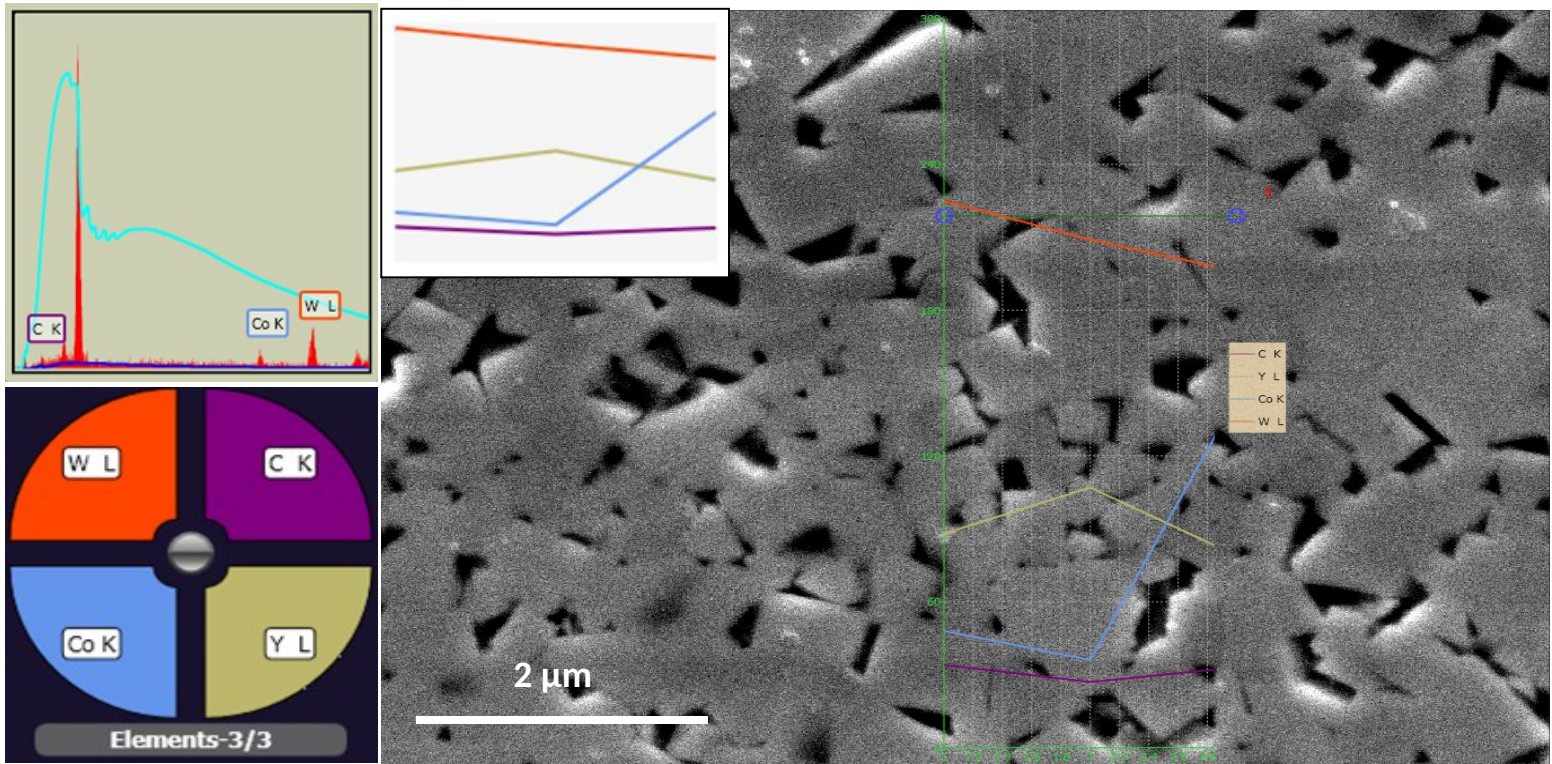
Fig 11: Line scanning of WC (1-3 µm) - 7.5 wt. % Co (1-3 µm) sample, microwave sintered at 1400 ° C

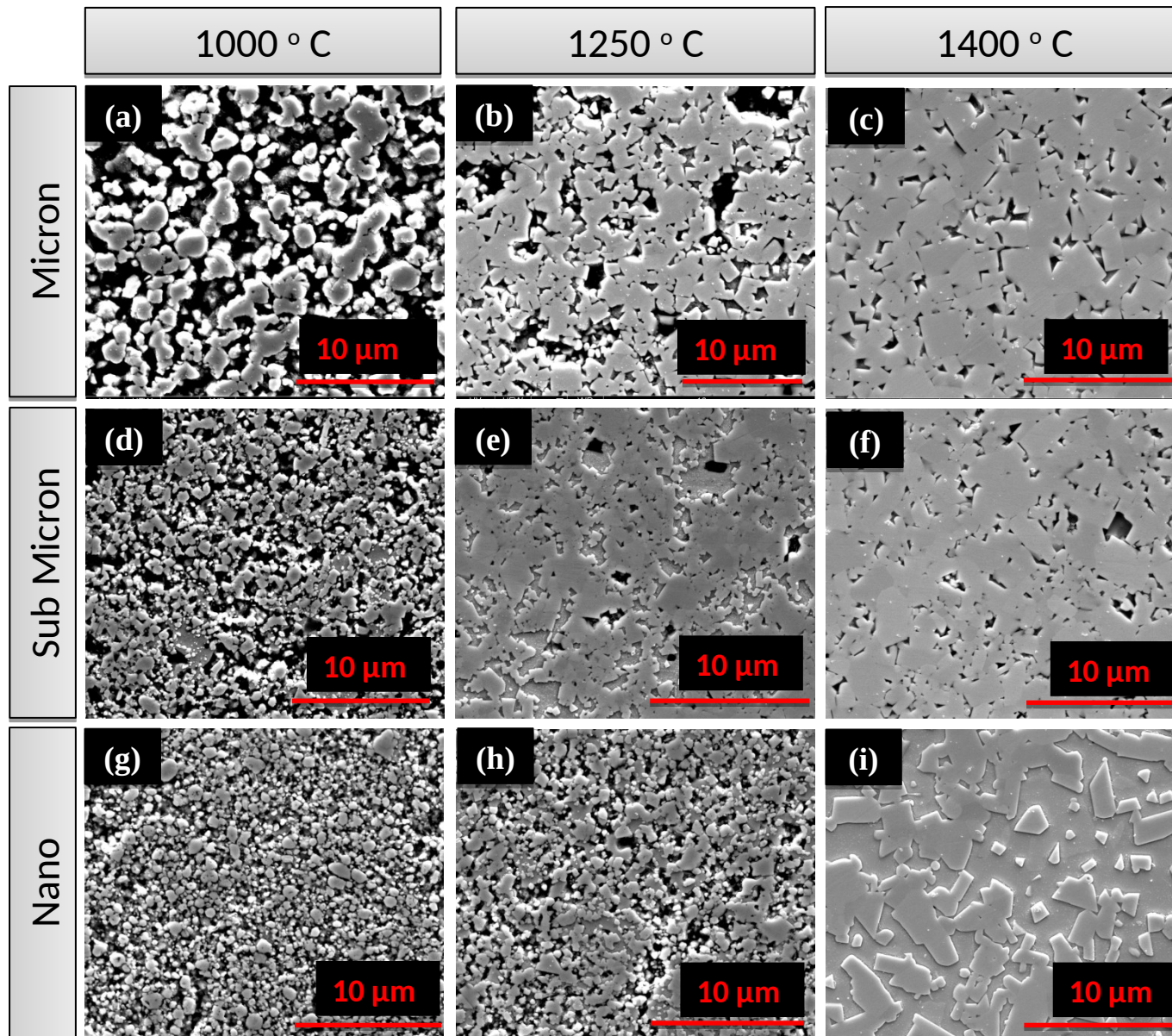| Sample Number	Composition	Size of WC Particles (Avg.)	Size of Co Particles (Avg.)	Weight of Mixed Powder (g)	Compaction Pressure (MPa)	Sintering Temperature ($^{\circ}$ C)	Heating Rate ($^{\circ}$C/min)	Holding Time (Min)
1	WC-7.5Co	1-3 µm	1-3 µm	2.0	50	1000	40	60
2	WC-7.5Co	1-3 µm	1-3 µm	2.0	50	1250	40	60
3	WC-7.5Co	1-3 µm	1-3 µm	2.0	50	1400	40	60
4	WC-7.5Co	500 nm	500 nm	2.0	50	1000	40	60
5	WC-7.5Co	500 nm	500 nm	2.0	50	1250	40	60
6	WC-7.5Co	500 nm	500 nm	2.0	50	1400	40	60
7	WC-7.5Co	100 nm	100 nm	2.0	50	1000	40	60
8	WC-7.5Co	100 nm	100 nm	2.0	50	1250	40	60
9	WC-7.5Co	100 nm	100 nm	2.0	50	1400	40	60

Table 1: Mixing and processing conditions of WC-Co powders

Microwave Furnace Model	MW-L0316V
Output power	3kW
Maximum operating temperature	1600°C
Maximum heating rate	50 ^{o}C/min
Temperature measurement	Infra-Red sensor, 450-2250°C (Raytek)
Temperature Control	PID controller with ramp and soak
Maximum frequency	2450 MHz
Overall Size	800 mm (W) x 800 mm (D) x 1800 mm (H)
Atmosphere	Air, Argon, Hydrogen, Nitrogen
Cooling	Water, 2m^3/h

Table 2: Features of the microwave furnace.

Mechanical Properties and Microstructural Behavior of Pulse Plasma Sintered WC - Co

Rumman Md Raihanuzzaman*, Marcin Rosinski[1], Zonghan Xie, Reza Ghomashchi*

School of Mechanical Engineering, The University of Adelaide,

South Australia 5005, Australia

[1]GeniCore, Warsaw, Poland

Statement of Authorship

Title of Paper	Mechanical Properties and Microstructural Behavior of Pulse Plasma Sintered WC - Co
Publication Status	☐ Published ☐ Accepted for Publication ☑ Submitted for Publication ☐ Unpublished and Unsubmitted work written in manuscript style
Publication Details	Raihanuzzaman RM, Marcin Rosinski, Zonghan Xie, Reza Ghomashchi Mechanical Properties and Microstructural Behaviour of Pulse Plasma Sintered WC – Co, International Journal of Refractory Metals and Hard Materials (Under Review)

Principal Author

Name of Principal Author (Candidate)	Md Raihanuzzaman Rumman		
Contribution to the Paper	I was responsible for the literature review required for this work, and designed the framework for the experimental conditions. I carried out the mechanical property and microstructural behaviour analysis, wrote the first draft of the manuscript and incorporated and addressed all comments and suggestions by other authors in subsequent revisions of the manuscript. Interpretation of data was primarily my responsibility.		
Overall percentage (%)	85%		
Certification:	This paper reports on original research I conducted during the period of my Higher Degree by Research candidature and is not subject to any obligations or contractual agreements with a third party that would constrain its inclusion in this thesis. I am the primary author of this paper.		
Signature		Date	22/12/15

Co-Author Contributions

By signing the Statement of Authorship, each author certifies that:
  i.   the candidate's stated contribution to the publication is accurate (as detailed above);
  ii.   permission is granted for the candidate in include the publication in the thesis; and
  iii. the sum of all co-author contributions is equal to 100% less the candidate's stated contribution.

Name of Co-Author	Reza Ghomashchi		
Contribution to the Paper	I was supervisor of this work, and contributed to outlining the scope of this work and refining the manuscript.		
Signature		Date	23/12/2015

Name of Co-Author	Zonghan Xie		
Contribution to the Paper	I was joint supervisor for the work, and contributed to refining the manuscript.		
Signature		Date	15/01/2016

Name of Co-Author	Marcin Rosinski		
Contribution to the Paper	I have conducted the pulse plasma compaction and sintering of the powder samples, and jointly contributed in refining the manuscript.		
Signature		Date	05/02/2016

Manuscript details

Manuscript number   IJRMHM_2016_83

Title   Mechanical Properties and Microstructural Behavior of Pulse Plasma Sintered WC - Co

Article type   Research Paper

Abstract   Tungsten carbides-based inserts have been considered as one of the dominant hard materials in the cutting industry, receiving great interest for their excellent combination of mechanical properties. Pulse plasma sintering (PPS) process has been applied to a series of WC-Co samples with varying sintering temperature, initial particle size and sintering pressure in order to study the mechanical and microstructural behaviour. The quality of the products as well as the mechanical properties and microstructural features this process yields are commendable and worth looking into. A high hardness of more than 2000 HV has been achieved while a maximum fracture þÿ t o u g h n e s s   o f   1 5 . 3   M P a" m   w a in samples that were sintered at 1100 oC and 100 MPa. Microstructural features like grain growth and other properties are discussed with respect to the varying parameters. While grain size shows an incremental pattern with increasing temperature, it was still possible to limit them to a great extent ensuring high mechanical properties. The effect of sintering pressure in the range of 60-100 MPa, while

keeping sintering temperature constant, was found to be almost negligible.

Corresponding Author   Md. Raihanuzzaman Rumman

Corresponding Author's Institution   The University of Adelaide

Order of Authors   Md. Raihanuzzaman Rumman, Marcin Rosinski, Zonghan Xie, Reza Ghomashchi

Submission files included in this PDF

File Type	File Name
Cover Letter	Cover Letter.docx
Highlights	Research Highlights.docx
Manuscript File	Manuscript.docx
Figure	Figures.pptx
Table	Tables.pptx

To view all the submission files, including those not included in the PDF, click on the manuscript title on your EVISE Homepage, then click 'Download zip file'.

Request for Publication

Wednesday, Feb 10, 2016

Editor
International Journal of Refractory Metals and Hard Materials

Title: **"Mechanical Properties and Microstructural Behavior of Pulse Plasma Sintered WC - Co"** by Rumman

Md Raihanuzzaman, Marcin Rosinski, Zonghan Xie and Reza Ghomashchi

Dear Editor

I am pleased to submit another article entitled **"Mechanical Properties and Microstructural Behavior of Pulse Plasma Sintered WC - Co"** by Rumman Md Raihanuzzaman, Marcin Rosinski, Zonghan Xie and Reza Ghomashchi for publication in your journal, which is the third article in this series of work (One published and one currently under review). The manuscript has not been previously published, is not currently submitted for review to any other journal, and will not be submitted elsewhere before one decision is made. All authors are fully aware of the progress and state of this paper.

I would appreciate if it is kindly considered and processed for publication on the journal.

Sincerely yours,

Rumman Md Raihanuzzaman
School of Mechanical Engineering, The University of Adelaide, Adelaide, Australia 5000
E-mail: raihan.rumman@adelaide.edu.au
Tel: +61 (08) 8313 4185, Fax: +61 (08) 8313 4367

Research Highlights

- Effect of pulse plasma sintering process, temperature, and particle size on mechanical properties of WC was studied.
- Crack initiation, propagation and grain size were analyzed to discuss mechanical properties.
- Quantitative measurement of porosity was carried out in reconfirming density and hardness behavior.
- Overall, microstructural characteristics were analyzed to explain hardness and fracture toughness.

Mechanical Properties and Microstructural Behavior of Pulse Plasma Sintered WC - Co

Rumman Md Raihanuzzaman*, Marcin Rosinski[1], Zonghan Xie, Reza Ghomashchi*

School of Mechanical Engineering, The University of Adelaide, South Australia

[1]GeniCore, Warsaw, Poland

Phone: +61 (0) 8 8313 4185

Email: raihan.rumman@adelaide.edu.au, reza.ghomashchi@adelaide.edu.au

Abstract

Tungsten carbides-based inserts have been considered as one of the dominant hard materials in the cutting industry, receiving great interest for their excellent combination of mechanical properties. Pulse plasma sintering (PPS) process has been applied to a series of WC-Co samples with varying sintering temperature, initial particle size and sintering pressure in order to study the mechanical and microstructural behaviour. The quality of the products as well as the mechanical properties and microstructural features this process yields are commendable and worth looking into. A high hardness of more than 2000 HV has been achieved while a maximum fracture toughness of 15.3 MPa√m was recorded in samples that were sintered at 1100 ℃ and 100 MPa. Microstructural features like grain growth and other properties are discussed with respect to the varying parameters. While grain size shows an incremental pattern with increasing temperature, it was still possible to limit them to a great extent ensuring high mechanical properties. The effect of sintering pressure in the range of 60-100 MPa, while keeping sintering temperature constant, was found to be almost negligible.

Keywords: Cemented carbides; Pulse Plasma Sintering; Microstructure, Mechanical Properties, Compaction

1. Introduction

Powder metallurgy is considered one of the most effective methods for the fabrication of cemented carbides. The process chain can be segmented into several stages that usually changes depending on the requirements of the product. The process usually starts from initial powders that may go through a milling stage and then into compaction. Compaction and sintering, which are two important processes, can also be carried out together. This in effect not only allows for better efficiency in terms of time and energy consumption, but can also contribute in achieving high mechanical properties and desired microstructural features like grain size and growth. In order to cater for the desired requirements within the field of powder metallurgy, a few integrated compaction and sintering processes have been employed on cemented carbides [1-3].

Sintering is arguably the most important step of the manufacturing process for these series of cemented carbides [4-6]. It can be roughly classified into two types; namely sintering without pressure and sintering with applied pressure. When pressure-less sintering is used, it is imperative to employ a separate compaction process prior to heating in order to be able to generate the green samples. Plasma sintering is now finding application as a chosen sintering process due to their fast and effective diffusion processes rendering almost 100% theoretical density [7-10]. Pulse plasma sintering is one of the new pressure assisted integrated compaction and heating processes that are being explored for the manufacture of carbide tools [11, 12]. The advantage of using this process primarily comes from the idea that pressure and temperature are simultaneously applied during the process, which in effect saves time and energy and can even contribute towards faster densification and diffusion during the process [13].

When conventional sintering is used to manufacture these hard materials, thermal energy is usually directed to the surface of the material, either through radiation or a convection process, which is then progressed to the rest of the material which is a slow process altogether [14-16]. The heating rate is often set low in this process and can take several hours to complete, which is only one stage of the manufacturing process. In addition, a pre-compaction process also needs to be carried out in order to produce green samples [17]. Pulse plasma sintering in contrast is a modern sintering process where plasma assisted sintering can be achieved at a relatively low temperature taking advantage of the rapid heating rate of the process. The pulse current used is considered as an

important feature towards heating of powder particles. Within the short duration and frequently generated current pulse, spark discharges are generally ignited in the pores of the sample that undergo a simultaneous compaction. These generated spark discharges are capable of removing the gaseous content including oxygen from the surface of the material, creating an easier path for particles or grains to bond together, irrespective of the presence or state of the liquid or binder phase of the material [18]. The compressive stress applied in this process results in having better contact among particles and is capable of improving densification mechanisms, namely grain boundary diffusion or even initiate plastic deformation or grain boundary sliding [19, 20].

The aim of this paper is to discuss the mechanical properties and microstructural features of a range of pulse plasma sintered WC - 7.5 wt. % Co samples that are different in terms of sintering temperature, initial particle size and pressure applied during the heating process.

2. Pulse Plasma Sintering:

The pulse plasma sintering process is unique in terms of efficiency of the heating process involved. In this process the reaction is initiated by periodically generated high current electric pulses that are charged at a maximum of 6kV by the energy source, which is a battery of capacitors. During this process energy is released on to the powder particles for repeated duration of a fraction of a second (frequency 1-20Hz), while they are already under a constant set pressure. This process of heating by very narrow high-current pulses with duration in the order of hundreds of microsecond, along with the applied pressure on the powders help the particles reach the ignition temperature faster in comparison with conventional heating processes. From a physical point of view, compressed particles are heated by Joule heating at contact points with the help of repeated spark discharges occurring between particles and within pores helping faster diffusion [21], along with building momentum of atoms due to the plasma ion-atoms interaction that are active during the sintering process. Fig. 1 shows a schematic diagram of a pulse plasma sintering unit of Genicore company while Fig. 2 shows the behavior of pulse current during a battery of capacitors discharge of PPS unit model GC_A_V2L200HV.

3. Experimental Procedure

In this study, three different sizes of WC and Co particles were used, namely 1~3 µm, 500 nm and 100nm, with an average of 0.1 (wt. %) total oxygen, 0.06 (wt. %) free carbon and 6.10–6.18 (wt. %) carbon content in the WC particles. A fixed composition of WC - 7.5 wt. % Co was used throughout the whole study while sintering temperature, pressure and initial particle size of the samples were varied. Powders were first mixed using a high-energy ball mill with a 5:1 ball to powder ratio, using Ti coated WC balls and jar. The speed of rotation was set at 500 rpm and was used for 5 minutes to mix the powders under dry conditions. Powders were then compacted into graphite dies and sintered simultaneously using the PPS unit.

Approximately 5g of powder mixture was poured into a graphite die, with inner and outer diameters of 12 mm and 30 mm, respectively. A high temperature BN lubricant/mould release agent spray was applied on the inner wall of the die before pouring the powder mixture and placing the upper punch. To get the actual temperature reading of the die and the powders/compacts, temperature was measured by pyrometer on the surface of the graphite die. The final sintering temperature was set at 1000 - 1200 $^{\circ}$C, with a heating rate of 100 $^{\circ}$C/min and a holding time of 5 minutes at the sintering temperature (Fig. 3). In the PPS method, the powder is heated by periodically repeated electric high-current pulses with amplitude of about dozens kA. While the current flows through material to be sintered, the surfaces of the particles are heated temporarily to very high temperature, of the order of several thousand degrees Celsius [12]. After the current flow stops, the temperature decreases very quickly to the settled sintering temperature. No commercial grain growth inhibitors such as Chromium (Cr_3C_2), or Vanadium Carbide (VC) [22] or binders were used in this study other than Co. For most of these samples, a pressure of 100 MPa was used while some samples were tested at 60 MPa just to be able to briefly observe the effect of pressure on these series of samples. Finally, controlled cooling was carried out (100°C/min) to bring the samples down to room temperature before they were taken out from the dies. A list of the samples, along with their processing conditions, is given in Table 1.

The sintered samples were sectioned longitudinally, mounted and conventionally prepared (down to 1 µm diamond paste) for metallographic analysis. For etching, Murakami reagent (10 g potassium ferricyanide K_3Fe (CN)$_6$, sodium hydroxide (NaOH), and 100 ml water) was used where necessary. Density measurements on the WC-Co samples were carried out using Archimedes method, by weighing them in both water and air. Hardness tests were conducted on polished surfaces of WC-Co samples using a Vickers hardness tester at 30 kgf load. The

results are averages of at least 10 indentations. The equation that was used for Vickers hardness calculation is given below:

$$HV = \frac{2 F sin \frac{136°}{2}}{d^2}$$ ………………………………………………..

…………………………………………………….. (1)

Here,

HV = Vickers Hardness,

F = Force applied during the test and

d = Diagonal average length of the indentation.

For microstructural analysis including crack length measurements, a QUANTA 450 FE-SEM was used, while porosity measurements were carried out using optical microscopy (Zeiss Axio Vision Software). Since the sintered samples were quite small in size (~11.5 mm diameter, 1.5-4.5 mm long), fracture toughness values were calculated using the following equation [23]:

$$K_{1c} = 0.016 \sqrt{(E \div H)} (P \div C^{3/2})$$ ………………………………………………...……………………………………

(2)

Where E is Young's modulus, H is the hardness of the material measured using a Vickers Hardness tester, P is the indentation load, and c is the average indentation crack length [11]. The crack lengths, where applicable, were measured from the initiation points, along the edges of the indentation marks, till the end of the propagation. For all calculations, E= 625 GPa was used. [24-28].

4. Results and Discussion

SEM micrographs of WC and Co initial powders sized at 1-3 µm, separately and in mixed forms are shown in Fig 4. The reason for the initial observation was to check the size and shape of the particles. Since particle size was one of the parameters that were varied in this study, it was of importance that powders of specific size range reflected accordingly before proceeding further with consolidation. The observations also help in identifying the change in behaviour after sintering takes place. Both WC and Co particles were mostly found to have spherical shapes, which is one of the desired characteristics of the initial particles that need to be compressed further [29,

30]. This observation was important to verify that high energy ball milling, used for mixing purposes only, did not have an effect on size or shape of any of the particles involved in the composition. Some research studies have successfully illustrated that [31-33] high energy ball milling (HEBM) can essentially help refine WC-Co particles when applied for several hours. This study used HEBM for a few minutes resulting in no signs of refinement, and has only illustrated a homogeneous mixture of WC and Co particles (Fig. 4d). During the initial processing of WC and Co particles, including the mixing stage, it is important to ensure that a homogeneous mixture of powder sample is prepared as it plays a crucial role towards facilitating a proper bonding between particles. In addition it also contributes in terms of keeping grain growth [1, 22, 34] almost even across all particles, along with other parameters (grain growth inhibitors, sintering temperature, holding time, heating rate etc) that also factor in during sintering. The brownish/reddish area in Fig 4(d) indicates the presence of Co particles, along with the possibility that some of the particles may have gone through initial agglomeration due to their softer nature as opposed to WC particles.

Fig 5 shows the XRD analysis of a micron sample of mixed WC-Co particles before sintering was carried out. The diffraction peaks illustrated in the figure suggest that the samples consist of WC and Co particles only without the presence of any other phase. The presence of other phases like η-WC (a carbon deficient form of tungsten carbide that results in a harder, more brittle cemented carbide part) [15] has been referred in literature, which can be considered as a microstructural defect if present in high concentration, eventually leading the material to fail, structurally. Co peaks are found to be extremely difficult to identify, due to the very high massive absorption coefficient of the WC phase, especially for compositions with low Co content. Traces of Co are usually seen at 37, 44, 52, 65 and 75 2theta (2θ) degree angles, indicating reasonably low intensities. This behaviour remains almost constant in all samples that were prepared in this study, and is even applicable after sintering.

Density is one of the important properties that sintered materials are tested for in general, before hardness and other tests are carried out. The changes in density with respect to sintering temperature, initial particle size and sintering pressure are illustrated in Fig. 6. The sample numbers indicate the difference in terms of sintering temperature where it was ranged between 1000 and 1200 ºC. For one of the nano samples (sample 3 for Nano and sample 4 for Sub Micron and Micron), sintering was carried out at a lower pressure of 60 MPa just to be able to observe if employing a lower pressure would greatly affect any particular behaviour. Since it did not

result in having any significant deviation in terms of mechanical behaviour, which will also be elaborated in other figures, it suggests that initial particle size and sintering temperature, along with the unique features of pulse plasma sintering had effective contributions in achieving the set of behaviour for these series of sintered WC-Co samples. Density was found to have displayed an incremental behaviour with increasing sintering temperature irrespective of the size of initial particles. Although the density of nano, sub and micron size are different at lower temperature but they all tend to reach full density number with increasing temperature. This may be attributed to the idea that factors like powder morphology and homogeneity play a more dominant role towards densification at lower temperature while pressure and temperature start to influence the behaviour while particles reach higher temperature. Lowering sintering pressure at 1200 °C did cause a slight drop in density although it was quite insignificant. However, this is one of the reasons why a higher pressure was chosen for this study since sintering temperature has already been brought down by a great extent as opposed to conventional practices [2, 35, 36]. It is also important to highlight that almost fully dense WC-Co samples were successfully fabricated at this low sintering temperature range without inclusion of any commercial grain growth inhibitors. . In PPS process, due to the extremely short duration of the high temperature and its rapid decrease to the settled sintering temperature, the growth of the WC grains is hampered since the precipitation of the tungsten carbide dissolved in cobalt is restricted. This in effect again hints that the process may have contributed in inducing such behaviour in these sintered WC-Co samples. In comparison with conventional liquid phase sintering [14, 16, 37], higher density can quite effectively be obtained in PPS samples, which is attributed to the fact that every particle is heated almost simultaneously in PPS process ensuring faster surface to core heating resulting in rapidly reaching sintering temperature altogether. This along with simultaneous compression may result in achieving improved grain boundary diffusion, plastic deformation and grain boundary sliding [19, 20]. In contrast, during conventional sintering, sample surfaces tend to reach sintering temperature first, which then slowly gets transferred to the centre [38].

Fig. 7 shows the changes in hardness behaviour with respect to varied sintering conditions in WC – 7.5 wt. % Co samples. When hardness is tested in cemented carbides, samples need to reach specific values in order to meet industrial requirements based on their area of application. It is understood that there is a minimum threshold for cemented carbides when it comes to hardness which primarily defines the quality of the product. Achieving high hardness is always desirable for WC-Co samples, and it also encourages the process to be modified to an extent, including the incorporation of commercial grain growth inhibitors. Some studies have

already suggested that it is possible to achieve the hardness of around 1900 HV in these series of WC-Co samples with the presence of commercial inhibitors like VC, Cr_3C_2, Mo_2C, NbC and so on [39]. In some cases it is also required that the sintering process goes through several stages in order to be able to achieve that high hardness point. In our study, it was observed that hardness showed an incremental behaviour with increasing sintering temperature for all three types of initial particle size, reaching a maximum of around 2000 HV. This is significantly higher than what can be achieved from a conventional approach [2, 14]. In addition, the fact that no grain growth inhibitors was used in this study also makes it a more effective approach in reaching such high hardness values. Grain growth is a critical phenomenon here as it is thought to be primarily responsible for hardness decrease in hard materials [34, 40]. The reason why nano particles displayed higher hardness values compared to the rest of the samples could be attributed to the prevention of grain growth by a great extent. Like the density behaviour discussed earlier as a function of pressure, for hardness as well, a drop in pressure (sample 3 for Nano and sample 4 for Sub Micron and Micron) did not seem to have caused much deviation in hardness results. The hardness values observed at 1000 ºC are quite low irrespective of the type of powders used, which can be attributed to the light bonding between particles as shown in the inset.

Fracture toughness is an influential property for hard materials since a combination of high hardness and reasonable fracture toughness is of great interest for these series of brittle materials. Depending on the size of samples, different methods can be applied to measure fracture toughness of a material [41, 42]. Since the size of the samples studied for this work was kept small in order to prevent pressure gradients along the length, conventional tests were not applicable. However, with the help of hardness values, using equation 2, fracture toughness was calculated. Fig. 8 shows the fracture toughness behaviour in WC- 7.5 wt. % Co samples with respect to sintering temperature, initial particle size and pressure (a low pressure of 60 MPa was applied on Nano sample 3, Sub Micron Sample 4 and Micron sample 4). For all three types of samples, the starting temperature of 1000 ºC resulted in relatively low fracture toughness values. In order to be able to display high fracture toughness, it is critical that a proper WC-Co-WC bond is formed, which is quite strong in nature in the sense that a presence of Co between WC particles would work as a resistance against crack propagation due to its preference towards deformation rather than brittle failure. At low temperature, it is possible that a proper bonding between the particles is somewhat missing, which would make the sample more prone to cracking. In addition, at low temperature, it is also possible that the mobility of binder, which is Co in this study, is compromised to an extent since the temperature involved is not high enough to either induce a proper WC-Co-

WC bond among particles or melt Co particles that could eventually generate a liquid phase. When temperature was raised to 1100 °C and beyond, fracture toughness values were found to have improved significantly, indicating better bonding among particles. The fact that a temperature above 1100 °C resulted in a slight drop in fracture toughness could be attributed to the grain growth which is directly related to the temperature involved during sintering. When there is presence of larger WC grains in the samples, cracks would tend to become trans-granular in addition to being intergranular, helping cracks propagate relatively fast within WC, which is more brittle in nature as opposed to WC-Co. Considering all samples and their fracture toughness behaviour, it can be said that 1100 °C brought out the best fracture toughness behaviour in WC-Co samples regardless of their initial particle size. Based on the understanding we have on fracture toughness, it is safe to assume that it is more likely to be influenced by factors like final sintering temperature and grain growth than initial particle size, unless final grain size is almost identical to initial particle size.

The analysis of fracture toughness requires a clear understanding of the hardness behaviour, including crack patterns or how they generate and evolve. Fig. 9 shows a typical image of a hardness impression (d) along with some preliminary surface images of samples sintered at 1100 °C (a-c). In most samples, cracks were found to have generated from the corners and propagated without further branching out. The crack lengths were higher in samples that were sintered at low temperatures indicating incomplete bonding between particles, resulting in low fracture toughness values. With increasing temperature, particles or grains tend to join better, allowing less room for cracks to channel through. It can either reflect in the form of smaller crack length, secondary cracks generating from primary ones, or multiple smaller cracks instead of a long, propagating one. Since Co is softer in nature as opposed to WC, and works as a binder between two WC particles or grains at elevated temperatures, an even distribution of Co is essential not only to ensure better bonding, but also to work as a resisting force against crack propagation by absorbing the energy dissipated by cracks and through plastic deformation rather than permanently breaking, like WC. Fig. 10 (a, b) shows inter and trans-granular crack paths along with presence of a secondary or branched out crack. However, based on the microstructural observation, it was primarily intergranular cracks that were formed as a result of hardness impressions. Intergranular cracks suggest that cracks were propagating along grain boundaries, referring to the idea that grains containing several WC-WC bonds are quite strong in nature. The deflection and diminishing patterns of cracks may also be thought of as an indication that Co was present, which effectively work towards ensuring crack arrests through deformation rather than brittle failure.

Porosity is one of the microstructural features that are responsible for aiding cracks to propagate within sintered samples. Although the understanding of porosity is related to density analysis, the former is analysed from a microstructural perspective while the latter is a physical property measured directly and quite accurately. It is often requires a quantitative measurement method [43, 44] that considers the binder content even though it is present in low concentration. The grey level thresholding during quantitative measurements may pick up some of the binders as porosity. In order to observe the nature of porosity present in these series of sintered samples, a closer look at the samples, both surface and along the cross section, has been taken. Fig. 11 shows the distribution of porosity in some of the micron samples with respect to changing temperature and pressure. The red marked areas are pores and the blue/green areas are identified as WC [7]. It appears that with increasing temperature, porosity tends to gradually decrease within the samples. It also justifies the density behaviour discussed earlier, Fig 6. The majority of the pores were found to have displayed the characteristics of an A-type porosity where the diameters of the pores are between 1 and 10 µm.

Fig. 12 shows some SEM micrographs of the samples that were sintered at different temperatures. The three different types of samples based on initial particle size are also labelled. In all range of powder size, it was seen that particles tend to bond better with increasing temperature, although microstructural behaviour between samples sintered at 1100 ºC and 1200 ºC have not been much different except for the slight difference in terms of porosity and grain size. Fig. 12 (i) shows the surface microstructure of a nano WC-Co sintered sample where a low pressure of 60 MPa was applied, while 100 MPa was used for the rest. This was done to observe whether pressure brings any significant changes to the microstructure for a specific set temperature. More discussions on the effects of pressure on microstructural behaviour can be found in our previous work [7]. Theoretically, if final sintering temperature is around the melting point of a binder, a liquid phase is expected to form which may improve the sintering process to an extent. However it is only applicable when a very high temperature around the melting point of the binder is involved, which is inconvenient in terms of time and energy consumption, grain growth and some mechanical properties of this series of hard materials. The images in Fig. 12 indicate that particles/grains have not gone through a great extent of growth during sintering, which can be attributed to the relatively low sintering temperature used in this study as opposed to conventional sintering. Furthermore, unlike most conventional approaches, compression and heating are carried out simultaneously in pulse plasma

sintering, which may also contribute to achieving such high mechanical properties without compromising the microstructural features like grain growth and porosity.

As part of the microstructural analysis, three distinct features were also looked for, that may come in the form of an impurity or defect [45].

- **Clusters:** Clusters are defined as groups of WC grains that are significantly larger than the average measured grain size, and are thought to have formed during the heating stage of the sintering process through WC coalescence. It could also be a result of Oswald ripening which is often found as a post sintering microstructural feature. If present in abundance, these clusters of WC can be identified as a weak spot in the carbide microstructure. Although, conform to expectations, some typical clusters were observed in the images, they were not found in abundance. However, clusters can be eliminated by the homogeneity of binder present in the composition, which essentially helps WC particles or grains join with other WC particles by deforming to an extent, and smoothening the rough edges of their brittle WC counterparts.
- **Binder lakes (blk):** Binder lakes are primarily described as a group or pool of Co binder particles within the structure, generated in liquid state of Co while channelling through open pores. This phenomenon was not observed in the samples we have tested which can be attributed to the fact that a sintering temperature well below the melting point of the binder was used in this study, indicating a solid state sintering occurring between particles. In addition, using high pressure also helps WC grains and binders simultaneously channel towards open pores, eliminating the chances of binder lake formation within the structure of the carbide tools.
- **Eta Phase (Eta-1, Eta-2, Eta-3)**: Eta phase is basically a form of carbon deficiency in sintered WC that leaves the product susceptible to quick brittle failure. This is a phenomenon that is usually seen when synthesis of WC-Co sintering samples start from elemental W, C and Co particles rather than mixing WC and Co. Insufficient carbon content would result in having improper formulation of carbide powder, eventually leading to poor mechanical properties and microstructural behaviour. Presence of this phase has also been mentioned in some microwave sintered samples. XRD traces in this study along with the SEM observations suggest the absence of such a phase within the microstructure.

The mechanical behaviour of the samples discussed earlier also suggests that pulse plasma process along with the involvement of high pressure, low sintering temperature and a homogenous mixture of WC and Co jointly contributed in phasing out the impurities of the samples by a great extent.

It is often seen that traces of cobalt or any binder within the carbide composition is hard to find before or after sintering. In order to observe whether there are Co traces between WC grains, a line scanning was conducted between a few WC grains (Fig. 13). It was seen that Co, although in limited concentration, was present between WC grains.

5. Conclusion

Several WC – 7.5 wt. % Co samples were pulse plasma sintered with varying sintering temperature, initial particle size and sintering pressure (limited samples). Density, hardness and fracture toughness were primarily tested and analysed, showing an almost incremental behaviour with increasing temperature. When pressure was reduced from 100 MPa to 60 MPa for some samples while keeping other parameters constant, negligible deviation was observed in terms of mechanical properties suggesting that pressure may not be the most influential parameter within the tested range, and can only effect significantly in addition to varying other parameters like sintering temperature, state of sintering, initial particle size and so on. Using 1100 $^{\circ}$C sintering temperature led to demonstrating the optimum combination of mechanical and microstructural behaviour.

References

[1] Fang Z, Eason JW. Study of nanostructured WC-Co composites. International Journal of Refractory Metals and Hard Materials. 1995;13:297-303.

[2] Song J-W, Raihanuzzaman RM, Hong S-J. Consolidation of WC-Co Alloys by Magnetic Pulsed Compaction and Evaluation of their Mechanical Properties. Powder Technology. 2012;235: 723–7.

[3] Shao G, Duan X, Xie J, Yu X, Zhang W, Yuan R. Sintering of nanocrystalline WC-Co composite powder. Reviews on Advanced Materials Science. 2003;5:281-6.

[4] "Microwave sintering of Metals," http://www.azom.com/article.aspx?ArticleID=937).

[5] Carroll D. Sintering and microstructural development in WC/Co-based alloys made with superfine WC powder. International Journal of Refractory Metals and Hard Materials. 1999;17:123-32.

[6] Sunil BR, Sivaprahasam D, Subasri R. Microwave sintering of nanocrystalline WC–12Co: Challenges and perspectives. International Journal of Refractory Metals and Hard Materials. 2010;28:180-6.

[7] Rumman MR, Xie Z, Hong S-J, Ghomashchi R. Effect of spark plasma sintering pressure on mechanical properties of WC–7.5 wt% Nano Co. Materials & Design. 2015;68:221-7.

[8] Song J-W, Raihanuzzaman RM, Hong S-J. Consolidation of WC–Co alloys by magnetic pulsed compaction and evaluation of their mechanical properties. Powder Technology. 2013;235:723-7.

[9] Jia C-C, Tang H, Mei X-Z, Yin F-Z, Qu X-H. Spark plasma sintering on nanometer scale WC–Co powder. Materials Letters. 2005;59:2566-9.

[10] Song X, Liu X, Zhang J. Neck Formation and Self-Adjusting Mechanism of Neck Growth of Conducting Powders in Spark Plasma Sintering. Journal of the American Ceramic Society. 2006;89:494-500.

[11] Michalski A, Siemiaszko D. Nanocrystalline cemented carbides sintered by the pulse plasma method. International Journal of Refractory Metals and Hard Materials. 2007;25:153-8.

[12] Michalski A, Rosinski M. Pulse Plasma Sintering and Applications. Advances in Sintering Science and Technology: Ceramic Transactions. 2010;87:219.

[13] Michalski A, Siemiaszko D, Jaroszewicz J, Rosiński M, Psoda M. Nanocrystalline cemented carbides sintered by the pulse plasma method. Solid State Phenomena: Trans Tech Publ; 2006. p. 245-50.

[14] Raihanuzzaman RM, Han S-T, Ghomashchi R, Kim H-S, Hong S-J. Conventional sintering of WC with nano-sized Co binder: Characterization and mechanical behavior. International Journal of Refractory Metals and Hard Materials. 2015.

[15] Breval E, Cheng J, Agrawal D, Gigl P, Dennis M, Roy R, et al. Comparison between microwave and conventional sintering of WC/Co composites. Materials Science and Engineering: A. 2005;391:285-95.

[16] Demirskyi D, Borodianska H, Agrawal D, Ragulya A, Sakka Y, Vasylkiv O. Peculiarities of the neck growth process during initial stage of spark-plasma, microwave and conventional sintering of WC spheres. Journal of Alloys and Compounds. 2012;523:1-10.

[17] Oghbaei M, Mirzaee O. Microwave versus conventional sintering: A review of fundamentals, advantages and applications. Journal of Alloys and Compounds. 2010;494:175-89.

[18] Michalski A, Rosiński M. Sintering diamond/cemented carbides by the pulse plasma sintering method. Journal of the American Ceramic Society. 2008;91:3560-5.

[19] Rahaman MN. Ceramic processing: Wiley Online Library; 2006.

[20] Guillon O, Gonzalez-Julian J, Dargatz B, Kessel T, Schierning G, Räthel J, et al. Field-Assisted Sintering Technology/Spark Plasma Sintering: Mechanisms, Materials, and Technology Developments. Advanced Engineering Materials. 2014;16:830-49.

[21] Rosinski M, Fortuna E, Michalski A, Pakiela Z, Kurzydlowski K. W/Cu composites produced by pulse plasma sintering technique (PPS). Fusion Engineering and Design. 2007;82:2621-6.

[22] Morton C, Wills D, Stjernberg K. The temperature ranges for maximum effectiveness of grain growth inhibitors in WC–Co alloys. International Journal of Refractory Metals and Hard Materials. 2005;23:287-93.

[23] Xie Z-H, Hoffman M, Cheng YB. Microstructural Tailoring and Characterization of a Calcium α-SiAlON Composition. Journal of the American Ceramic Society. 2002;85:812-8.

[24] Cha SI, Hong SH, Kim BK. Spark plasma sintering behavior of nanocrystalline WC–10Co cemented carbide powders. Materials Science and Engineering: A. 2003;351:31-8.

[25] Doi H, Fujiwara Y, Miyake K, Oosawa Y. A systematic investigation of elastic moduli of WC-Co alloys. Metallurgical and Materials Transactions. 1970;1:1417-25.

[26] Coromant S. Modern metal cutting: a practical handbook: Sandvik Coromant; 1994.

[27] Upadhyaya G. Materials science of cemented carbides—an overview. Materials & Design. 2001;22:483-9.

[28] Jaensson BO, Sundström BO. Determination of Young's modulus and poisson's ratio for WC☐ Co alloys by the finite element method. Materials science and engineering. 1972;9:217-22.

[29] Fuller KA, Malm WC, Kreidenweis SM. Effects of mixing on extinction by carbonaceous particles. Journal of Geophysical Research. 1999;104:941-54.

[30] Murthy J, Venkataraman B. Abrasive wear behaviour of WC–CoCr and Cr 3 C 2–20 (NiCr) deposited by HVOF and detonation spray processes. Surface and Coatings Technology. 2006;200:2642-52.

[31] Butler BG, JUN L, Fang ZZ, Rajamani RK. Production of nanometric tungsten carbide powders by planetary milling. International journal of powder metallurgy. 2007;43:35-43.

[32] Kimmel ER, Shaffer ME, Pinkowski TR, Harris GL. Method of producing monotungsten carbide powder. Google Patents; 1987.

[33] Xueming M, Ling Z, Gang J, Yuanda D. Preparation and structure of bulk nanostructured WC-Co alloy by high energy ball-milling. Journal of materials science letters. 1997;16:968-70.

[34] Choi K, Hwang N. Effect of VC addition on microstructural evolution of WC–Co alloy: mechanism of grain growth inhibition. Powder Metallurgy. 2000;43:168-72.

[35] Raihanuzzaman RM, Song J-W, Hong S-J. Evaluation of mechanical properties and processing conditions of WCCo alloys fabricated by magnetic pulsed compaction. Journal of alloys and Compounds. 2012;536:S211-S5.

[36] Raihanuzzaman RM, Xie Z, Hong SJ, Ghomashchi R. Powder refinement, consolidation and mechanical properties of cemented carbides—An overview. Powder Technology. 2014;261:1-13.

[37] Tandon R, Johnson J. Liquid-phase sintering. ASM Handbook. 1998;7:565-73.

[38] SUN L, JIA C-c, LIN C-g, CAO R-j. VC addition prepared ultrafine WC-11Co composites by spark plasma sintering. Journal of Iron and Steel Research, International. 2007;14:85-9.

[39] Yaman B, Mandal H. Spark plasma sintering of Co–WC cubic boron nitride composites. Materials Letters. 2009;63:1041-3.

[40] Agrawal D, Cheng J, Seegopaul P, Gao L. Grain growth control in microwave sintering of ultrafine WC-Co composite powder compacts. Powder Metallurgy. 2000;43:15-6.

[41] Sigl LS, Fischmeister H. On the fracture toughness of cemented carbides. Acta Metallurgica. 1988;36:887-97.

[42] Chermant J, Osterstock F. Fracture Toughness of Cemented Carbides. ECF2, Darmstadt 19782012.

[43] Martínez V, Echeberria J. Hot isostatic pressing of cubic boron nitride–tungsten carbide/cobalt (cBN–WC/Co) composites: effect of cBN particle size and some processing parameters on their microstructure and properties. Journal of the American Ceramic Society. 2007;90:415-24.

[44] Amberg S, Doxner H. Porosity in cemented carbide. Powder Metallurgy. 1977;20:1-10.

[45] Walz T, "Building Superior Brazed Tools," http://www.carbideprocessors.com/pages/carbide-parts/carbide-defects.html).
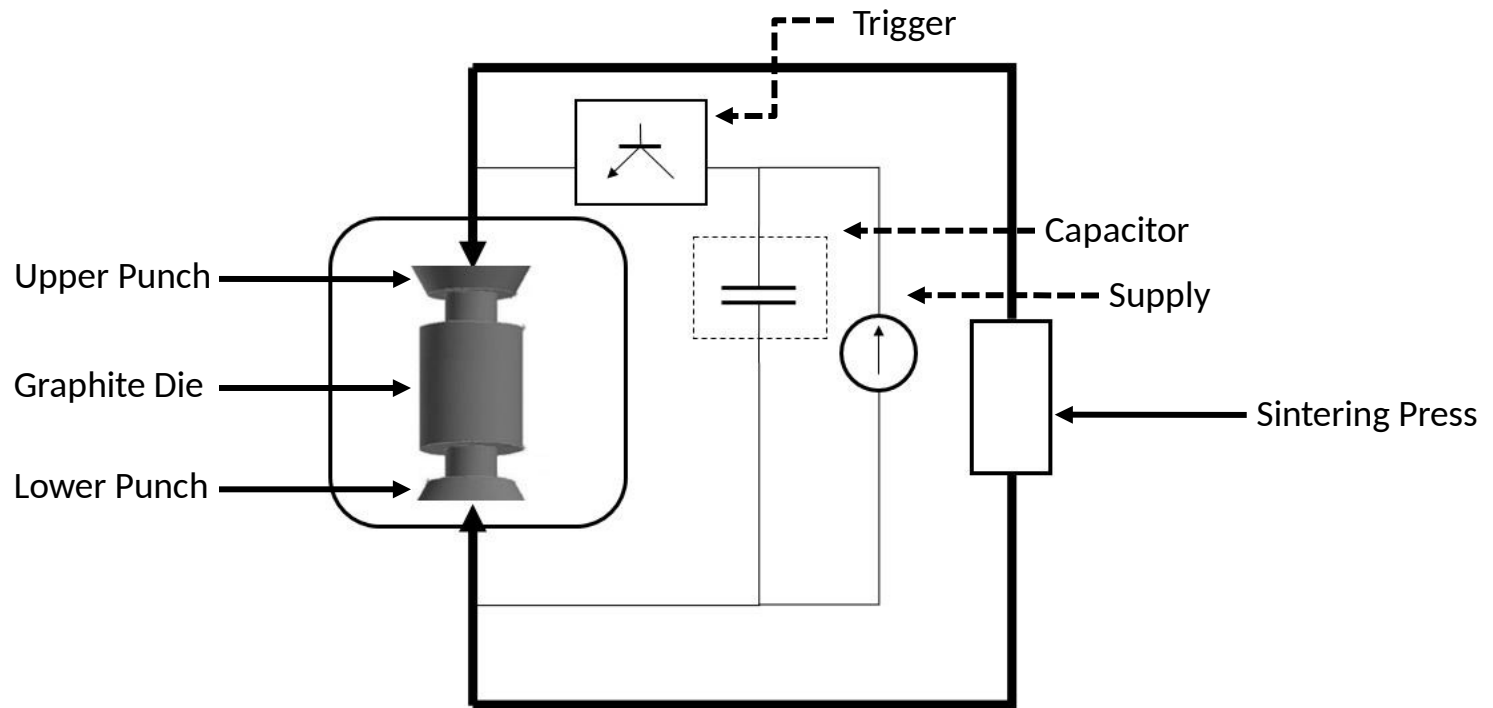
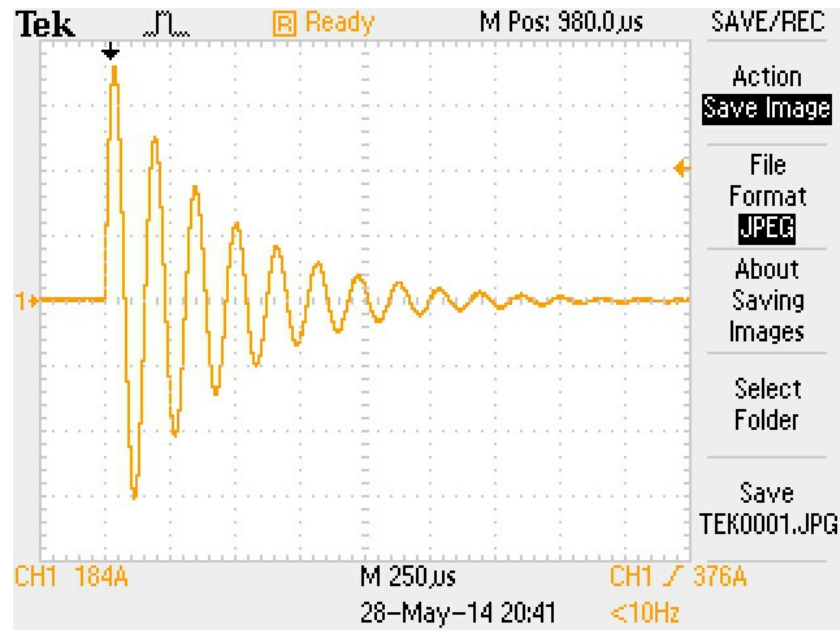Fig. 1. Schematic diagram of a pulse plasma compaction (PPC) unit model GC_A_V2L200HV [www.genicore.pl].

Fig. 2. Behavior of pulse current during a battery of capacitors discharge of PPC unit model GC_A_V2L200HV [www.genicore.pl].
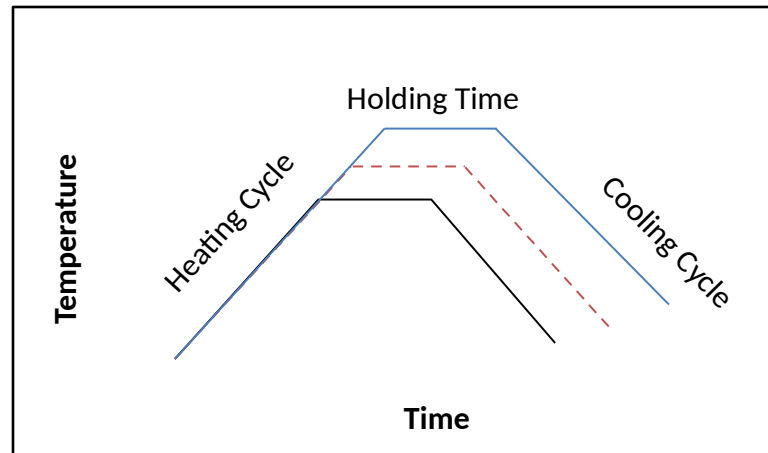
Fig. 3. Schematic representation of the temperature and pressure during pulse plasma sintering
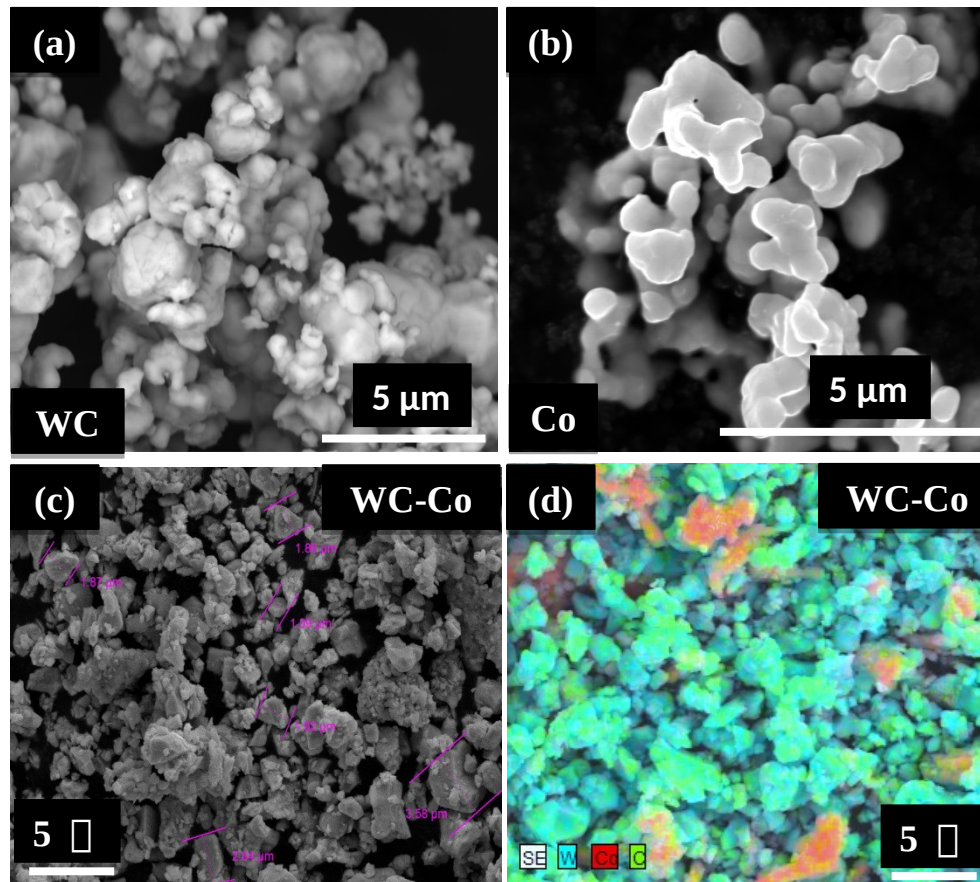
Fig 4: SEM micrographs (SE) of (a) initial WC powders (b) initial Co powders (c) mixed WC-7.5 wt.% Co powders and (d) EDX image of mixed WC-7.5 wt. % Co powders
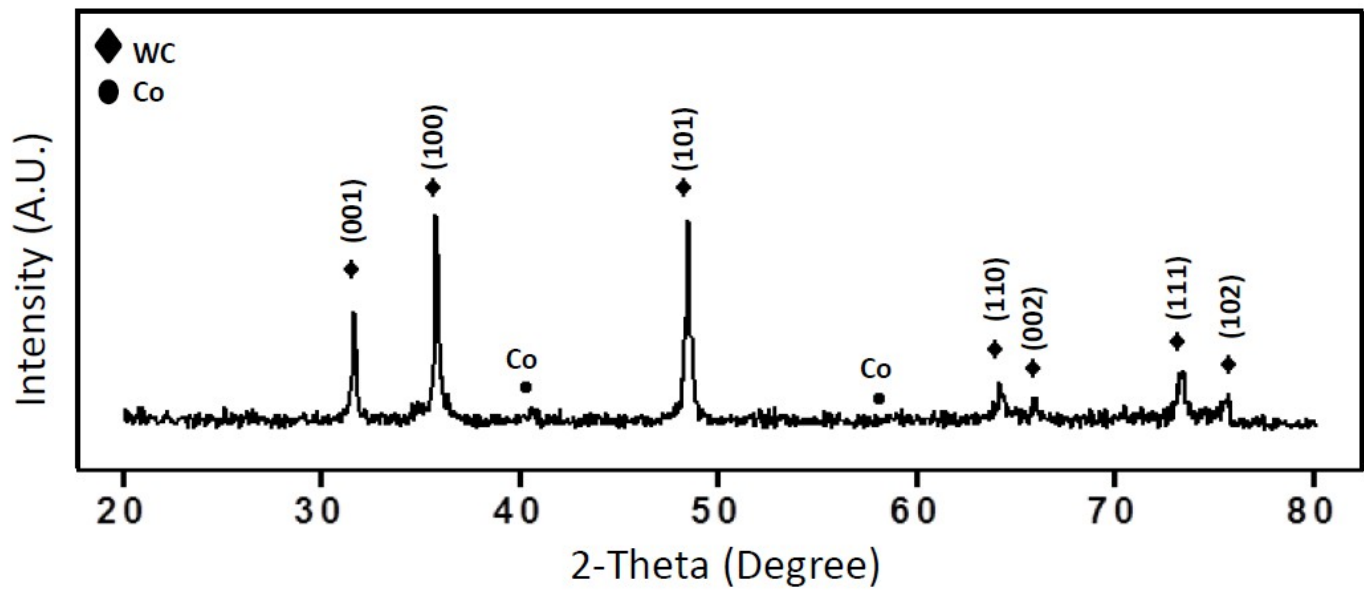
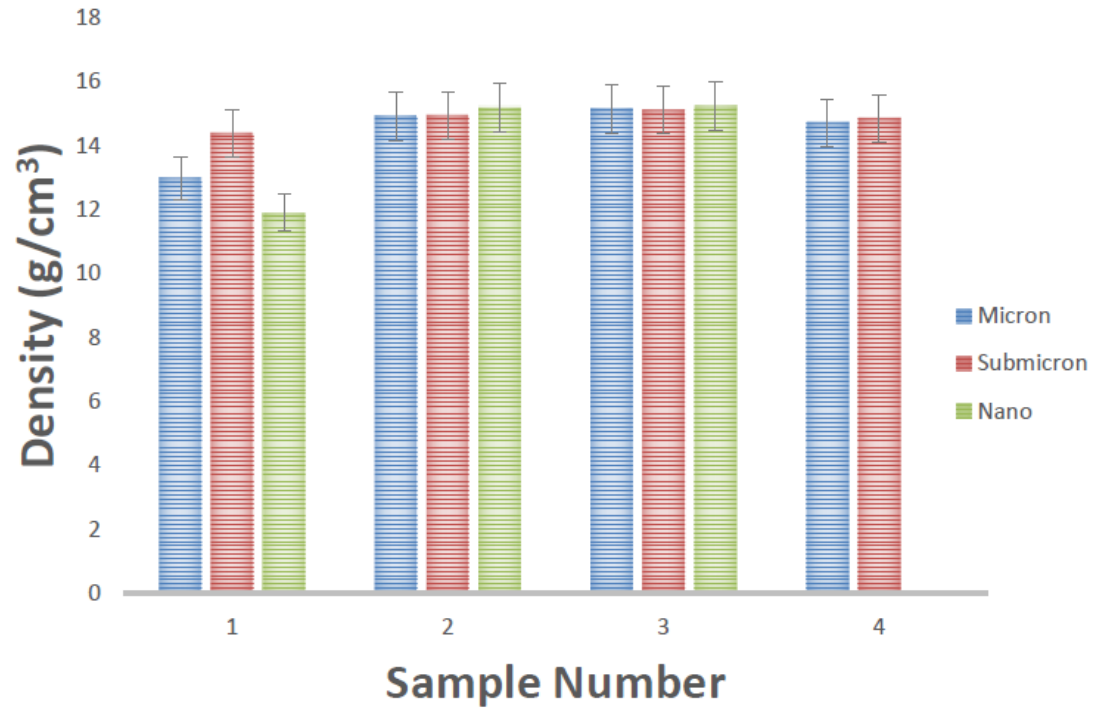Fig 5: XRD pattern of WC - 7.5 wt. % Co Powders

Fig 6: Changes in density of sintered WC - 7.5 wt. % Co with varying sintering temperature and initial particle size.
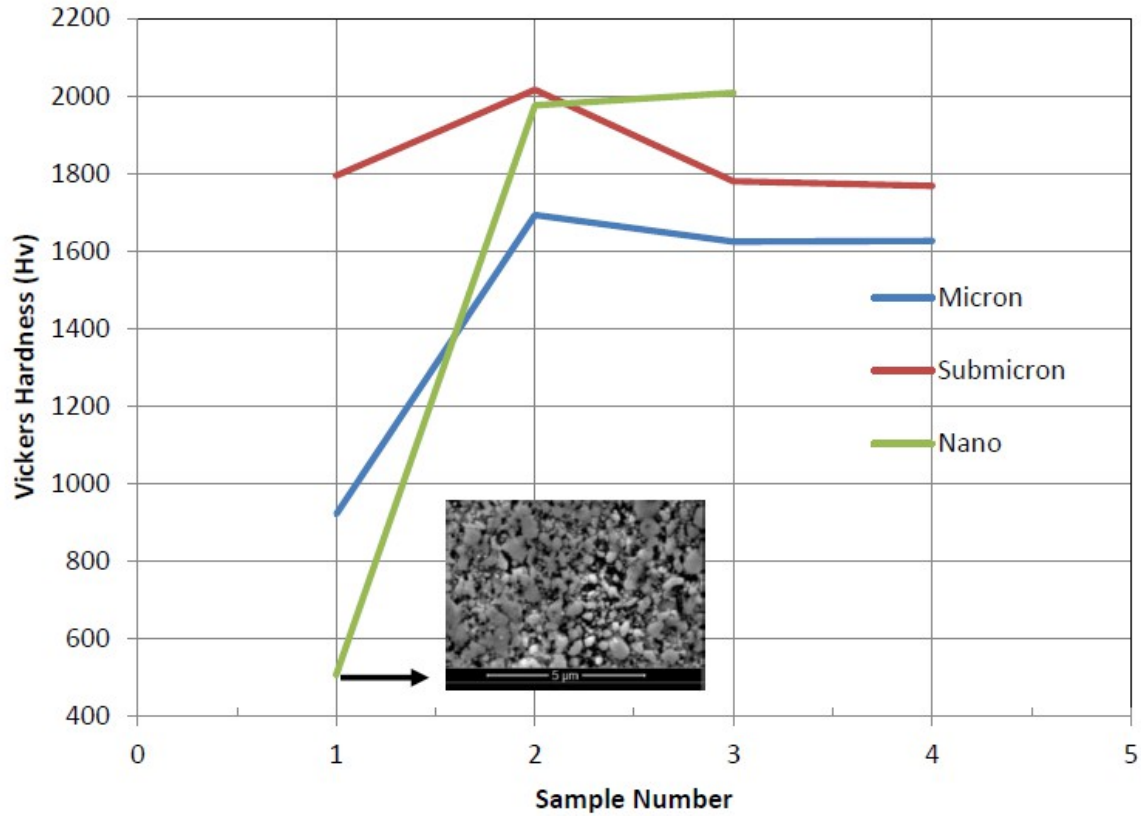
Fig 7: Changes in hardness behavior of sintered WC - 7.5 wt. % Co with varying sintering temperature and initial particle size.
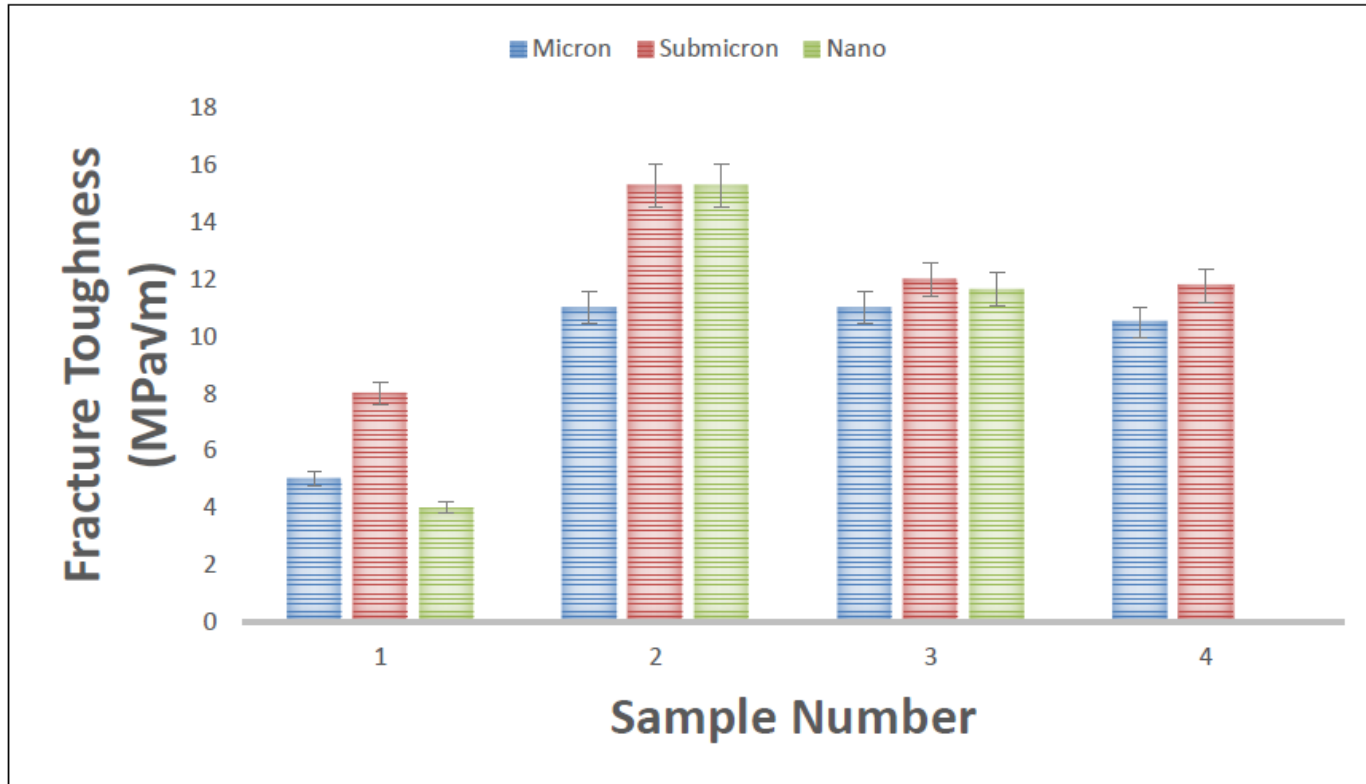
Fig 8: Changes in fracture toughness of sintered WC - 7.5 wt. % Co with varying sintering temperature and initial particle size.
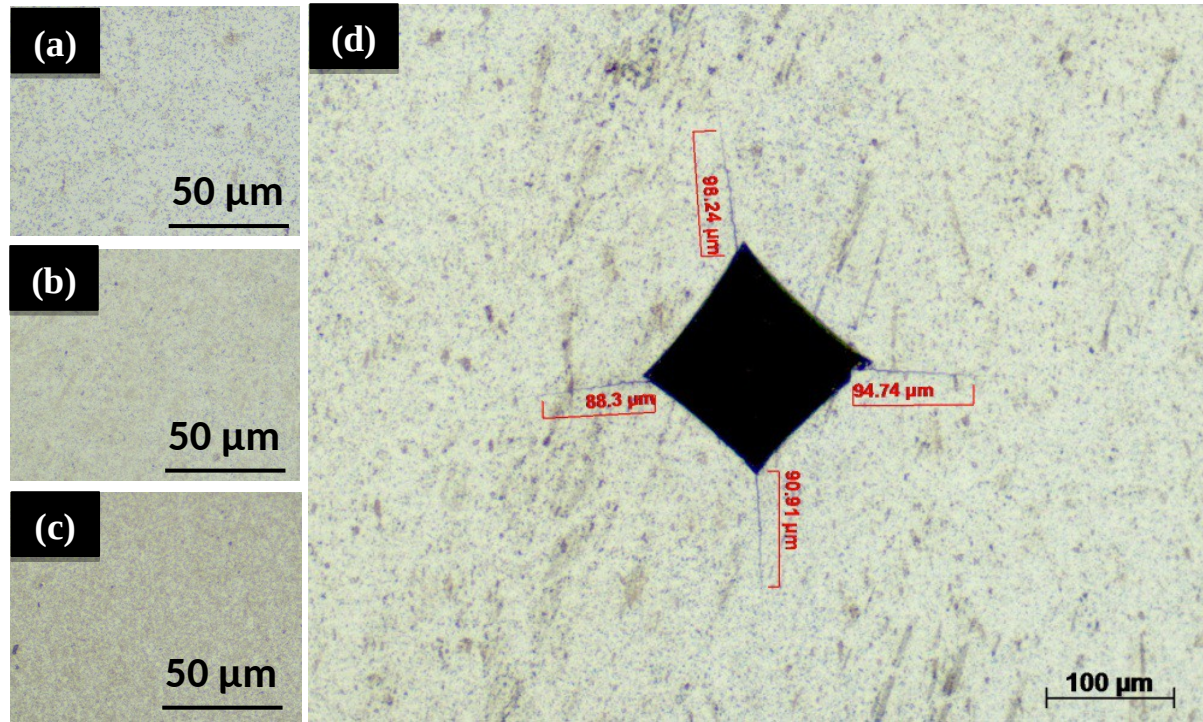
(a)

50 μm

(b)

50 μm

(c)

50 μm

(d)

98.24 μm

88.3 μm

94.74 μm

90.61 μm

100 μm

Fig 9: Optical micrographs of pulsed plasma samples sintered at 1100 °C (a) Micron (b) Submicron (c) Nano. The typical representation of cracks generated along the indentations are shown in (d) which is a micron sample sintered at 1100 °C.
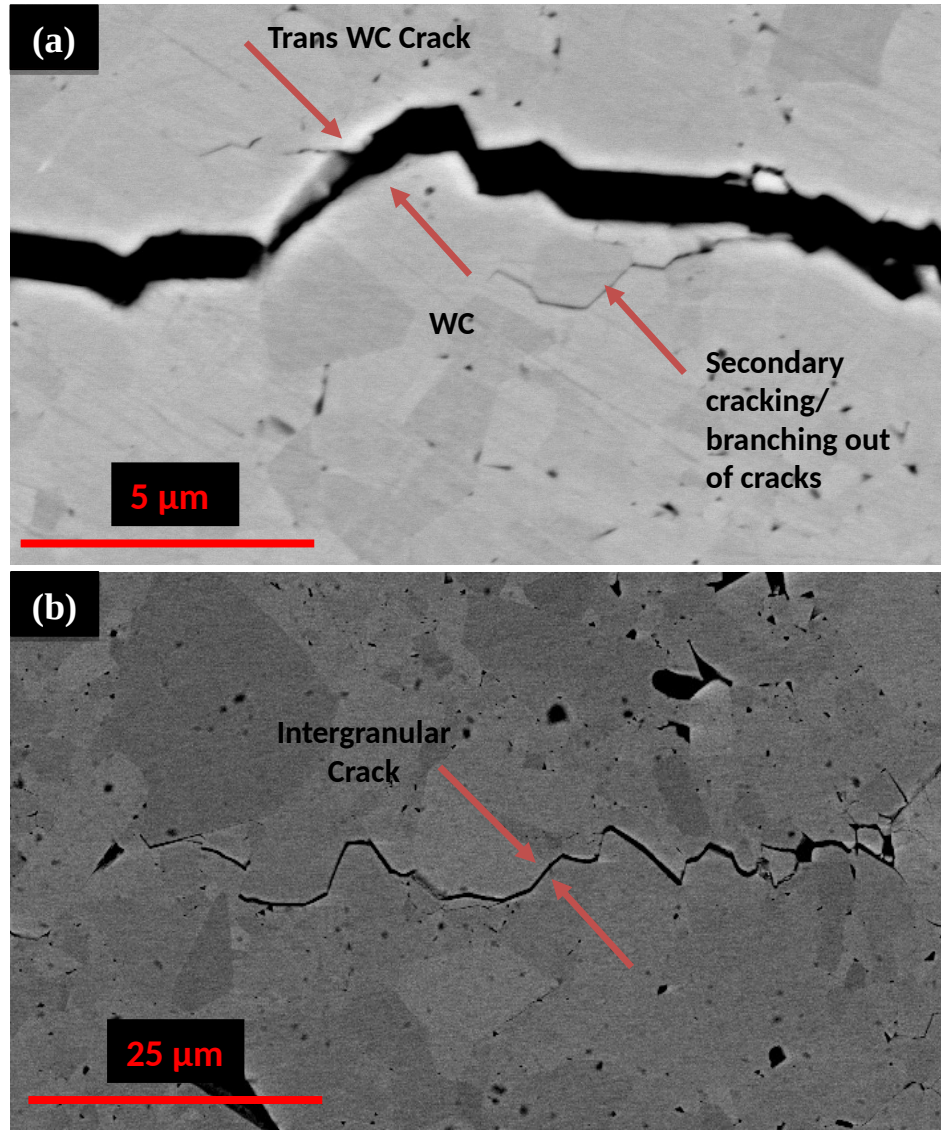
Fig 10: Crack path showing (a) trans WC and (b) intergranular crack propagation and presence of a secondary or branched out crack. This WC - 7.5 wt. % Co sample was sintered at 1200 ^{o} C.
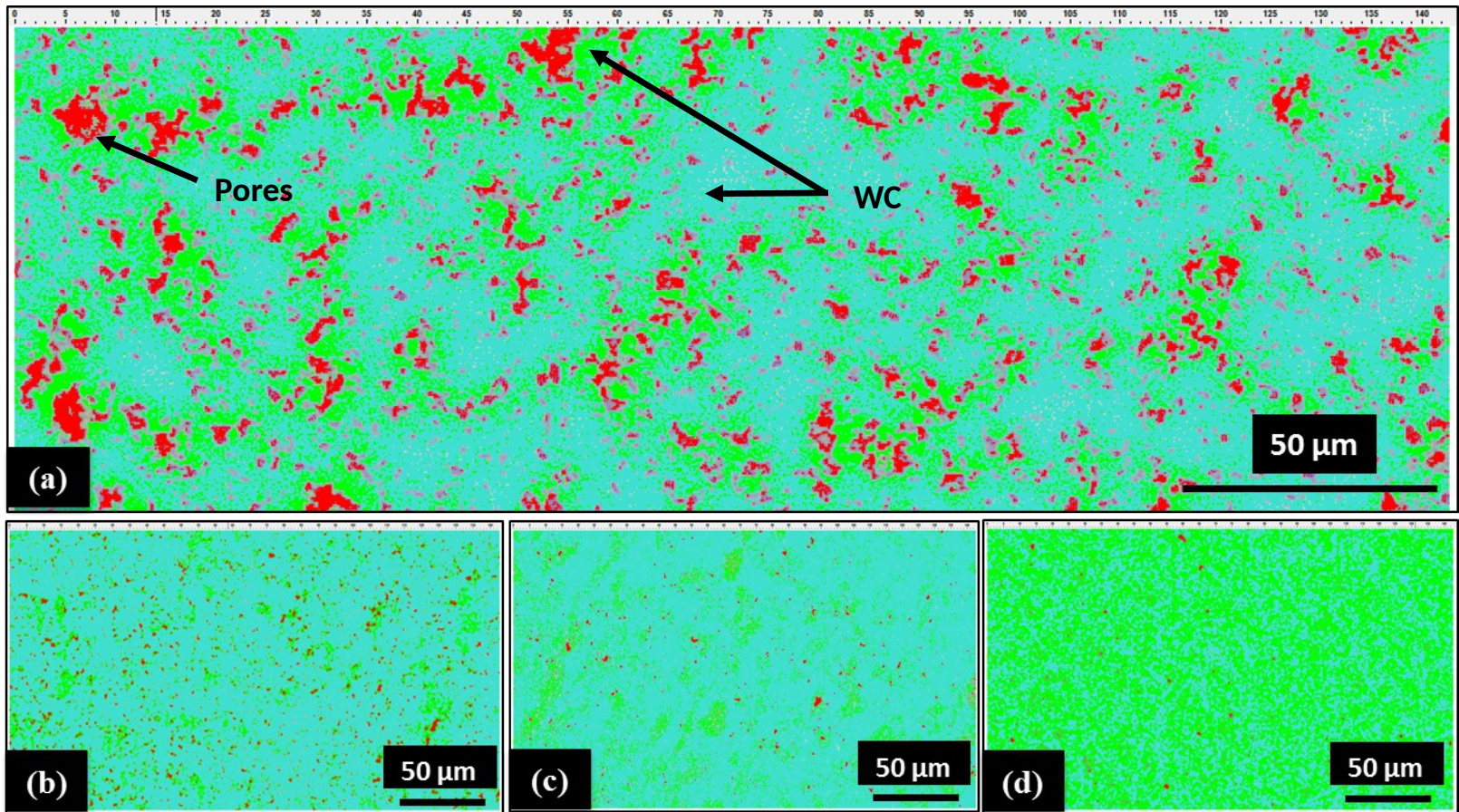
Fig 11: (a) A typical porosity content profile of a sample sintered at a low temperature. The figure shown here is a micron sample sintered at 1000 ^{o} C. (b) Porosity content of a micron sample sintered at 1100 ^{o} C (c) Porosity content of a sub micron sample sintered at 1100 ^{o} C (d) Porosity content of a nano sample sintered at 1100 ^{o} C

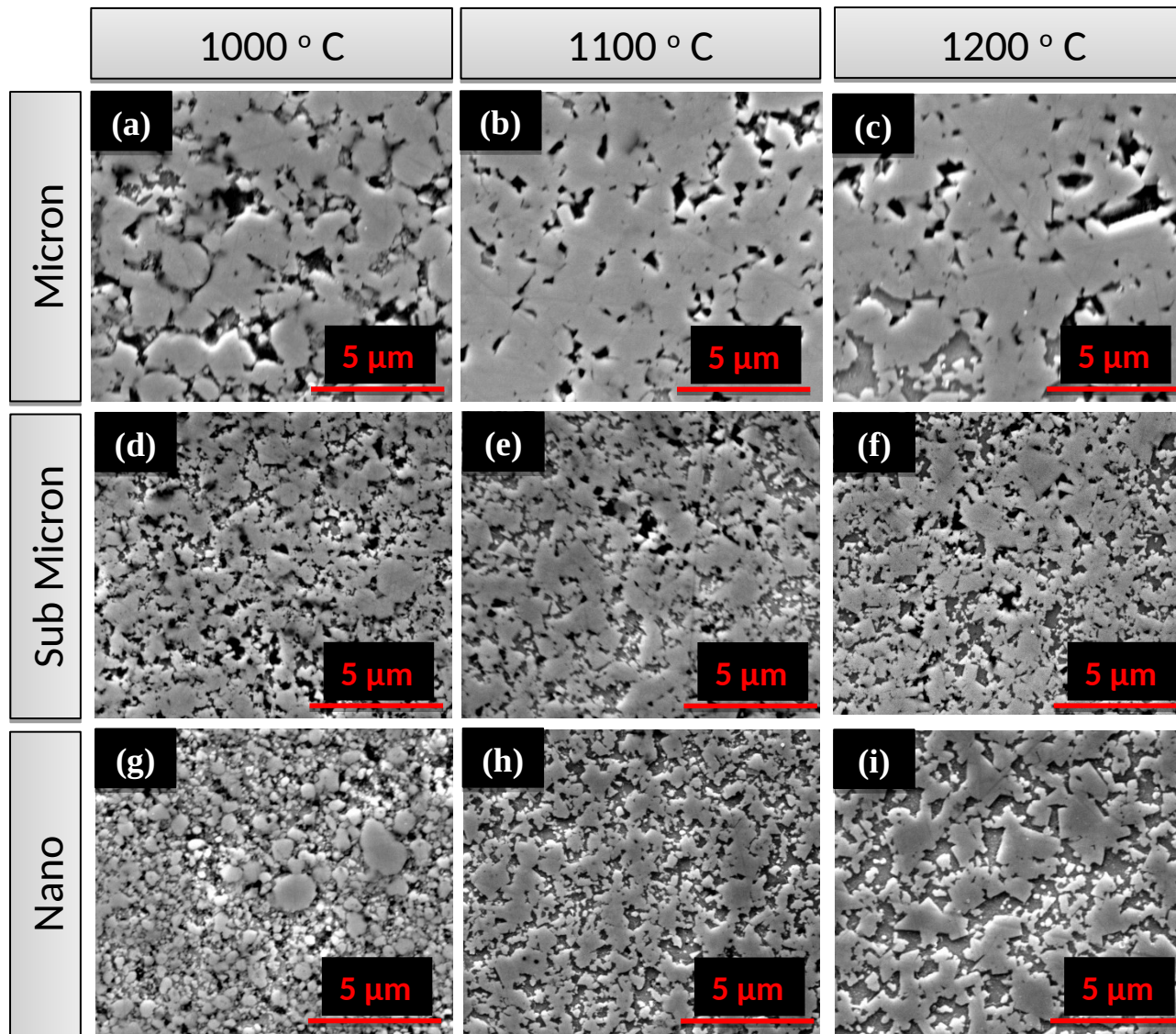|	1000 °C	1100 °C	1200 °C
Micron	(a) 5 μm	(b) 5 μm	(c) 5 μm
Sub Micron	(d) 5 μm	(e) 5 μm	(f) 5 μm
Nano	(g) 5 μm	(h) 5 μm	(i) 5 μm

Fig 12: SEM secondary electron images of WC-7.5wt. % Co samples sintered at different temperatures.
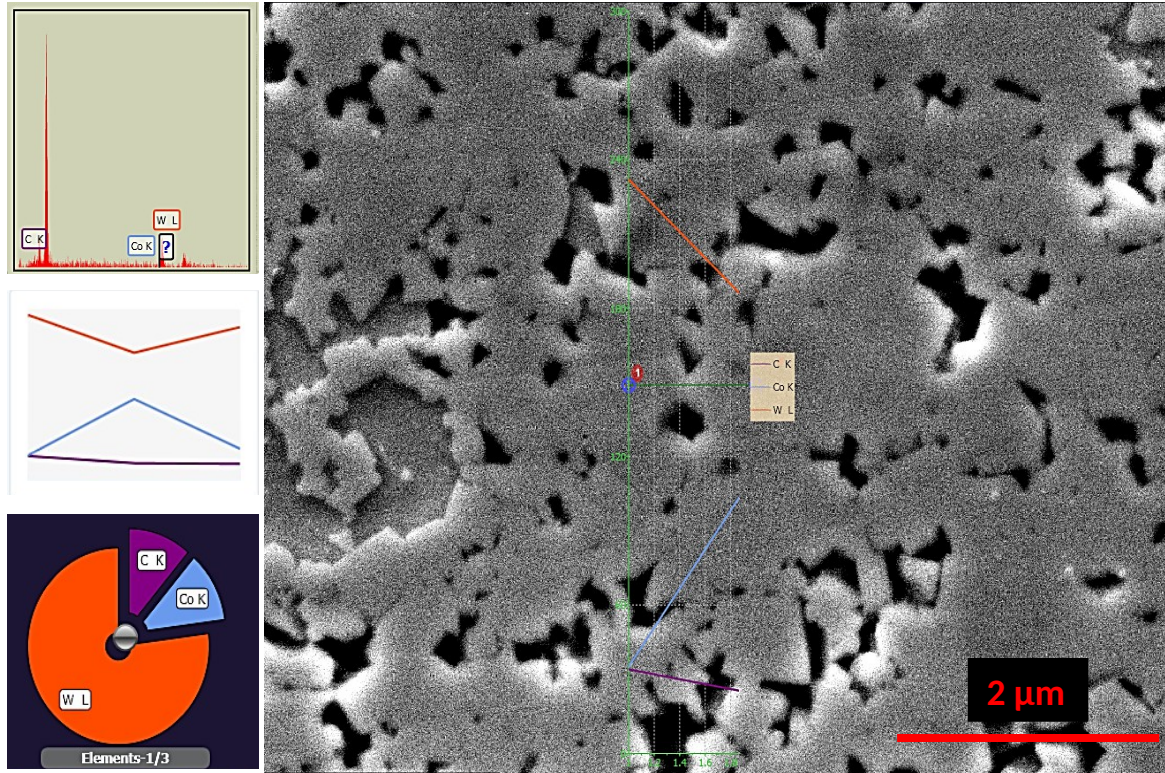
Fig 13: Line scanning of WC (1-3 µm) - 7.5 wt. % Co (1-3 µm) sample, pulse plasma sintered at 1200 $^{\circ}$ C

Sample Number	Composition	Powder Size	Compaction Pressure (MPa)	Sintering Temperature ($^{\circ}$C)	Heating Rate ($^{\circ}$C/min)	Holding Time (min)	Cooling Rate
Micron 1	WC-7.5Co	1-3 Micron	100	1000	100	5	
Micron 2	WC-7.5Co	1-3 Micron	100	1100	100	5	
Micron 3	WC-7.5Co	1-3 Micron	100	1200	100	5	
Micron 4	WC-7.5Co	1-3 Micron	60	1200	100	5	
Sub Micron 1	WC-7.5Co	500 nm	100	1000	100	5	
Sub Micron 2	WC-7.5Co	500 nm	100	1100	100	5	Natural Cooling
Sub Micron 3	WC-7.5Co	500 nm	100	1200	100	5	
Sub Micron 4	WC-7.5Co	500 nm	60	1200	100	5	
Nano 1	WC-7.5Co	100 nm	100	1000	100	5	
Nano 2	WC-7.5Co	100 nm	100	1100	100	5	
Nano 3	WC-7.5Co	100 nm	60	1200	100	5	

Table 1: Mixing and processing conditions of WC-Co samples

Sample Number	Diameter	Weight	Thickness
Micron 1	11.5 mm	6.16 gm	4.5 mm
Micron 2	11.6 mm	6.03 gm	3.7 mm
Micron 3	11.7 mm	2.89 gm	1.7 mm
Micron 4	11.6 mm	3.46 gm	2.1 mm
Sub Micron 1	11.6 mm	5.43 gm	3.5 mm
Sub Micron 2	11.7 mm	5.32 gm	3.3 mm
Sub Micron 3	12.4 mm	5.07 gm	2.9 mm
Sub Micron 4	11.6 mm	2.56 gm	1.5 mm
Nano 1	11.6 mm	5.25 gm	4.2 mm
Nano 2	11.6 mm	5.38 gm	3.2 mm
Nano 3	11.7 mm	5.22 gm	3.1 mm

Table 2: Physical specification of WC-Co samples

CONCLUSIONS AND FURTHER SUGGESTIONS

The use of four different sintering techniques, namely conventional sintering (CS), microwave sintering (MS), spark plasma sintering (SPS) and pulse plasma sintering (PPS) have been used on three different types of WC – 7.5 wt. % Co samples; micron, submicron and nano, for the first time in an attempt to make a four way comparison between all these different processes. Sintering technique was the most significant parameter that was changed during this study. In addition, another critical parameter was varied in this study, which is the initial particle size, which was found to be quite different from the final grain size observed in the samples. Furthermore, sintering temperature was varied between 1000 and 1400 °C, although it was not possible to use the exact same temperature range for all processes as they widely vary in nature. Finally sintering pressure was varied in two parts of this study.

The purpose of using different sintering techniques was to observe the differences most of them yield in contrast with conventional sintering, a process that has been used by industries for more than a century. In addition, these sintering processes were categorized based on the number of steps required. Where microwave and conventional sintering were of similar nature in terms of number of steps; pre-compaction and sintering, spark and pulse plasma sintering were found to be quite similar in terms of time required for sintering, and steps involved during the process. The heating and cooling rates of these two processes were compatible as well, although the generated frequency in pulse plasma sintering was more intense than what we observed for spark plasma sintering. In other words, microwave and conventional sintering are pressure less heating techniques and require an additional stage of compaction. Since pressure is not employed during the heating and cooling cycle in these two processes, employment of a relatively higher temperature is often observed. In order to make these two processes compatible with the plasma methods, a wider range of temperature was used.

Initial particle size, the second varying parameter in this study, is directly related to the process that is being used for sintering and the final temperature that is involved, although there are other parameters that factor in behind drawing a relationship between initial particle

and final grain size. Industrially, the practice of using grain growth inhibitors relate to the idea that they contribute in keeping the grain growth under control. However through careful observations of all our studies, it can be conclusively said that compositions without inclusions of commercial inhibitors also displayed equally strong, or even improved mechanical behaviour compared to samples that used growth inhibitors as part of the composition. In addition, using lower sintering temperature during plasma processes resulted in displaying limited grain growth in samples, eventually leading to improved mechanical properties. Sintering processes that did not use pressure needed to be carried out for longer period of time and at higher temperature in order for the particles to bond together.

An idea behind using a wide range of sintering temperature was to identify if it was possible to achieve similar or better mechanical and microstructural behaviour at a low temperature in comparison with the standard conventional temperature required to reach that threshold. It was eventually found out that PPS and SPS processes are capable of displaying significantly better mechanical behaviour at low temperatures, attributing to their enhanced and rapid diffusion and bonding mechanisms. When low temperature succeeds in displaying better mechanical properties, it can fairly demonstrate the ability to control grain growth, which of course is related to the mechanical behaviour observed in those sintered samples. Out of all sintering processes, the use of pulse plasma sintering indicated the best mechanical behaviour as well as microstructural features, including solid state bonding between particles and grains at low sintering temperature. Conventional sintering was found to display relatively low mechanical properties, namely hardness (~1352 HV/13.26 GPa) and fracture toughness (4.5 MPa $\sqrt{m}$), primarily due to the absence of pressure and inclusion of high sintering temperature, helping grain growth in the process. In contrast, it was possible to reach a maximum of 2000 HV hardness with fracture toughness of 15.3 MPa $\sqrt{m}$ in plasma sintered samples.

Some of the core findings of this study are listed below:

- With an increase in milling time, finer particles of metallic Co binder got more homogeneously distributed around coarse WC (Chapter 3).
- Grain size in the sintered samples has been found to reduce with increasing milling time (Chapter 3).

- Relative density and hardness both increased due to slight drop in grain size and improved Co distribution (Chapter 3).

- Although coarse particles of WC went through uneven breaking during high-energy ball milling, the greater homogeneity of nano Co within WC matrix helped overcome the bonding adversities, and resulted in displaying reasonably high mechanical property (Chapter 3).

- For conventional sintering, lower fracture toughness values were attributed to lack of large Co particles acting as crack arrestor and also higher percentages of WC–WC contact in the nano-Co binder samples (Chapter 4).

- Sintering temperatures at which the samples were treated for several hours, did not seem to have quite an impact on the properties, and primarily contributed towards stabilizing the homogeneity from a microstructural point of view (Chapter 4).

- WC was found to be the dominant phase in all sintered samples, although Co was homogeneously distributed as a combined result of using high energy ball milling of powders, employing MPC for pre-compaction and several hours of conventional sintering for phase stabilization (Chapter 4).

- When SPS was used, hardness increased in the samples with increasing SPS pressure reaching a maximum of 1925 HV (18.88 GPa) (Chapter 5).

- Porosity reduced in the SPS samples with increased homogeneity in terms of size and distribution, both on the surface and along cross section, with incremental sintering pressure (Chapter 5).

- While the decrease in crack length showed an increase in hardness and fracture toughness, it was difficult to identify the contribution of binder phase (nano cobalt) in terms of limiting crack propagation, as WC was the dominant phase around the cracks and throughout the microstructure (Chapter 5).

The nature of this study is quite extensive in the sense that it covers almost all the parameters involved during sintering process, and uses a wide range to be able to identify changes in behaviour or patterns for specific conditions.

Future work will involve further investigation on sintering mechanisms and how they resolve one of the most critical questions; whether the presence of plasma can be confirmed during the use of these modern sintering methods. A part of the future study with focus on individual

plasma sintering processes to determine the criteria and boundary conditions for the generation of plasma. It would be of interest to know the frequency of the plasmas and the maximum local temperature they are capable of producing, and how they affect cemented carbides. In addition, a variance in terms of composition, or presence of binder content, with and without commercial grain growth inhibitors, and how that is influenced by plasmas would be another promising avenue to explore. It is also important to understand the mechanism of consolidation during sintering and explore the simultaneous application of pressure (or indeed the lack of it for pressure-less processes) and temperature on microstructural evolution during sintering processes using a combination of EBSD and TEM analyses. This should eventually lead to modelling of diffusion during each respective sintering processes.